STEREOCHEMICAL STUDIES, AND KINETICS OF ENVIRONMENTAL AVERAGING PROCESSES IN SOME ORGANOMETALLIC ACETYLACETONATE COMPLEXES OF TIN(IV), GERMANIUM(IV), AND SILICON(IV)

Kenneth Aaron Hersh

A THESIS

in

The Department

of

Chemistry

Presented in Partial Fulfillment of the Requirements for the Degree of Master of Science at
Concordia University
Sir George Williams Campus
Montreal, Canada

February, 1975

STEREOCHEMICAL STUDIES, AND KINETICS OF ENVIRONMENTAL AVERAGING PROCESSES IN SOME ORGANOMETALLIC ACETYLACETONATE COMPLEXES OF TIN(IV), GERMANIUM(IV), AND SILICON(IV)

Kenneth Aaron Hersh

ABSTRACT

The stereochemistry of $XYM(acac)_2$ complexes (where X = CH_3, C_6H_5; Y = CH_3, C_6H_5, Cl; and M = Sn, Ge, Si; acac = $CH_3COCHCOCH_3$-) has been investigated by dynamic nmr methods. These complexes are predominantly *cis* in chloroform-d, bromoform or chloroform-d-carbon tetrachloride solutions with a small amount ($\leq$ 5%) of the *trans* form present in some of the complexes (*e.g.*, when X = C_6H_5, Y = Cl, M = Sn, Ge, Si and when X = CH_3, Y = Cl and M = Ge). Attempts to assess the structure of $(CH_3)_2Sn(acac)_2$ in solution by variable temperature nmr techniques proved unsuccessful; also, the structure of $(C_6H_5)_2Ge(acac)_2$ could not be unequivocally assigned. Kinetics of configurational rearrangements which exchange acac ring protons

between the two nonequivalent sites in the case of the methylchloro and phenylchloro complexes, along with exchange of methyl groups in $(C_6H_5)_2Sn(acac)_2$ have been determined by nmr line-broadening in dichloromethane, chloroform-d, bromoform, and chloroform-d-carbon tetrachloride solutions. First-order rate constants at 25°, activation energies, and entropies of activation for the exchange process are, respectively, for $(C_6H_5)_2Sn(acac)_2$: 369 ± 58 ($CDCl_3$) and 281 ± 37 sec^{-1} (CH_2Cl_2), 8.1 ± 0.3 ($CDCl_3$) and 7.4 ± 0.3 kcal/mole (CH_2Cl_2), -21.7 ± 1.4 ($CDCl_3$) and -24.5 ± 1.2 eu (CH_2Cl_2); for $(CH_3)ClSn(acac)_2$ in $CDCl_3$, 36 ± 3 sec^{-1}, 14.6 ± 1.1 kcal/mole, and -4.3 ± 3.7 eu; for $(C_6H_5)ClSn(acac)_2$ in $CDCl_3$ and $CHBr_3$ they are, 4.1 ± 0.9 and 2.9 ± 0.4 sec^{-1}, 12.7 ± 2.0 and 14.7 ± 0.8 kcal/mole, -15 ± 6 and -9.4 ± 2.4 eu; for $(C_6H_5)ClGe(acac)_2$ in $CDCl_3$-CCl_4 they are, 9.4 sec^{-1}, 12.8 ± 1.2 kcal/mole, -13 ± 4 eu; for $(C_6H_5)ClSi(acac)_2$ in $CDCl_3$-CCl_4 they are, 4.2 x 10^3 sec^{-1}, 6.4 ± 1.0 kcal/mole and -22 ± 5 eu. Substitution of chloride in $Cl_2Sn(acac)_2$ by phenyl or methyl groups increases the lability in the order Cl_2Sn < $(C_6H_5)ClSn$ < $(CH_3)ClSn$ < $(C_6H_5)_2Sn$. The same effect is observed in the case of the analogous germanium and silicon complexes. A mechanistic analysis of the coalescence behaviour of methyl resonances and acac ring proton signals in nmr spectra of $RClM(acac)_2$ complexes (when M = Sn, R = CH_3, C_6H_5; when M = Ge, Si, R = C_6H_5) suggests that

configurational rearrangements in these proceed *via* twist motions through trigonal prismatic transition states. Rearrangements in $(C_6H_5)_2M(acac)_2$ (M = Sn or Ge) are also believed to occur *via* a twist mechanism on the basis of activation parameters reported here and those obtained from the intermolecular ligand exchange process in the $(C_6H_5)_2Sn(acac)_2$-$(CH_3)_2Sn(acac)_2$ system. The environmental averaging process for $(CH_3)ClGe(acac)_2$ in $CDCl_3$-CCl_4 solution was found to be second-order in complex concentration. Activation parameters are E_a = 6.0 ± 0.3 kcal/mole, $\Delta S^{\ddagger}$ = -30 ± 1 eu, and k_{25} = 1.6 x 10^2 $M^{-1}sec^{-1}$. Rearrangements are viewed as occurring *via* a germanium-oxygen bond rupture as a first step to yield a five-coordinate intermediate. The rate determining sequence is thought to involve proper orientation of two five-coordinate species to form a bis-acac bridged dimer.

Dedicated to Essie and Cheryl who waited in the wings so patiently

and

To my parents who instilled upon me the value of an education and can now see the fruits of their labours

BIOGRAPHICAL SKETCH

The author, son of Mr. and Mrs. Morris B. Hersh was born July 7, 1947 in Montreal, Quebec, Canada. His secondary education was completed in June 1964, at Northmount High School in Montreal.

From September of 1964 until June of 1965 he attended the Montreal Institute of Technology.

In September of 1965, he entered Sir George Williams University where he graduated in June 1970 with a B.Sc. degree with a Major in Chemistry.

The author entered the Graduate Chemistry program at Sir George Williams University in September 1970.

He is co-author of (1) "A Nuclear Magnetic Resonance Study of the Structure of Diphenylbis(2,4-pentanedionato)tin(IV) Complex" by N. Serpone and K.A. Hersh, Inorg. Nucl. Chem. Letters, 7, 115 (1971); (2) "Kinetic Analysis of the Configurational Rearrangements in, and the Stereochemistry of Some Organotin(IV) β-ketoenolate Complexes" by N. Serpone and K.A. Hersh, Inorg. Chem., 13, 2901 (1974); (3) "Stereochemistry of, and Kinetics of Environmental Averaging Processes in Some Organogermanium-(IV) and Organosilicon(IV) Chelates" by N. Serpone and K.A. Hersh, J. Organometal. Chem., IN PRESS; (4) Kinetics of Environmental Averaging, and the Stereochemistry of $(CH_3)ClGe(acac)_2$. A Case of a Second Order Process" by K.A. Hersh and N. Serpone, Can. J. Chem., IN PRESS.

ACKNOWLEDGEMENT

I wish to express sincere thanks to Dr. N. Serpone for his continued patience, guidance, and advice throughout this work. A more dedicated mentor cannot be found.

I would also like to thank Professors L.D. Colebrook and R.A. Westbury for serving on my research committee.

I also wish to thank Doug Bickley for the many discussions concerning the mechanisms of environmental averaging processes in chelate complexes.

TABLE OF CONTENTS

LIST OF TABLES

LIST OF FIGURES

I. INTRODUCTION

In the past several years the chemistry of various β-ketoenolate complexes of transition and past transition metals has received considerable attention (1-9). Of particular interest has been the correlation of molecular structure, and kinetic lability with respect to configurational rearrangements (e.g., racemization, isomerization, and ligand exchange). However, little attention has been paid to organometallic β-ketoenolate complexes of group IV (Si, Ge, Sn) elements with regard to stereochemistry and, to an even lesser extent configurational rearrangements in the chelate rings.

It has been established that dialkyl and diaryltin(IV) form six-coordinate (10-16), monomeric (13,17-19) complexes with β-ketoenols (12-14,17), 8-hydroxyquinoline (10,11,13,15,18) and tropolone (19). There has, however, been much controversy over the structure of many of these and analogous complexes. This is mainly due to the fact that these complexes which are of the type $R_2M(dik)_2$ can assume two different configurations, a cis and a trans structure. These are illustrated below.

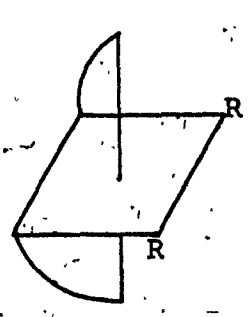

CIS

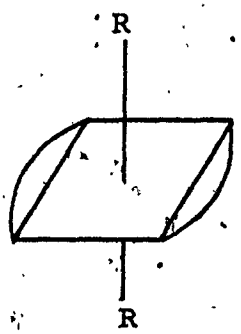

TRANS

Compounds of the type $Sn(acac)_2X_2$ (X = Cl; Br, I, or F; 'acac' = anion of acetylacetone) have been found to have a dipole moment of 6-7D (20-22), indicating a predominantly cis structure in solution. Also, coincidence of bands in the Sn-O and Sn-Cl regions in the infrared and Raman spectra of $Sn(acac)_2Cl_2$ is consistent with a cis structure (23). Nmr spectra of the dichloro and diiodo, $X_2Sn(acac)_2$, complexes exhibit two resonance signals of equal intensity in the methyl region (21,23,24-27). Kawasaki and coworkers (26,28,29) first attributed these two resonances to a distorted trans structure featuring localized double bonds; however, the weight of other evidence necessitates the assignment of the cis configuration. Low temperature nmr spectra (30) of $Sn(acac)_2F_2$, which exhibits two methyl resonances, supports the dipole moment data (20) and confirms the cis configuration. Solid state infrared spectral evidence (30) also confirms this assignment but contradicts the work of Cox and coworkers (31). Jones (30) has reported data on $Sn(dpm)_2X_2$ (X = Cl, Br, I, or F; 'dpm' = anion of dipivaloylmethane) in which the nmr spectra exhibited two equivalent t-butyl resonances indicative of a cis structure. A recent intensive nmr and infrared study (32) of $X_2Sn(acac)_2$ (X = Cl, Br, I, or F) complexes has shown that these possess the cis structure in solution and in the solid state, and that stereochemical non-rigidity follows the order F >I > Br ≥ Cl. Moessbauer(33,34) and single crystal diffraction studies (35) of $Cl_2Sn(acac)_2$

also reveal a cis stereochemistry in the solid state.

Controversy over the stereochemistry of $(CH_3)_2Sn(acac)_2$ in the solid state has been solved from the x-ray diffraction results of Miller and Schlemper (36). They have found the compound to have the trans configuration in which the molecules possess a center of symmetry, i.e., the arrangement of the methyl groups (CH_3-Sn-CH_3) is rigorously trans. However, the configuration in solution is still uncertain. In 1964 McGrady and Tobias (14) suggested that the compound adopts the trans structure in chloroform-d solutions on the basis of the magnitude of the Sn-CH_3 spin-spin coupling constants and their similarity to values of the aquo-dimethyltin(IV) cation. This cation was shown to have trans methyl groups from Raman and infrared spectra (14). Kawasaki and coworkers (37) assigned the trans structure on the basis of the vibrational spectra of the crystalline compound. In a later study, McGrady and Tobias (12) also assigned the trans structure to $(CH_3)_2Sn(acac)_2$ in the crystalline state, and in benzene and carbon tetrachloride solutions on the basis of further vibrational evidence. More recent Raman studies (38) also support the trans configuration in the solid and solution states. The studies have ruled out the possibility of a trans to cis isomerization reaction owing to the nearly identical polarizability tensors for the symmetric SnC_2 stretching vibration at 510 cm^{-1} in the solution and solid state Raman spectrum of the dimethyltin complex (38).

The appearance of only a single acetylacetonate methyl resonance (12) for $(CH_3)_2Sn(acac)_2$ in the room temperature nmr spectrum led to the deduction of a trans structure; this evidence is of limited value because of the possibility of a rapid exchange process taking place that time-averages the acetylacetonate methyl signals on the nmr time scale. On the basis of the magnitude of the quadrupole splitting in the Moessbauer spectrum (33,39,40) the trans configuration was assigned to $(CH_3)_2Sn(acac)_2$. Moore and Nelson (41) have reported measurements of molar polarizations and refractivities at 4358 Å for benzene and cyclohexane solutions and reported dipole moments (static) of 2.95 and 3.19D, respectively. The cis structure was assigned in consideration of these dipole moments. This is also supported by Hayes and coworkers (42) who found dielectric relaxation times of 5.3×10^{-2} sec and a dipole moment (dynamic) of 1.76D indicative of a dipolar cis structure.

It was originally suggested (13) that $(C_6H_5)_2Sn(acac)_2$ should exist as a cis or trans isomer with the cis form producing two enantiomers. However, failing to resolve these enantiomers over a D-lactose chromatographic column, Nelson and Martin (13) concluded that this compound possesses the trans configuration in solution, although existence of the cis form was not precluded. Observation (12) in the room temperature nmr spectrum of only one methyl signal, and vibrational spectra closely similar to those of the corresponding dimethyltin complex led to the

formulation of a trans structure. On the other hand, Moessbauer studies (33,39) indicate a cis structure in the solid state. This cis geometry is supported by recent variable temperature nmr studies (43). From small values of the dipole moment (13) (3.78D in C_6H_6 and 4.02D in $C_{12}H_{12}$) found in earlier studies it was deduced that the compound assumed the trans configuration in solution. However, in a recent report Moore and Nelson (41) have proposed a cis structure on the basis that the presence of this dipole moment rules out the non-polar trans structure. Atomic polarization (42) and dielectric relaxation studies (44) support the existence of the cis form in solution although these latter studies did not preclude a mixture of cis and trans isomers, with the former predominating.

Haloalkyltin(IV) acetylacetonates, $RXSn(acac)_2$ (R = alkyl; X = Cl, Br, or I), were assigned a trans stereochemistry by Kawasaki and coworkers (29) on the basis of nmr evidence, presumably from room temperature nmr spectra. A later report (45) on $RXSn(acac)_2$ complexes explains the temperature dependence of the nmr spectrum of $(CH_3)ClSn(acac)_2$ in terms of a cis $\rightleftharpoons$ trans isomerization reaction. Nmr studies (28) on $(C_6H_5)XSn(acac)_2$ (X = Cl or Br) complexes in chloroform-d and bromoform revealed four methyl and two acetylacetonate ring proton nmr resonance signals; these were suggested as arising from a linear C_6H_5-Sn-X stereochemistry and from a distorted acetyl-

acetonate ring structure, for example, a structure containing "somewhat localized double bonds". Such a distorted structure has also been proposed (26,28,29,46) for $X_2Sn(acac)_2$ (X = Cl, Br, or I) chelates but has since been shown (32) to be incorrect. Furthermore, the coalescence phenomena of the ring proton resonances in the limited variable-temperature nmr data available on the phenylchlorotin(IV) acetylacetonate complex (in $CHCl_3$ and $CHBr_3$) was misinterpreted (28) in terms of hindered internal rotation of the phenyl group around the Sn-C bond (E_a = ca. 3 kcal/mole). Moessbauer studies (33) have suggested a cis structure for both the methyl- and phenylchlorotin(IV) acetylacetonates although this was quite difficult to ascertain as the predicted quadrupole splittings for the cis and trans structures are too similar (calculated values for trans-$(CH_3)ClSn(acac)_2$ and trans-$(C_6H_5)ClSn(acac)_2$ are 1.94 mm/s and 1.78 mm/s respectively and for the cis complexes, 2.03 mm/s and 1.87 mm/s respectively; observed values were 1.78 mm/s and 1.77 mm/s).

Organogermanium(IV) complexes with β-diketones have received little attention (47,48). Mehrotra and Mathur (49) reported the synthesis of the monomeric, six-coordinate $(C_6H_5)_2Ge(acac)_2$ complex and of $(t\text{-}C_4H_9)_3Ge(acac)$ suggested as being five-coordinate. Dichlorogermaniumbisacetylacetonate, $Cl_2Ge(acac)_2$, has been found to be monomeric (50) and a weak electrolyte in ionizing

solvents (51). Infrared and preliminary x-ray crystallographic studies (31) have suggested a cis structure for this compound. The large dipole moments observed for $Cl_2Ge(acac)_2$ (7.4D) (52) and $Br_2Ge(acac)_2$ (8.7D) (53) led Osipov and coworkers (52) to postulate a cis configuration in equilibrium with an ionic species $Ge(acac)_2Cl^+$; however, there is some doubt of an appreciable amount of this species present (54). Nmr studies by Pinnavaia and coworkers (54) on $Cl_2Ge(AA)_2$ (AA = acac, dpm, and pvac; 'pvac' = anion of pivaloylacetone) complexes suggest that these compounds exist as an equilibrium mixture of both cis and trans isomers in solution. In the nmr spectrum of $Cl_2Ge(acac)_2$ there are two equally intense methyl resonances, indicating that the complex adopts primarily the cis configuration in solution; however, a remaining methyl and methylene resonance strongly suggests the presence of an appreciable amount of trans isomer, believed to be in the range of 15-20% (54). Pure trans-$Cl_2Ge(acac)_2$ has been isolated (30) by aging a saturated chloroform solution. The nmr spectrum of this aged solution exhibits one ring proton and one methyl resonance. The chemical shift of the trans isomer corresponds to the one attributed to a contaminant by Smith and Wilkins (24), who had originally postulated the cis structure for this compound in solution. The analogous dibromo complex has been assigned (30) the trans structure in the solid state because of the similarity of the low energy infrared spectrum to that of the trans-Cl_2Ge-

$(dpm)_2$. Similar results have been obtained with $X_2Ge(dpm)_2$ (X = Cl, Br) from hexane solutions although pure cis-$X_2Ge(dpm)_2$ (X = Cl,I) has been isolated (30) by crystallization from dipivaloylmethane at 0°, and then aging for several days. Pinnavaia (54) has concluded that the general case for $Cl_2Ge(dpm)_2$ is that the crystal first formed from hexane contains a mixture of the cis and trans forms but the cis structure predominates in solution.

The complex $Cl_2Si(acac)_2$ has recently been synthesized by Thompson (55,56). Nmr spectra exhibited no splitting or broadening of the acetylacetonate methyl signals even at temperatures as low as -60°. This would indicate a trans structure for the complex. However, from other work with complexes of the type $M(acac)_2Cl_2$ (M = group IV metal) (24,57) the position of the ring proton resonance (δ = 5.93 ppm) is consistent with an ionic or dipolar cis complex. Of course, the possibility that this complex behaves anomalously cannot be precluded, and the compound may be structurally similar to trans-diacetoxybisacetylacetonatosilicon(IV), for which resonance signals occur in the same region. These results would indicate a probable trans structure (55). However, although $(CH_3CO_2)_2Si(acac)_2$ does exist predominantly in the trans form in the solid state and in freshly prepared solutions, it has been found to isomerize in solution to the cis structure to yield an equilibrium mixture ([cis]/[trans] = 1.6) (9,58,59). On the basis of infrared spectral evidence of

the complexes of the type $RClSi(acac)_2$ (R = methyl or phenyl), West (60) deduced their hexacoordinate nature but was unable from the available information to assign a particular configuration. His attempts to synthesize $(CH_3)_2Si(acac)_2$ yielded an open chain compound for which there was no apparent explanation. Steric hindrance was ruled out as the steric requirement of the chlorine atom is approximately equal to that of a methyl group and the compound $(CH_3)ClSi(acac)_2$ is chelated. It was postulated (60) that the presence of the electronegative chlorine atom on the silicon apparently increases the acidity of the silicon by sufficient withdrawal of electrons so that chelation can take place in the $RClSi(acac)_2$ complexes.

One application of silicon β-diketonate complexes has been in the area of hardening of silicon rubber (61). A silicon complex $(CH_3)XSi(acac)_2$ (X = Cl or OAc) is first obtained by treating CH_3SiX_3 with Ac_2CH_2. Then, 0.6 parts of the resulting complex dissolved in 1.5 parts $CHCl_3$ is added to 10 parts of organopolysiloxane, having silanol end groups, to give a completely hardened polymer.

It was, therefore, decided to investigate the stereochemical nature and stereochemical lability of compounds of the type $XYM(acac)_2$, where X is methyl or phenyl, Y is methyl, phenyl, or chlorine, and M is either tin, germanium, or silicon. An analysis of the probable mechanisms for the environmental averaging of acetylacetonate

ring protons and/or acetylacetonate methyl groups has also been undertaken. These make up the subject of the present thesis.

II. EXPERIMENTAL

A. Synthesis of Compounds

1. Reagents and Solvents

Reagent grade anhydrous ether, benzene, hexane and carbon tetrachloride were purchased from Anachemia Chemicals. Dichloromethane was Fisher Scientific Certified Reagent Grade. The above solvents were dried by refluxing over calcium hydride (Fisher Purified) for at least 12 hours prior to distillation. Diphenyltin dichloride, dimethyltin dichloride, phenyltin trichloride, methyltin trichloride, dimethylgermanium dichloride, methylgermanium trichloride, diphenylgermanium dichloride, diphenyl dichlorosilane, dimethyl-dichlorosilane, phenyl trichlorosilane, methyl trichlorosilane and thallous carbonate were purchased from Alfa Inorganics and used without further purification. Tetraphenylgermane and germanium tetrachloride were purchased from Research Organic/Inorganic Chemical Corp. and were used without further purification. Acetylacetone (2,4-pentanedione, Fisher certified Reagent), sodium metal (J.T. Baker), absolute ethanol (Commercial Alcohols Ltd.), hexachloro-2-propanone (Aldrich Chemical Corp), pyridine (purified, J.T. Baker) and deuterium oxide (Merck, Sharp and Dohme) were used as purchased and without further purification. Aluminum trichloride anhydrous was Fisher Certified Reagent Grade.

2. General Techniques

Syntheses and handling of compounds for physical measurements were carried out under anhydrous conditions in a dry nitrogen atmosphere, using a nitrogen-filled Glove Bag (Instruments for Industry and Research) containing a dish of phosphorus pentoxide. All glassware, including side-arm flasks and modified fritted glass funnels of the type described by Holah (62) and Fay and Pinnavaia (63) was cleaned with alcoholic potassium hydroxide and/or aqua regia, washed with water and then dried in an oven at 140°C for at least one hour prior to use. All filtrations were accomplished under nitrogen. The compounds were stored in a desiccator containing Drierite.

3. Isolation of Products and Purification

In all cases, after the starting materials were allowed to react the products were obtained by the following techniques. The mixtures produced from the reaction of the starting materials were repeatedly filtered through a modified fritted glass funnel until a clear solution was obtained. In the case of the tin and germanium compounds the solution was reduced to about one-half the original volume by passing a gentle stream of nitrogen gas over the surface of the solution while heating (ca. 60°) the flask with a heat gun. Approximately 10 ml of hexane was then added and the solution concentrated further until the first signs of turbidity. The flask was subsequently stoppered

and placed in a freezer (ca. -4°) to allow crystallization to occur (about 1-3 hours). Should crystallization not have occurred more solvent was removed and the process repeated until the desired product was obtained. The supernatant fluid was decanted under nitrogen and the resulting solid was recrystallized by first dissolving it in a minimum amount of dichloromethane followed by addition of about 10 ml of hexane; the solvent again was removed until the first signs of turbidity. The product was crystallized as described above. The solid product was filtered and initially dried by running a stream of nitrogen gas through the modified fritted glass funnel and then dried in vacuo for at least 0.5 hours.

In the case of the silicon compounds which tended to decompose more readily the solvent was removed under partial vacuum from a water aspirator while applying heat to the flask from a heat gun. In all cases, the purity of the products was checked from their nmr and infrared spectra, and from melting points.

4. Melting Points

Melting points were measured with a Gallenkamp melting point apparatus (model MF-370). The capillaries were sealed with modeling clay in a glove bag. Reported melting points are uncorrected.

5. Elemental Analyses

Samples were submitted for elemental analysis in screwcap vials secured with vinyl tape.

Elemental analyses were determined by Galbraith Laboratories, Knoxville, Tennessee. In two cases, chlorine determinations were done by the author.

6. Sodium Acetylacetonate.-

The sodium salt of acetylacetonate was prepared by standard methods (12,64). To a solution of acetylacetone in anhydrous ether was added small pieces of metallic sodium. The mixture was stirred for two hours at which time a white solid was produced. After filtering and washing with cold anhydrous ether, the product was dried *in vacuo*. Unreacted sodium particles were manually removed.

7. Thallium Acetylacetonate.-

To a solution of acetylacetone (4.51 g, 0.0451 mol) in 200 ml of absolute ethanol was added 10.57 g of thallous carbonate, Tl_2CO_3, (0.0225 mol). This mixture was stirred and refluxed for 3 hours until the solution became clear. At this time the hot solution was filtered through a coarse modified fritted glass funnel (62,63) to remove any undissolved impurities. The filtrate was allowed to cool under a stream of nitrogen gas until the first

signs of crystallization. The stoppered flask was placed in a freezer (ca. -4°) to allow complete crystallization. The white crystals were then collected and washed with cold (-4°) absolute ethanol and dried in vacuo. Yield produced was 8.13 g (61.2% of theoretical). Mp 157-159°: Lit., (13) mp 153-154°.

8. Phenylgermanium Trichloride.-

This compound was synthesized by the method of Rijkens and Van der Kerk (65). To a Carius combustion tube (250 mm long, i.d. 8 mm) was added 3.19 g of germanium tetrachloride, $GeCl_4$, (0.0149 mol). A mixture of tetraphenyl germane, $(C_6H_5)_4Ge$, (2.32 g, 0.00609 mol), and freshly sublimed aluminum trichloride, $AlCl_3$, (0.16 g, 0.00120 mol) was first homogenized and then placed in the tube in a manner which allowed maximum wetting of the solids. The tube was flame-sealed at atmospheric pressure and subsequently placed in a tightly secured steel pipe. The latter was placed in an oven for seven hours at 125°C. After cooling, the products were distilled and the desired phenylgermanium trichloride, $C_6H_5GeCl_3$, removed at 128-150°C (50 mm). Lit., (65) bp 105-106° (13 mm). The purity of the product was verified from its infrared and nmr spectra.

9. Diphenylbis(2,4-pentanedionato)tin(IV).-

A 70% yield of this product was obtained by the

reaction of 4.90 g (0.0143 mol) of diphenyltin dichloride, $(C_6H_5)_2SnCl_2$, with 3.83 g (0.0314 mol) of sodium acetylacetonate, Na(acac), in 100 ml of dichloromethane. The mixture was stirred for three hours and then filtered. The filtrate was processed as described earlier and the white product recrystallized from dry dichloromethane-hexane solutions. The yield was 4.70 g. Mp 124-126°(dec). Lit., (12) mp 125°. Lit., (17) mp 125-126°. Lit., (16) mp 127°. Chemical shifts (9.8 g/100 ml; $CDCl_3$/TMS; ca. 37°): δ = 5.41 ppm (-CH=) and 1.98 ppm (CH_3).

10. Dimethylbis(2,4-pentanedionato)tin(IV).-

To a 150 ml solution of dimethyltin dichloride, $(CH_3)_2SnCl_2$, (2.51 g, 0.0114 mol) in dichloromethane was added sodium acetylacetonate, Na(acac), (3.05 g, 0.0250 mol). The mixture was stirred for three hours and then filtered through a modified fritted glass funnel. The filtrate was processed as described above and the white product was subsequently obtained by recrystallization from dichloromethane-hexane solutions. Yield 1.20 g (30% of theoretical). Mp179-180°(dec). Lit., (37) mp 177-178°. Chemical shifts (10.3 g/100 ml; $CDCl_3$/TMS; ca. 37°): δ = 5.32 ppm (-CH=), lit., (12) 5.27 ppm; 1.96 ppm (CH_3); 0.89 ppm (Sn-CH_3), lit., (12) 0.49 ppm. J(^{117}Sn-CH_3) 99.2 Hz, lit., (12) 95.0 Hz; J(^{119}Sn-CH_3) 103.8 Hz, lit., (12) 99.3 Hz.

11. Phenylchlorobis(2,4-pentanedionato)tin(IV).-

Sodium acetylacetonate, Na(acac), (1.61 g, 0.0132 mol), was added to phenyltin trichloride, $C_6H_5SnCl_3$, (1.81 g, 0.00599 mol), in 75 ml of dichloromethane. The mixture was refluxed for about three hours and then filtered hot. The desired white product was recrystallized from dry dichloromethane-hexane solutions. Yield 1.84 g (72% of theoretical yield). Mp 149-150°. Lit., (17) mp 149-152°.

Anal. Calcd. for $C_{16}H_{19}O_4ClSn$: C, 44.75; H, 4.46; Cl, 8.25; Sn, 27.64. Found: C, 44.60; H, 4.47; Cl, 8.42; Sn, 27.56.

Chemical shifts in $CDCl_3$/TMS (8.8 g/100 ml; ca. 37°), δ = 2.07 ppm (CH_3) and 5.50 ppm (-CH-).

12. Methylchlorobis(2,4-pentanedionato)tin(IV).-

Sodium acetylacetonate, Na(acac), (2.87 g, 0.0235 mol), was added to 2.58 g of methyltin trichloride, CH_3SnCl_3, (0.0107 mol) in 75 ml of dichloromethane. The mixture was refluxed for ca. 4 hours and then filtered hot. The desired white product was recrystallized from dry dichloromethane-hexane solutions. Yield 1.00 g (25% of theoretical yield). Mp 135-137°. Lit., (17) mp 135-136°. The purity of this product was verified by nmr and infrared spectra. Substitution of thallous acetylacetonate for sodium

acetylacetonate yielded 72% of the product. Chemical shifts in $CDCl_3$/TMS (15.8 g/100 ml; ca. 28°), δ −0.86 ppm ($Sn-CH_3$), 2.04 ppm ($acac-CH_3$), 5.51 ppm (acac-CH—). $J(^{117}Sn-CH_3)$ 119.2 Hz, $J(^{119}Sn-CH_3)$ 124.6 Hz.

13. Diphenylbis(2,4-pentanedionato)germanium(IV).-

This compound was synthesized by reacting 2.69 g of diphenylgermanium dichloride, $(C_6H_5)_2GeCl_2$, (0.00904 mol), and thallous acetylacetonate, Tl(acac), (5.00 g, 0.0164 mol) in 75 ml of dichloromethane. The resulting mixture was stirred for about two hours, filtered and the filtrate processed as described earlier. The white product was recrystallized from dry dichloromethane-hexane solutions. Yield 1.70 g (49% of theoretical yield). Mp 134-136°(dec), bp 243° (1.0 mm). Lit., (49) bp 201° (0.6 mm).

Anal. Calcd. for $C_{22}H_{24}O_4Ge$: C, 62.17; H, 5.69. Found: C, 59.01; H, 5.38.

Purity of the product was confirmed by the absence of OH and uncomplexed CO bands in the infrared spectrum. This white compound tends to decompose over a few days as evidenced by a change in color. The unsatisfactory analysis is probably the result of rapid decomposition of this compound. A low carbon analysis has also been reported by others (49).

Chemical shifts in $CDCl_3$-CCl_4/TMS (10.3 g/100 ml; ca. 31°), δ 1.93 ppm (CH_3) and 5.31 ppm (-CH—).

14. Phenylchlorobis(2,4-pentanedionato)germanium(IV).- This compound was obtained in 67% yield by adding 6.29 g of thallous acetylacetonate, Tl(acac), (0.0208 mol) to 2.66 g of phenylgermanium trichloride, $C_6H_5GeCl_3$, (0.0104 mol) in 75 ml of dichloromethane. The mixture was stirred for 30 minutes and filtered. The desired product was recrystallized from dry dichloromethane-hexane solutions. This compound tended to form an intractable oil; it was necessary to induce crystallization by scratching the sides of the flask with a spatula while evaporating the solvent with a stream of nitrogen gas. Yield 2.65 g. Mp 143-145°(dec). Lit., (47) mp 140-145°.

Anal. Calcd. for $C_{16}H_{19}O_4ClGe$: C, 50.13; H, 5.00. Found: C, 43.89; H, 4.46.

Chemical shifts in $CDCl_3$-CCl_4/TMS (17.6 g/100 ml; ca. 31°), δ = 2.08 ppm (CH_3) and 5.60 ppm (-CH=).

Purity of the freshly prepared product was ascertained from nmr and infrared spectra. Rapid decomposition (ca. 2-3 days) results in an unsatisfactory analysis. A gravimetric determination of chlorine (47) produced 9.10% (calcd. 9.25%).

15. Methylchlorobis(2,4-pentanedionato)germanium(IV).- To prepare this compound, 6.15 g of thallous acetylacetonate, Tl(acac), (0.0213 mol), was added to a

75 ml dichloromethane solution of methylgermanium trichloride, CH_3GeCl_3, (2.29 g, 0.0118 mol). The mixture was stirred for 35 minutes. The desired white compound was recrystallized from dry dichloromethane-hexane solutions. Yield 1.20 g (32% of theoretical yield). Mp 128-132°(dec). Lit., (47) mp 128-132°.

Anal. Calcd. for $C_{11}H_{17}O_4ClGe$: C, 41.12; H, 5.33. Analyses on two separate samples gave; C, 25.98, 25.98; H, 3.98, 3.13. A gravimetric determination of chlorine on a freshly prepared sample in this laboratory gave 11.0% (calcd. 11.04%).

Purity was also verified by the absence of OH and uncomplexed CO bands in the infrared spectrum. The compound tends to decompose over a period of a few days. Chemical shifts in $CDCl_3$-CCl_4/TMS (17.6 g/100 ml; ca. 31°); δ = 1.11 ppm (Ge-CH_3); δ = 2.07 ppm (CH_3-acac) and 5.57 ppm (-CH =acac).

16. Phenylchlorobis(2,4-pentanedionato)silicon(IV).-

This complex was prepared by the addition of 5.20 g of thallous acetylacetonate, Tl(acac), (0.0171 mol) to 7.96 g of phenyltrichlorosilane, $C_6H_5SiCl_3$, (0.0377 mol) in 75 ml of dichloromethane. The mixture was stirred for 10 minutes and filtered. The desired white product was recrystallized from dry dichloromethane-hexane solutions. A reddish side product tended to form on standing so that further recrystallizations were necessary to remove this

red decomposition product. Mp 119-121° (dec); lit., (47), ca. 135°.

Anal. Calcd. for $C_{16}H_{19}O_4ClSi$: Cl, 10.49. Found. Cl, 10.65.

Purity was further verified by the absence of OH and uncomplexed CO bands in the infrared spectrum. The compound decomposes over a period of hours. Chemical shifts in $CDCl_4$-CCl_4/TMS (10.8 g/100 ml; ca. 28°), δ =2.00 ppm (CH_3) and 5.58 ppm (-CH-).

17. Methylchlorobis(2,4-pentanedionato)silicon(IV).-

This complex was synthesized by the reaction of thallous acetylacetonate, Tl(acac), (4.34 g, 0.0143 mol) and methyl trichlorosilane, CH_3SiCl_3, (4.71 g, 0.0315 mol) in 50 ml of dichloromethane. The mixture was stirred for 10 minutes and filtered. The white product was recrystallized from dichloromethane-hexane. Because of its rapid decomposition a consistent melting point was difficult to obtain. The compound underwent constant decomposition upon heating.

Anal. Calcd. for $C_{11}H_{17}O_4ClSi$: Cl, 12.6 Found (47): Cl, 13.5.

The purity of this compound was verified by the absence of OH and uncomplexed CO bands in the infrared spectrum. This product decomposes in a matter of minutes.

Chemical shifts in $CDCl_3$-CCl_4/TMS (12.6 g/100 ml; 75.6°), δ = 2.07 ppm (Si-CH_3), 2.20 ppm (CH_3-acac), and 6.54 ppm (-CH=).

B. Nuclear Magnetic Resonance Spectra

1. Preparation of Solutions

a) Solvents

Deuteriochloroform, for use as a nmr solvent, was obtained by the method of Paulsen and Cooke (66) but with a slight modification (30). Hexachloro-2-propanone was reacted with deuterium oxide in the presence of pyridine. Excess deuterium oxide was removed from the crude product by cooling the mixture to ca. -4° and filtering through glass wool. Deuteriochloroform was further dried by refluxing over calcium hydride for at least four hours prior to distillation into septum sealed storage bottles containing molecular sieves (Type 4A). The solvent was ascertained to be ca. 99% atom pure from its nmr spectrum.

Bromoform (J.T. Baker Reagent Grade) was purified by distillation over molecular sieves (Type 4A) before use.

The solvent mixture of deuteriochloroform and carbon tetrachloride consisted of 53.5% by weight of deuteriochloroform and 46.5% by weight of carbon tetrachloride. This $CDCl_3$-CCl_4 mixture allowed complexes to be

studied by nmr at temperatures well below the freezing point of deuteriochloroform (freezing point of the mixture is -86.9°C (67)).

b) Solutions

Solutions of known concentration were prepared under anhydrous conditions (12) in a dry nitrogen atmosphere in a glove bag.* These were then filtered through a membrane filter (Metricel Alpha-8-0.2 μ) in order to remove any undissolved particles which can alter the resolution of the nmr spectrometer.

After preparation, the solutions were transferred to oven dried 5 mm o.d. polished nmr tubes (Wilmad #505-PS) and the sample tubes were subsequently flame-sealed in vacuo, after degassing by the freeze-thaw-refreeze method. When these nmr samples were further required, they were stored in liquid nitrogen.

2. General Variable Temperature Techniques

Proton chemical shifts (± 0.01 ppm and coupling constants (± 0.3 Hz) were obtained with a Varian

---

* When rigorous anhydrous conditions were not maintained, we observed some turbidity in the nmr solutions, indicating possible hydrolysis by trace amounts of water. These solutions were discarded.

Associates A-60-A high resolution spectrometer operating at 60.00 MHz. Sweep widths were calibrated using a $CHCl_3$/TMS standard or by the audio frequency sideband technique. Variable temperature nmr spectra were run in the frequency sweep mode on a HA-100 high-resolution spectrometer operating at 100.00 MHz and equipped with a V-6040 variable temperature controller and a V-4343 variable temperature probe. Probe temperatures were measured from chemical shift differences between nonequivalent protons of methanol (-85° to $40^{\circ}C$) or 1,2-ethanediol (40° to $80^{\circ}C$) using a modified version of the Van Geet equation (vide infra), unless otherwise noted, in the appropriate temperature ranges.

3. Systematic Errors

In the study of kinetics of configurational rearrangements by the variable temperature nmr method there are various possible experimental errors which can affect the lineshape, and therefore the accuracy of the results. Various instrument errors have been discussed by different authors, particularly by Allerhand and coworkers (68). In this work attempts were made to reduce or eliminate these errors.

Instrument error, which is the main source of experimental error in variable temperature nmr studies includes instrument instability, calibration error and

spectral distortion. Normally, the operating temperature of the Varian HA-100 spectrometer is ca. 28°; however, when the temperature is varied using a gas-flow probe there is an alteration of the quality of the magnetic field at the sample. An equilibration time of a minimum of seven minutes was allowed for each sample at each new temperature. Temperature stability also depends on the gas-flow rate and the spinning rate which in this case were kept as constant as possible with only slight adjustments made when deemed necessary. At each new temperature there is a corresponding change in field homogeneity. This was maximized to account for the drifts caused by the temperature change and by the instrument itself.

Instability errors due to sweep rate, frequency, and static magnetic fields were minimized by averaging at least five spectra at each temperature. Also, the homogeneity was optimized between scans to offset any minor field fluctuations. In addition, the internal locking nature of the spectrometer compensates for these errors by minimizing the frequency drift while the spectrum is being scanned.

Spectral distortions result from the excessive use of electronic filtering, saturation effects, and mismatch of sweep and recorder response. These were minimized by using the smallest necessary radio frequency amplitude

to eliminate saturation, by employing a slow sweep rate (0.2-0.1 Hz/sec), and by using the least amount of electronic filtering. It has been noted (68) that attempts to improve the signal to noise ratio may lead to distortion of the lineshapes. Damping of the output signal was sometimes necessary owing to the low solubility of some of the tin compounds and/or to weak absorption regions (-CH- region) in others. However, this still resulted in somewhat noisy spectra with consequent larger errors than desired.

The presence of any undissolved particles can also affect the resolution. Poor resolution can arise from the random motion of the particles through the influence of convection currents caused by temperature changes. The homogeneity cannot be adjusted quickly enough to account for this condition. Consequently, any undissolved particles were removed (vide supra).

Probe temperatures were measured by the chemical shift differences between the nonequivalent protons of either methanol (-85° to 40°C) or 1,2-ethanediol (40° to 80°C). The resulting temperatures may be read from published curves as reported by Varian Associates (69,70).

Recently Van Geet (71,72) has noted that the Varian curves (70) are in error with respect to the temperatures attainable on the A-60 spectrometer. Indeed, these findings were further confirmed by Neuman and Jonas (73)

and by Yamamoto and Yanagesawa (74). The Varian equations, derived from the published graphs (70) are

$$T = 460 - 1.64(\nu_{CH_2} - \nu_{OH}) \qquad 1$$

for 1,2-ethanediol in the range 20° to 200°C, and

$$T = 479 - 1.94|\Delta\nu| \qquad 2$$

for methanol in the range -60° to +40°C where $\Delta\nu$ is the chemical shift difference between the methyl and hydroxyl proton resonances. On the other hand, the Van Geet equation for 1,2-ethanediol is

$$T = 466.0 - 1.694(\nu_{CH_2} - \nu_{OH}) \qquad 3$$

and for methanol

$$T = 435.5 - 1.193|\Delta\nu| - 29.3|10^{-2}\Delta\nu|^2 \qquad 4$$

Van Geet reports that equation 3 is accurate to within ±0.3° in the range 37° - 137°C, and that equation 4 fits the data with a RMS error of 0.6° over the range -53° to 47°C.

Similarly, this discrepancy probably also exists for HA-100 spectra. However because Van Geet equations are not available for HA-100 operations, they were derived from the appropriate Van Geet A-60 equations. To accomplish this the HA-100 chemical shifts were converted to equivalent A-60 chemical shifts. Since;

$$\delta_{(A-60)}\ ppm = \frac{\text{observed shift freq.(Hz)} \times 10^6}{60 \times 10^6}$$

and

$$\delta_{(HA-100)}\ ppm = \frac{\text{observed shift freq (Hz)} \times 10^6}{100 \times 10^6}$$

Since

$$\delta_{(A-60)}\,ppm = \delta_{(HA-100)}\,ppm.$$

then

observed shift freq(A-60)(Hz) = 0.6 (observed shift freq (HA-100)(Hz))

Therefore, the Van Geet equations are altered as follows:

For methanol

$$T = 435.5 - 1.193|0.6\Delta\nu| - 29.3(10^{-2}(0.6\Delta\nu))^2$$

or

$$T = 435.5 - 0.7158|\Delta\nu| - 29.3(0.006\Delta\nu)^2 \qquad 5$$

and for 1,2-ethanediol

$$T = 466.0 - 1.694|0.6\Delta\nu|$$

or

$$T = 466.0 - 1.0164|\Delta\nu| \qquad 6$$

for the temperature limits stated earlier. In general, a discrepancy of $\sim 4^{\circ}$ is evident between the Varian and the Van Geet temperatures in the low temperature region and becomes progressively smaller towards ambient temperatures. Such discrepancy may lead to some small errors in the activation parameters; e.g., 0.4 to 1.6 kcal/mole in E_a and 1 to 5 eu in $\Delta S^{\ddagger}$(32,75).

4. Processing of NMR Spectra

The nuclear magnetic resonance experiment can provide access to the mean lifetime τ_i of an absorbing nucleus at the site giving rise to the mean resonance absorption (93). The reciprocal of the mean lifetime, $1/\tau_i$, is the first-order rate constant for transfer of the resonating nucleus out of the i^{th} site. When it is possible to assign values of the transverse relaxation time, T_2, the chemical shift separation between the two protons, $\delta\nu$, and the fractional populations at the two sites, P_A and P_B, at a given temperature it is possible to calculate a realistic lineshape as a function of the exchange rate. This lineshape function is given (77) by suitable modifications of the Bloch pheromenological equations as developed by Gutowsky and Holm (78) but retaining terms involving the transverse relaxation times (equation 7):

$$v = \frac{\left(P\left[1 + \tau\left(\frac{P_B}{T_{2A}} + \frac{P_A}{T_{2B}}\right)\right] + Q\left[R + \tau\left(\frac{1}{T_{2B}} - \frac{1}{T_{2A}}\right)\frac{\delta\omega}{2}\right]\right)\omega_1 M_0}{P^2 + R^2 + \tau^2\left(\frac{1}{T_{2B}} - \frac{1}{T_{2A}}\right)^2\left(\frac{\delta\omega}{2}\right)^2 + 2R\left(\frac{1}{T_{2B}} - \frac{1}{T_{2A}}\right)\frac{\delta\omega}{2}} \qquad 7$$

where

$$P = \tau\left[\frac{1}{T_{2A}T_{2B}} - \Delta\omega^2 + \left(\frac{\Delta\omega}{2}\right)^2\right] + \frac{P_A}{T_{2A}} + \frac{P_B}{T_{2B}}$$

$$Q = \tau\left[\Delta\omega - \frac{\delta\omega}{2}(P_A - P_B)\right]$$

$$R = \Delta\omega\left[1 + \frac{\tau}{T_{2A}} + \frac{\tau}{T_{2B}} + \frac{\delta\omega}{2}(P_A - P_B)\right]$$

and $$\tau = \frac{\tau_A\tau_B}{\tau_A + \tau_B} \qquad 8$$

where v is the transverse component of the resultant magnetic moment perpendicular to the rotating field H_1, which is proportional to the absorption intensity; ω_1 is the applied rotating radiofrequency field; $\Delta\omega$ is the difference in the frequencies (radians/sec) of the applied radiofrequency and the frequency center of the two resonance components; $\delta\omega$ is the difference of the resonance frequencies (radians/sec) corresponding to the sites A and B; τ_A and τ_B are the mean lifetimes for a stay on the A and the B sites; P_A and P_B are the fractional populations of the A and the B sites; T_2, is the transverse relaxation time in the absence of exchange; M_O, is the equilibrium value of the z component of the resultant magnetic moment.

Various methods (68,81,82) have been suggested to determine τ_i from the experimental lineshape data for the cases presented in this thesis which are those of

uncoupled two-site exchange systems. A reliable method for evaluating exchange rates from the spectral data consists of matching the observed spectra with a series of calculated spectra in which the exchange rate is varied. With the advent of high speed digital computers, comparison of experimental spectra and calculated spectra are now possible on an almost point by point basis. This method of complete lineshape analysis has become widely accepted as the most satisfactory of known methods (68,79,80). Two methods were employed in this work and are described below.

Mean lifetimes were calculated from nmr spectra recorded in an appropriate solvent over an appropriate temperature range. The complexes of interest in this work were examined in the solvents and at the temperature ranges shown in Table I.

Whenever possible, the following spectral parameters were selected from the nmr spectra; $W_{1/4}$, $W_{1/2}$, $W_{3/4}$, the full linewidths at one-quarter, one-half, and three-quarters of maximum height; $\delta\nu_e$, the chemical shift difference between the two proton resonances (78); and R, the ratio of the maximum intensity to minimum central intensity, $(\nu_A + \nu_B)/2$ (83).

Table I.- Temperatures at Which Complexes in This Work Were Investigated.

Complex	Solvent	Temperature Range (^{o}C)
$(C_6H_5)_2Sn(acac)_2$	$CDCl_3$	-53.7 to -12.7
	CH_2Cl_2	-56.8 to 3.0
$(C_6H_5)ClSn(acac)_2$	$CDCl_3$	-42.6 to 58.7
	$CHBr_3$	15.5 to 80.7
$(CH_3)ClSn(acac)_2$	$CDCl_3$	-44.5 to 29.5
$(C_6H_5)_2Ge(acac)_2$	$CDCl_3$-CCl_4	-80.0 to -28.0
$(C_6H_5)ClGe(acac)_2$	$CDCl_3$-CCl_4	-53.9 to 62.2
	$CDCl_3$	-55.0 to 50.2
$(CH_3)ClGe(acac)_2$	$CDCl_3$-CCl_4	-80.7 to 23.1
$(C_6H_5)ClSi(acac)_2$	$CDCl_3$-CCl_4	-78.5 to 33.7
	CH_2Cl_2	-80.0 to 36.2
$(CH_3)ClSi(acac)_2$	$CDCl_3$-CCl_4	-75.6 to 28.0

Average values of these parameters for five spectral scans are summarized in Tables II to IX.* To further process the spectral data it was necessary to determine two additional parameters for each set of data, namely the chemical shift separation in the absence of exchange, $\delta\nu$, and the transverse relaxation time in the absence of exchange, T_2.

The chemical shift separation in the absence of exchange, $\delta\nu$, can be obtained from the very slow exchange limit. The value for $\delta\nu$ is then assumed to be a constant (provided this limit is accessible) throughout the exchange region. Early investigators of restricted rotation of N,N-disubstituted amides often assumed that the $\delta\nu$ in the absence of exchange was indeed a constant. However, this assumption has resulted in serious systematic errors in the activation parameters (68), as $\delta\nu$ often varies with temperature probably owing to a certain degree of molecular association (84). Therefore, an improved technique was used whereby compensation is made for the change of $\delta\nu$ with temperature (85).

A plot is drawn of $\delta\nu$ vs temperature in which the linear portion in the slow exchange region is extrapolated into the intermediate and fast exchange regions.

---

* In these tables, LF means lowfield; HF stands for highfield.

Table II.- Spectral Parameters and Lifetimes for Exchange of Acetylacetonate CH_3 Groups for $(C_6H_5)_2Sn(acac)_2$ in $CDCl_3$.

Temp. °C	R		$\delta\nu_e$, Hz	Linewidths, Hz						$\tau \times 10^2$ sec
				$W_{1/4}$		$W_{1/2}$		$W_{3/4}$		
	LF	HF		LF	HF	LF	HF	LF	HF	
-53.7	2.34	2.43	5.54[a]	-	-	3.18	3.18	1.69	1.69	18.4 ± 1.4[b]
-50.6	2.11	2.08	5.58[a]	-	-	3.83	3.88	1.92	1.92	15.1 ± 1.4
-48.4	1.73	1.78	5.59[a]	-	-	-	-	2.15	2.22	11.8 ± 0.9
-46.8	1.53	1.55	5.43[a]	-	-	-	-	2.60	2.75	9.87 ± 0.79
-43.3	1.18	1.19	4.66[a]	-	-	-	-	-	-	7.38 ± 0.07
-42.4	1.05	1.17	4.46[a]	-	-	-	-	-	-	6.60 ± 0.86
-39.4	-	-	2.53	-	-	-	-	-	-	5.61
-38.0 (T_c)	-		-	[a]		[a]		5.69		5.86
-33.4	-		-	[a]		5.84		3.57		3.90 ± 0.23
-27.6	-		-	6.54		3.85		2.24		2.53 ± 0.09
-22.1	-		-	5.05		2.90		1.66		1.75 ± 0.05
-12.7	-		-	3.55		2.06		1.14		0.99 ± 0.05

[a] Not used to obtain τ. [b] One standard deviation.

Table IIIA.- Spectral Parameters and Lifetimes for Exchange of Acetylacetonate CH_3 Groups for $(C_6H_5)_2Sn(acac)_2$ in CH_2Cl_2 in the Temperature Range -56.8 to -37.4°.

Temp. °C	R		$\delta\nu_e$, Hz	Linewidths, Hz						$\tau \times 10^2$ sec
				$W_{1/4}$		$W_{1/2}$		$W_{3/4}$		
	LF	HF		LF	HF	LF	HF	LF	HF	
-56.8	3.37	3.34	6.11[a]	-	-	2.75	2.40	1.39	1.25	20.3 ± 3.3[b]
-53.8	3.12	3.26	6.32[a]	-	-	3.00	2.68	1.54	1.51	16.0 ± 1.7
-51.7	2.99	2.96	6.31[a]	-	-	2.97	2.65	1.48	1.39	15.7 ± 1.3
-48.8	2.36	2.30	6.42[a]	-	-	3.70	3.60	1.93	1.83	11.3 ± 0.9
-48.4	2.02	1.99	6.40[a]	-	-	4.27	4.29	2.10	1.86	10.4 ± 1.0
-46.8	1.69	1.78	6.33[a]	-	-	-	-	2.83	2.36	8.02 ± 0.81
-45.0	1.82	1.79	6.30[a]	-	-	-	-	2.74	2.27	8.20 ± 0.90
-42.3	1.47	1.51	5.77[a]	-	-	-	-	3.09	2.92	6.94 ± 0.34
-38.6	1.14	-	4.90	-	-	-	-	-	-	5.82 ± 0.77
-37.4 (T_c)	-		-	[a]		[a]		6,27		4.53

[a] Not used to obtain τ. [b] One standard deviation.

Table IIIB.- Spectral Parameters and Lifetimes for Exchange of Acetylacetonate CH_3 Groups for $(C_6H_5)_2Sn(acac)_2$ in CH_2Cl_2 in the Temperature Range -35.1 to 3.0°.

Temp. °C	R LF	R HF	$\delta\nu_e$, Hz	Linewidths, Hz $W_{1/4}$ LF	Linewidths, Hz $W_{1/4}$ HF	Linewidths, Hz $W_{1/2}$ LF	Linewidths, Hz $W_{1/2}$ HF	Linewidths, Hz $W_{3/4}$ LF	Linewidths, Hz $W_{3/4}$ HF	$\tau \times 10^2$ sec
-35.1	-	-	-	[a]		7.70		5.21		3.99 ± 0.35[b]
-30.5	-	-	-	8.73		5.46		3.25		2.84 ± 0.19
-24.8	-	-	-	6.40		3.82		2.13		1.92 ± 0.06
-17.5	-	-	-	5.20		2.87		1.51		1.40 ± 0.14
-9.5	-	-	-	3.83		2.18		1.22		0.99 ± 0.04
-6.0	-	-	-	3.5		1.88		0.95		0.78 ± 0.15
3.0	-	-	-	2.79		1.48		0.74		0.50 ± 0.12

[a] Not used to obtain τ. [b] One standard deviation.

Table IVA.- Spectral Parameters and Lifetimes for Exchange of Acetylacetonate -CH= Protons for $(C_6H_5)ClSn(acac)_2$ in $CDCl_3$ for the Temperature Range -42.6 to 28.5°.

Temp. °C	R LF	R HF	$\delta\nu_e$, Hz	Linewidths, Hz $W_{1/4}$ LF	$W_{1/4}$ HF	$W_{1/2}$ LF	$W_{1/2}$ HF	$W_{3/4}$ LF	$W_{3/4}$ HF	$\tau \times 10^2$ sec
-42.6	-	-	10.89[a]	-	-	-	-	-	-	-
-34.5	-	-	10.57[a]	-	-	-	-	-	-	-
-20.9	-	-	10.52[a]	-	-	-	-	-	-	-
-16.3	-	-	10.44[a]	-	-	-	-	-	-	-
-5.6	-	-	10.30[a]	-	-	-	-	-	-	-
2.0	-	-	10.14[a]	-	-	-	-	-	-	-
17.5	13.78	13.69	10.07[a]	3.35[a]	3.07[a]	-	1.54	-	0.88	24.3 ± 2.3[b]
28.5	4.00	4.03	9.71[a]	-	-	3.19	3.12	1.54	1.69	8.27 ± 0.57

[a] Not used to obtain τ. [b] One standard deviation.

Table IVB.- Spectral Parameters and Lifetimes for Exchange of Acetylacetonate -CH= Protons for $(C_6H_5)ClSn(acac)_2$ in $CDCl_3$ for the Temperature Range 37.3 to 58.7°.

Temp. °C	R LF	R HF	$\delta\nu_e$, Hz	Linewidths, Hz $W_{1/4}$ LF	$W_{1/4}$ HF	$W_{1/2}$ LF	$W_{1/2}$ HF	$W_{3/4}$ LF	$W_{3/4}$ HF	$\tau \times 10^2$ sec
37.3	1.29	1.35	8.31	-	-	-	-	-	-	4.17 ± 0.67[b]
44.2	1.34	1.36	8.22	-	-	-	-	-	-	4.23 ± 0.62
44.4	1.20	1.29	7.01	-	-	-	-	-	-	3.52 ± 0.13
46.0(T_c)	-		-	16.11[a]		11.64		8.64		2.90 ± 0.31
48.5	-		-	15.25[a]		10.42		6.14		2.30 ± 0.26
50.2	-		-	15.04[a]		10.46		7.55		2.46 ± 0.07
58.7	-		-	9.17[a]		5.25		3.16		1.36 ± 0.02

[a] Not used to obtain τ. [b] One standard deviation.

Table VA.- Spectral Parameters and Lifetimes for Exchange of Acetylacetonate -CH= Protons for $(C_6H_5)ClSn(acac)_2$ in $CHBr_3$ for the Temperature Range 15.5 to 50.6°.

Temp. °C	R		$\delta\nu_e$, Hz	Linewidths, Hz						$\tau \times 10^2$ sec
	LF	HF		$W_{1/4}$ LF	$W_{1/4}$ HF	$W_{1/2}$ LF	$W_{1/2}$ HF	$W_{3/4}$ LF	$W_{3/4}$ HF	
15.5	-	-	12.34[a]	-	-	-	-	-	-	-
19.4	-	-	12.35[a]	-	-	-	-	-	-	-
21.6	-	-	12.24[a]	-	-	-	-	-	-	-
23.0	-	-	12.29[a]	-	-	-	-	-	-	-
26.6	9.09	9.78	12.30[a]	4.80[a]	4.39[a]	2.18	2.24	1.11[c]	1.14[c]	16.1 ± 2.2[b]
29.2	5.98	6.42	11.98	5.93[a]	5.40[a]	2.87	2.83	1.46	1.52	10.5 ± 1.1
41.7	2.63	3.00	11.30	-	-	4.94	4.81	2.69	2.58	5.17 ± 0.21
44.9	1.41	1.51	9.39	-	-	-	-	4.93	4.55	3.12 ± 0.07
50.6	1.31	1.28	8.08	-	-	-	-	-	-	2.72 ± 0.12

[a] Not used to obtain τ. [b] One standard deviation. [c] Small error in $W_{3/4}$ leads to large error in τ.

Table VB.- Spectral Parameters and Lifetimes for Exchange of Acetylacetonate -CH= Protons for $(C_6H_5)ClSn(acac)_2$ in $CHBr_3$ for the Temperature Range 52.2 to 80.7°.

Temp. °C	R LF	R HF	$\delta\nu_e$, Hz	Linewidths, Hz $W_{1/4}$ LF	$W_{1/4}$ HF	$W_{1/2}$ LF	$W_{1/2}$ HF	$W_{3/4}$ LF	$W_{3/4}$ HF	$\tau \times 10^2$ sec
52.2	-	-	4.70	-	-	-	-	-	-	2.13
53.1(T_c)	-		-	16.98[a]		12.92		9.45		1.91 ± 0.03[b]
57.7	-		-	14.74[a]		8.90		5.49		1.36 ± 0.00
63.8	-		-	10.24[a]		5.97		3.38		0.95 ± 0.02
66.8	-		-	8.74[a]		4.83		2.81		0.79 ± 0.00
73.4	-		-	6.27[a]		3.58		1.95		0.55 ± 0.03
80.7	-		-	4.84[a]		2.61		1.33		0.35 ± 0.05

[a] Not used to obtain τ. [b] One Standard deviation.

Table VIA.- Spectral Parameters and Lifetimes for Exchange of Acetylacetonate -CH= Protons for $(CH_3)ClSn(acac)_2$ in $CDCl_3$ for the Temperature Range -44.5 to 4.5°.

Temp. °C	R LF	R HF	$\delta\nu_e$, Hz	Linewidths, Hz $W_{1/4}$ LF	$W_{1/4}$ HF	$W_{1/2}$ LF	$W_{1/2}$ HF	$W_{3/4}$ LF	$W_{3/4}$ HF	$\tau \times 10^2$ sec
-44.5	-	-	9.89[a]	-	-	-	-	-	-	-
-37.6	-	-	9.57[a]	-	-	-	-	-	-	-
-29.3	-	-	9.35[a]	-	-	-	-	-	-	-
-25.0	-	-	9.28[a]	-	-	-	-	-	-	-
-20.2	-	-	9.05[a]	-	-	-	-	-	-	-
-15.9	-	-	8.93[a]	-	-	-	-	-	-	-
-8.6	-	-	8.70[a]	-	-	-	-	-	-	-
-0.5	5.29	5.58	8.51[a]	4.76[a]	4.03[a]	2.31	2.10	1.21	1.20	14.6 ± 1.1[b]
4.5	2.98	3.06	8.01[a]	-	-	3.47	3.18	1.86	1.82	8.25 ± 0.36

[a] Not used to obtain τ. [b] One standard deviation.

Table VIB.- Spectral Parameters and Lifetimes for Exchange of Acetylacetonate -CH= Protons for $(CH_3)ClSn(acac)_2$ in $CDCl_3$ for the Temperature Range 7.5 to 29.5°.

Temp. °C	R LF	R HF	$\delta\nu_e$, Hz	Linewidths, Hz $W_{1/4}$ LF	$W_{1/4}$ HF	$W_{1/2}$ LF	$W_{1/2}$ HF	$W_{3/4}$ LF	$W_{3/4}$ HF	$\tau \times 10^2$ sec
7.5	2.00	2.14	7.44	-	-	4.85	4.25	2.55	2.29	6.59 ± 0.54[b]
11.5	1.22	1.29	6.04	-	-	-	-	-	-	4.39 ± 0.18
13.5	1.03	1.06	3.74	-	-	-	-	-	-	3.42 ± 0.07
16.0	-		-	12.59[a]		9.12		6.65		3.12 ± 0.12
21.5	-		-	9.03[a]		5.30		3.06		1.88 ± 0.04
26.5	-		-	6.58[a]		3.75		2.14		1.40 ± 0.02
29.5	-		-	4.74[a]		2.57		1.38		0.86 ± 0.06

T_c = 17.0°

[a] Not used to obtain τ. [b] One standard deviation.

Table VII.- Spectral Parameters and Lifetimes for Exchange of Acetylacetonate -CH= Protons for $(C_6H_5)ClGe(acac)_2$ in $CDCl_3$-CCl_4 Solutions.

Temp. °C	R		$\delta\nu_e$, Hz	Linewidths, Hz						$\tau_c \times 10^2$ sec
				$W_{1/4}$		$W_{1/2}$		$W_{3/4}$		
	LF	HF		LF	HF	LF	HF	LF	HF	
-53.9	-	-	21.64[a]	-	-	-	-	-	-	-
-31.7	-	-	20.92[a]	-	-	-	-	-	-	-
-8.1	-	-	20.55[a]	-	-	-	-	-	-	-
5.6	-	-	20.25[a]	-	-	-	-	-	-	-
13.2	24.58	24.81	20.06[a]	4.34	4.69	2.37	2.55	1.26	1.31	11.5 ± 1.3[b]
20.8	14.57	14.61	19.86[a]	5.48	5.90	3.11	3.37	1.73	1.86	7.39 ± 0.73
30.2	5.12	5.19	18.93	-	-	4.77	5.17	2.58	2.87	4.35 ± 0.23
38.9	1.87	1.89	16.43	-	-	-	-	6.06	6.20	2.17 ± 0.09
41.9	1.13	1.14	11.93	-	-	-	-	-	-	1.51 ± 0.03
44.5(T_c)	-	-	-	-	-	23.25		18.00		1.55 ± 0.21
53.2	-		-	21.17		12.40		7.40		0.82 ± 0.04
62.2	-		-	10.04		6.50		3.80		0.45 ± 0.02

[a] Not used to obtain τ. [b] One standard deviation.

Table VIIIA.- Spectral Parameters and Lifetimes for Exchange of Acetylacetonate -CH= Protons for $(CH_3)ClGe(acac)_2$ in $CDCl_3$-CCl_4 Solutions for the Temperature Range -80.7 to -36.8°.

Temp. °C	R LF	R HF	$\delta\nu_e$, Hz	Linewidths, Hz $W_{1/4}$ LF	$W_{1/4}$ HF	$W_{1/2}$ LF	$W_{1/2}$ HF	$W_{3/4}$ LF	$W_{3/4}$ HF	$\tau \times 10^2$ sec
-80.7	-	-	16.02[a]	-	-	-	-	-	-	-
-78.4	-	-	15.76[a]	-	-	-	-	-	-	-
-76.1	-	-	15.62[a]	-	-	-	-	-	-	-
-73.0	-	-	15.39[a]	-	-	-	-	-	-	-
-70.2	-	-	15.29[a]	-	-	-	-	-	-	-
-61.7	-	-	14.70[a]	-	-	-	-	-	-	-
-53.5	-	-	14.18[a]	-	-	-	-	-	-	-
-46.2	-	-	13.75[a]	-	-	-	-	-	-	-
-36.8	-	-	13.98[a]	-	-	-	-	-	-	-

[a] Not used to obtain τ.

Table VIIIB.- Spectral Parameters and Lifetimes for Exchange of Acetylacetonate -CH= Protons for $(CH_3)ClGe(acac)_2$ in $CDCl_3$-CCl_4 Solutions for the Temperature Range -31.0 to 23.1°.

Temp. °C	R		$\delta\nu_e$, Hz	Linewidths, Hz						$\tau \times 10^2$ sec
				$W_{1/4}$		$W_{1/2}$		$W_{3/4}$		
	LF	HF		LF	HF	LF	HF	LF	HF	
-31.0	3.54	3.43	12.83[a]	-	-	4.02	4.23	2.14	2.26	6.03 ± 0.32[b]
-23.0	1.96	1.93	11.45[a]	-	-	-	-	3.48	3.55	3.89 ± 0.07
-18.0	1.20	1.20	9.05	-	-	-	-	-	-	2.94 ± 0.26
-13.3 (T_c)	-	-	-	19.61[a]		15.02[a]		11.36		2.57
-5.5	-		-	15.76		9.67		5.92		1.85 ± 0.26
3.4	-		-	10.84		6.22		3.56		1.32 ± 0.07
13.6	-		-	6.53		3.65		2.08		0.86 ± 0.03
23.1	-		-	4.63		2.39		1.32		0.56 ± 0.07

[a] Not used to obtain τ. [b] One standard deviation.

Table IX.- Results from Computer Fitting of NMR Spectra of $(C_6H_5)ClSi(acac)_2$ in $CDCl_3$-CCl_4 Solutions.

Temperature °C	$\delta\nu_e$ Hz	$\tau_a \times 10^3$ sec	$\tau_b \times 10^3$ sec	k (= 1/2τ)[a] sec^{-1}
-78.5	34.85	-	-	-
-74.1	34.80	-	-	-
-69.6	33.75	35.7 ± 1.0[b]	33.9 ± 0.9[b]	29
-64.9	32.72	28.7 ± 0.9	26.9 ± 0.8	36
-61.3	34.71	19.8 ± 0.6	18.8 ± 0.6	52
-54.7(T_c)	34.40	12.7 ± 0.1	12.1 ± 0.1	81
-49.3	34.05	9.5 ± 0.2	7.9 ± 0.2	116
-33.7	33.95	-	-	-

[a] $\tau = \frac{\tau_a \tau_b}{\tau_a + \tau_b}$

[b] Standard error.

Such plots and extrapolations for the compounds of interest are presented in Figures 1 and 2. It is apparent that most of the complexes exhibit a linear relationship in the slow exchange region except for some curvature in the case of $(C_6H_5)_2Sn(acac)_2$, where there is some regression in the low temperature region believed to be a viscosity effect. In the case of $(C_6H_5)ClSi(acac)_2$, where there is no linear portion, an alternative computer digitization technique was utilized to process the nmr spectra and is described later.

Once the extent of the linearity below coalescence was established for each complex, data points in the linear portion were submitted to a single linear regression analysis using the program SLREG (see Appendix) on a Hewlett-Packard 2114A computer. The resulting slope and intercept were then used to calculate a corrected $\delta\nu$ for each temperature including those at and above coalescence.

For each temperature it was also necessary to determine the transverse relaxation time, $T_{2a} = T_{2b}$, in the absence of exchange. These were obtained from the relationship: $1/[\pi \times$ (linewidth in the absence of exchange)] (86). The linewidth in the absence of exchange can be obtained from the low and high temperature limits of exchange (vide infra). Ideally, these are equivalent, and a constant T_2 is used throughout the exchange region, provided T_2 is

Figure 1.- Temperature dependence of the chemical shift separation, $\delta\nu$, for the indicated organotin complexes.

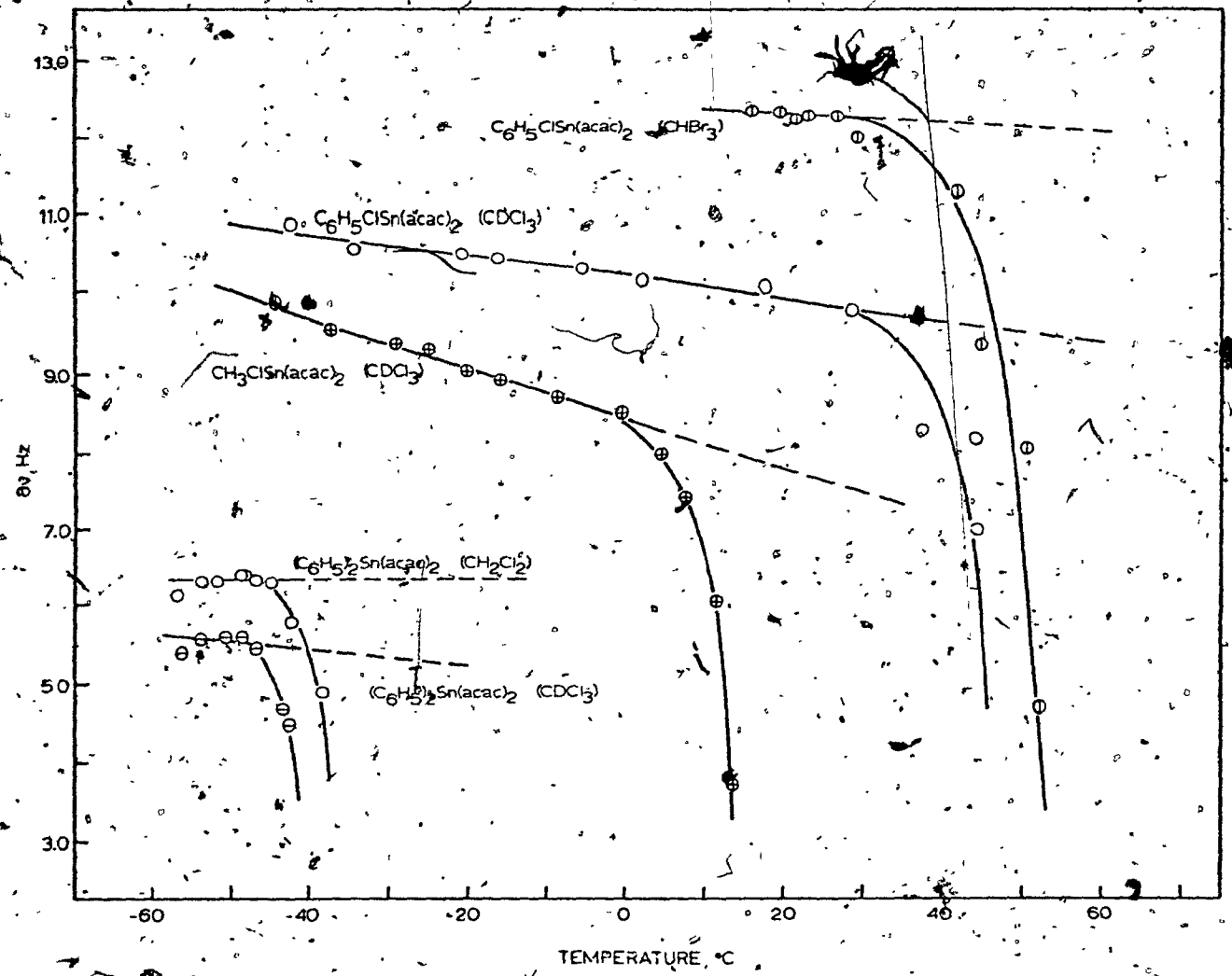
13.0
11.0
9.0
7.0
5.0
3.0
θ, Hz
$C_6H_5ClSn(acac)_2$ ($CHBr_3$)
$C_6H_5ClSn(acac)_2$ ($CDCl_3$)
$CH_3ClSn(acac)_2$ ($CDCl_3$)
$(C_6H_5)_2Sn(acac)_2$ (CH_2Cl_2)
$(C_6H_5)_2Sn(acac)_2$ ($CDCl_3$)
-60
-40
-20
0
20
40
60
TEMPERATURE, °C

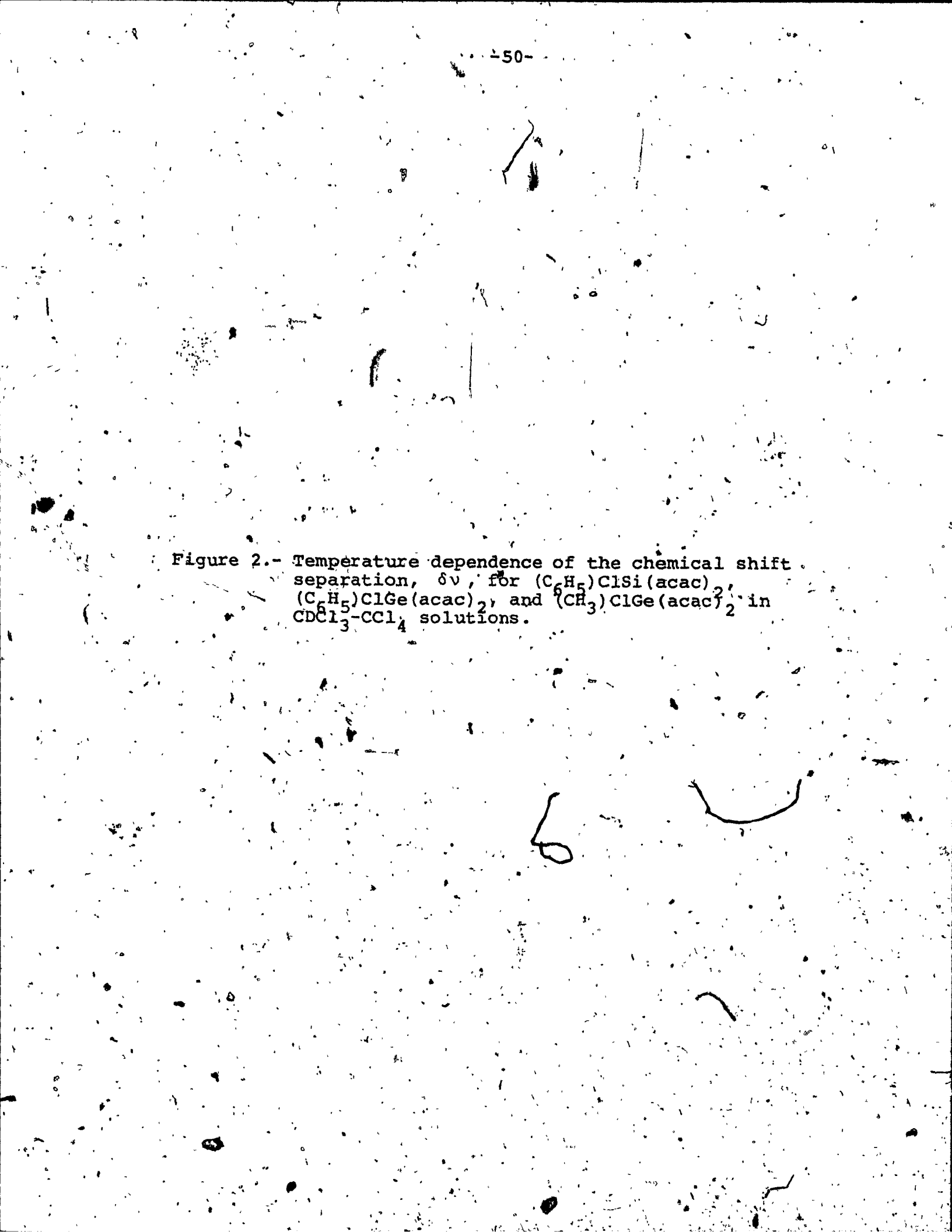

Figure 2.- Temperature dependence of the chemical shift separation, $\delta\nu$, for $(C_6H_5)ClSi(acac)_2$, $(C_6H_5)ClGe(acac)_2$, and $(CH_3)ClGe(acac)_2$ in $CDCl_3$-CCl_4 solutions.

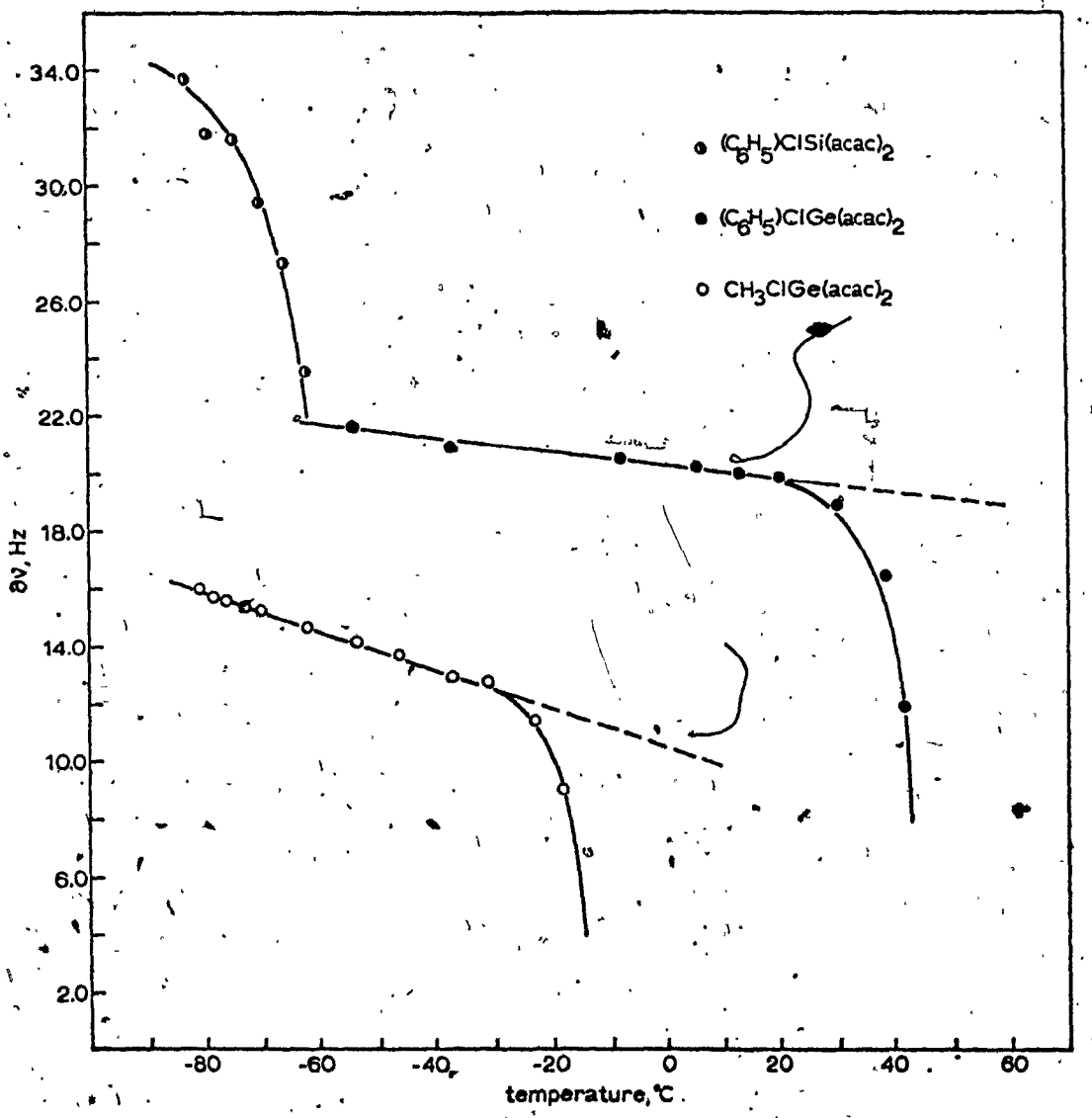
34.0
30.0
26.0
22.0
18.0
14.0
10.0
6.0
2.0
δν, Hz
-80
-60
-40
-20
0
20
40
60
temperature, °C
(C6H5)ClSi(acac)2
(C6H5)ClGe(acac)2
CH3ClGe(acac)2

independent of temperature. However, in the cases presented herein T_2 was determined to be temperature dependent (vide infra) so that another technique was necessary.

Following the method established by Fay and Lowry (87) the transverse relaxation times, $T_{2a} = T_{2b}$, were estimated from the linewidths of the acetylacetonate methyl resonance of $(CH_3)_2Sn(acac)_2$ in the appropriate solvents for $(C_6H_5)_2Sn(acac)_2$, $(CH_3)ClSn(acac)_2$, $(C_6H_5)ClSn(acac)_2$, $(C_6H_5)ClGe(acac)_2$, $(CH_3)ClGe(acac)_2$, and $(C_6H_5)ClSi(acac)_2$. The low solubility of the dimethyltin complex in bromoform precluded attempts to obtain reasonable -CH= linewidths. Appropriate values of the linewidths in the absence of exchange at the required temperature were read directly from the plots of Figure 3. The experimental data for the dimethyltin complex in the appropriate solvent are tabulated in Tables X to XII.

The parameters, $\delta\nu$, the chemical shift separation in the absence of exchange; T_2, the transverse relaxation time in the absence of exchange; and a value for the populations at both sites, $P_A = P_B = 0.5$, subsequently served as input parameters for the program NICKA (see Appendix) which was adapted for the Sir George Williams University CDC Cyber 70-72 computer. This is a Fortran program written (88,89) to compute a normalized lineshape over the frequency range of interest for a given set of

Table X.- Linewidths at One-Half of Maximum Height of Acetylacetonate Methyl and Ring Proton Resonances for $(CH_3)_2Sn(acac)_2$ in $CDCl_3$ Solutions.

Temperature °C	CH_3 Hz	Temperature °C	-CH= Hz
-48.9	1.66 ± 0.05[a]	-49.0	1.41 ± 0.05[a]
-40.6	1.55 ± 0.04	-39.2	1.32 ± 0.04
-25.6	1.33 ± 0.02	-29.4	1.26 ± 0.05
-17.4	1.27 ± 0.05	-15.9	1.16 ± 0.05
-8.6	1.16 ± 0.03	-2.8	1.01 ± 0.02
6.0	1.04 ± 0.04	13.4	0.91 ± 0.01
16.0	0.97 ± 0.04	30.0	0.81 ± 0.04
33.0	0.97 ± 0.03	44.9	0.92 ± 0.04
43.4	0.91 ± 0.02		

[a] One standard deviation

Table XI.- Linewidths at One-Half of Maximum Height of Acetylacetonate Methyl Resonances in Bromoform and Dichloromethane Solutions.

Temperature °C	$CHBr_3$ CH_3, Hz	Temperature °C	CH_2Cl_2 CH_3, Hz
16.5	1.39 ± 0.04[a]	-59.4	1.51 ± 0.08[a]
20.0	1.39 ± 0.05	-51.4	1.36 ± 0.03
25.0	1.28 ± 0.02	-42.8	1.31 ± 0.06
30.0	1.19 ± 0.05	-34.8	1.16 ± 0.03
43.4	1.03 ± 0.04	-25.6	0.98 ± 0.01
51.9	1.07 ± 0.02	-16.0	0.91 ± 0.04
59.2	1.00 ± 0.04	-9.7	0.85 ± 0.02
69.4	0.92 ± 0.03		
74.9	0.87 ± 0.03		
85.4	0.88 ± 0.02		

[a] One standard deviation.

Table XII.- Linewidths at One-Half of Maximum Height of Acetylacetonate Methyl and Ring Proton Resonances for $(CH_3)_2Sn(acac)_2$ in Deuteriochloroform-Carbon Tetrachloride Solutions.

Temperature °C	CH_3 Hz	-CH= Hz
-57.5	1.90 ± 0.00[a]	1.37 ± 0.03[a]
-44.0	1.50 ± 0.03	1.20 ± 0.01
-32.9	1.29 ± 0.04	1.22 ± 0.02
-20.8	-	1.06 ± 0.04
-19.7	1.16 ± 0.05	-
-7.5	-	1.10 ± 0.01
-6.7	1.11 ± 0.02	1.06 ± 0.03
2.2	1.09 ± 0.03	1.02 ± 0.05
11.8	1.04 ± 0.06	0.99 ± 0.06
26.1	0.97 ± 0.03	0.89 ± 0.04
45.9	0.96 ± 0.02	0.93 ± 0.06

[a] One standard deviation.

Figure 3.- Temperature dependence of the linewidths at one-half of maximum height for acetylacetonate methyl and ring proton resonances of $(CH_3)_2Sn(acac)_2$ in various solvents; $T_2 = 1/(\pi \times W_{1/2})$.

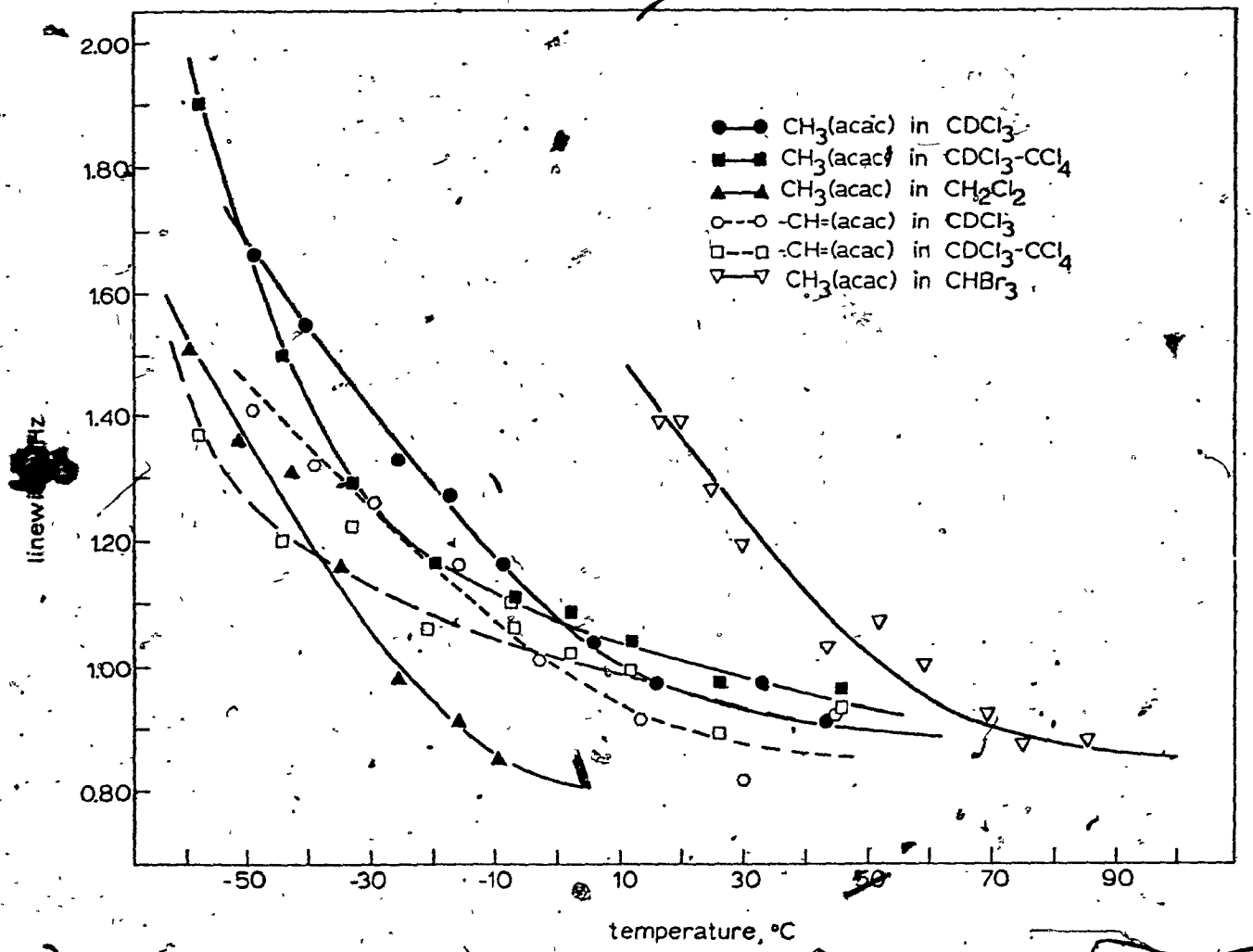
2.00
1.80
1.60
1.40
1.20
1.00
0.80
linewidth, Hz
-50
-30
-10
10
30
50
70
90
temperature, °C
CH3(acac) in CDCl3
CH3(acac) in CDCl3-CCl4
CH3(acac) in CH2Cl2
-CH=(acac) in CDCl3
-CH=(acac) in CDCl3-CCl4
CH3(acac) in CHBr3

input parameters. For the cases here the calculated spectra were computed at intervals of 0.005 Hz for a range of about 240 values of τ. A typical portion of the output of this program is exhibited in Table XIII. The resulting values of the calculated spectrum were subsequently compared to the experimentally determined data of the spectrum. This was accomplished by taking each experimental value and finding its position in the calculated series of values, and finally by interpolating the corresponding mean lifetime. For example, given the following experimentally determined values for a spectrum of a complex below coalescence; $B = 18.467$ ($B = \pi\delta\nu$), $T_{2a} = T_{2b} = 0.343$, $P_A = P_B = 0.5$, $R_A = R_B = 1.34$, $\delta\nu = 5.88$, $W_{1/4A} = W_{1/4B} = 12.93$, $W_{1/2A} = W_{1/2B} = 10.47$, $W_{3/4A} = W_{3/4B} = 3.07$, the appropriate excerpt from the printout from program NICKA is presented in Table XIII. The position of the experimental values were determined as indicated in the Table and the corresponding lifetimes were interpolated. $\delta\nu$ values were given a weighted factor of 2. The ten lifetimes were then averaged to produce a mean lifetime (τ) which was used in subsequent calculations. There were, of course, various limitations to this technique. In the case of $(C_6H_5)_2Sn(acac)_2$, $(C_6H_5)ClSn(acac)_2$ and $(CH_3)ClSn(acac)_2$ complexes, values of $W_{1/4}$ were not compared because of Sn-Hγ spin-spin coupling (90) which may broaden the lineshape in this region. For the other compounds, a specific $W_{1/4}$ may have been rejected due to poor homogeneity or to

Table XIII.- A Sample Computer Printout of a Calculated Spectrum Produced by Program NICKA and an Appropriate Comparison to Experimental Values to Obtain a τ Value.

B = 18.467 T2A = .343 T2B = .343 PA = .500 PB = .500

TAU	RATIO	FULL SEPARATION	WIDTH AT ONE-FOURTH	WIDTH AT ONE-HALF	WIDTH AT THREE-FOURTHS
.1000E-01	0.000	0.000	5.626	3.275	1.896
.1200E-01	0.000	0.000	6.512	3.824	2.221
.1400E-01	0.000	0.000	7.410	4.415	2.580
.1600E-01	0.000	0.000	8.295	5.053	2.985
.1800E-01	0.000	0.000	9.136	5.732	3.446
.2000E-01	0.000	0.000	9.905	6.438	3.978
.2200E-01	0.000	0.000	10.589	7.146	4.589
.2400E-01	0.000	0.000	11.184	7.827	5.271
.2600E-01	0.000	0.000	11.696	8.458	5.994
.2800E-01	0.000	0.000	12.135	9.023	6.710
.3000E-01	1.006	2.480	12.486	9.493	7.337
.3200E-01	1.030	3.700	12.711	9.824	7.789
.3400E-01	1.067	4.460	12.852	10.059	8.124
.3600E-01	1.113	5.020	12.936	10.229	8.378
.3800E-01	1.165	5.440	12.981	10.353	8.575
.4000E-01	1.223	5.780 ← (c)(d) 5.88	12.999	10.443 ← (g)(h) 10.49	8.731
.4200E-01	1.285	6.050	12.997	10.509	8.855
.4400E-01	1.350 ← (a)(b) 1.37	6.280	12.982	10.556	3.999
.4600E-01	1.418	6.480 (e)(f) → 12.93	12.957	10.589	3.472
.4800E-01	1.489	6.640	12.924	10.612 (i)(j) → 3.07	3.183
.5000E-01	1.563	6.780	12.887	10.626	2.974
.5200E-01	1.638	6.910	12.847	10.633	2.808
.5400E-01	1.716	7.020	12.803	10.635	2.671
.5600E-01	1.795	7.120	12.759	10.633	2.554

τ x 10²	
(a)	4.46
(b)	4.46
(c)	4.07
(d)	4.07
(e)	4.76
(f)	4.76
(g)	4.14
(h)	4.14
(i)	4.91
(j)	4.91
Average	4.47

asymmetry of the peak. In general, $W_{1/2}$ and $W_{3/4}$ were used except in extreme circumstances where excessive noise persisted. The ratios of intensity of maximum peak intensity to minimum central intensity $(\nu_A \pm \nu_B)/2$, were rejected in various comparisons owing to the fact that this parameter leads to large errors in τ when the central valley was too close to the baseline, such as in the case of $(C_6H_5)ClSn(acac)_2$ where an excessively noisy baseline made it difficult to obtain accurate ratios. In addition, values of $\delta\nu_e$ which fell on or too close to the least squares line plots (Figures 1 and 2) of $\delta\nu$ vs temperature were not used as they yielded anomalous values of τ.

After all the τ values had been extracted for each temperature from the digital output, they were submitted to program TAB (see Appendix) on a H-P 2114A computer. This program calculates the τ_A values by multiplying the average τ by a factor of two ($\tau_A = 2\tau$), produces the mean, standard and percentage deviations, the rate constant k, ln k, Log k and their appropriate mean, standard and percentage deviations and the reciprocal of the temperature in the form of $1/T \times 10^3$. These values were then presented in a manner ready for plotting. The calculated τ_A values for the complexes of interest are summarized in Tables II to VIII. The Arrhenius plots of Log k vs $1/T$ were then drawn. The resulting linear plots are presented in Figures 13 to 15 (see Section III).

In general, nmr studies were carried out at several temperatures above and below coalescence; lifetimes were calculated for all temperatures. In the particular case of $(CH_3)ClSn(acac)_2$, data points were collected between -44.5° and 29.5° ($T_c = 17.0^{\circ}$) and the appropriate data plotted in Figure 11. It is evident from the Figure that all the data points do not fall on the straight line, suggesting that data points too far removed from the coalescence temperature should be rejected. This is not unreasonable since lineshape parameters at the "anomalous" temperatures are not sensitive enough for changes in the rate of exchange. Similar procedures were used in the case of the other complexes investigated here.

After the above operation, lifetimes τ_A were submitted to program ACTP (76,91) (see Appendix) on the Sir George Williams University CDC Cyber 70-72 computer. This program performed a least squares analysis and subsequently calculated the activation parameters, E_{act}, $\Delta H^{\ddagger}$, $\Delta G^{\ddagger}$, $\Delta S^{\ddagger}$, and the random errors at the 95% probability limits.

In the case of $(C_6H_5)ClSi(acac)_2$ where there was no linear portion in the plot of $\delta\nu$ vs Temperature (Figure 2) it was not possible to use program NICKA to compare calculated and experimental values of lineshape parameters as described above. An alternative method was utilized in which experimental spectra were first digitized

on a point by point basis and then internally computer-fitted to obtain τ_a and τ_b at each temperature.

The initial requirement was to convert the nmr spectra to digital form. This was accomplished with the use of a Hewlett-Packard 2114A Computer, an Analog to Digital converter, a Moseley Autograph Model 7001AM X-Y Recorder, a Hewlett-Packard G-2B Null Detector, and a Hewlett-Packard F-3B Line Follower.

The function of the F-3B Line Follower is to produce analog electrical signals that represent graphical curves (9). The unit includes a control box and an optical pickup head which replaces the pen of the X-Y recorder. In order for it to be traced the spectrum is placed on the recorder with the baseline parallel to the recorder edge. The pick up head consists of a light and two photo-diodes in front of which is a semi-cylindrical lens through which the light is focused. The light illuminates the paper and is in turn reflected through to the two photo-diodes. The output of these diodes are within a balanced electrical circuit. If the illumination reaching the two diodes is equal there is a null condition, that is when the pickup head is directly on the spectral curve. When there is unequal illumination that is when the pickup head is off the curve, an error voltage is produced. This causes the servo system of the recorder to alter the tracking of the optical head until a null condition is again attained which

in doing so is actually placing the head over the curve. The movement of the head produces an analog electrical signal which is fed to an analog to digital converter; the error voltages to the servo system are not detected as they belong to a separate circuit.

The data from the analog to digital converter is recorded as a series of points of a X-Y plot (intensity versus frequency (in Hz)). The data are recorded on punched paper tape. The operation is coordinated by the Hewlett-Packard 2114A Computer using program LINDI (76,91).

The next step involves transfer of the digitized data from paper tape to magnetic tape. The data were not initially put directly on magnetic tape for two reasons; 1) The desire for a hardcopy of the digitization and, 2) memory restrictions within the Hewlett-Packard 2114A Computer. The transfer was managed by program TAPGH (76,91) using the H-P 2114A Computer, a H-P 2737A Punched Paper Tape Reader and a H-P 2020 Digital Tape Unit. The computer-fitting program NLINGH requires initial trial values of τ_a, the lifetime of a nucleus on site a; τ_b, the lifetime on site b; the chemical shift, with respect to some arbitrary zero, of the nucleus at site a and that of the nucleus at site b; the linewidth in the absence of exchange; and finally a scaling factor (given the value of 1500). The initial guesses of these values are also incorporated on the magnetic tape by program TAPGH, although the option

exists of keeping any combination of these variables constant for any spectrum. The linewidths at half-height of the acetylacetonate methyl and methylene resonances of $(CH_3)_2Sn(acac)_2$ were used as the standard for values of the linewidth in the absence of exchange at each temperature (Figure 3, Tables X-XII). All the other parameters in program TAPGH and NLINGH were, unless otherwise noted, allowed to vary.

The data prepared on magnetic tape by program TAPGH were then submitted to curve fitting. This was accomplished with program NLINGH (76,91) using the CDC Cyber 70-72 computer. The program looks for the best combination of the variable parameters such that the corresponding lineshape plot deviates by the sum of least squares of its points from that of the experimental plot. The calculation involves an iterative process whereby the computer uses the initial values of the variables to produce a spectrum which is then internally matched to the experimental spectrum. If the computer determines this to be a poor match it will select a new set of values depending on the initial limits and repeats the process. A printed copy of the calculated spectrum and the superimposed experimental spectrum is produced at each step of the iteration. As the program progresses two conditions can occur; If the initial values of τ_a and τ_b were good "guesses" then the computer will find what it considers a good match and continues to the next calculation (this may still be a bad fit) or if

the τ values were "far off" then the iteration limit will most probably be exceeded and the program terminated. When there is an unsatisfactory fit it is necessary to repeat the procedure and to reenter new initial "guesses" until an acceptable fit is obtained.

Some problems did occur when using the program to fit spectra where only one resonance line exists. In these cases the computer fit of experimental and calculated spectra were generally good; however, the τ_a and τ_b values from the printout may have varied by a factor as high as 100, even though the population in the two sites is experimentally equal. In addition the difference in the chemical shifts of sites a and b deviated markedly from the averaged difference obtained from computer fit of spectra below coalescence. To compensate for this problem, the chemical shifts of sites a and b were kept fixed in TAPGH and NLINGH for spectra above coalescence such that the difference, $\delta\nu$, was equal to the averaged $\delta\nu$ obtained from below coalescence spectral fits. Results of the computer fitting of experimental nmr spectra for $(C_6H_5)ClSi(acac)_2$ in $CDCl_3$-CCl_4 are summarized in Table IX.

5. Check of the Order of Kinetics of Configurational Rearrangements

The order of the kinetics of configurational rearrangements in the compounds of interest was checked

by accessing the mean residence times of solutions of either four or five different concentrations: for $(C_6H_5)_2Sn(acac)_2$ in $CDCl_3$, 0.04 to 0.12 M; $(CH_3)ClSn(acac)_2$ in $CDCl_3$, 0.16 to 0.52 M; $(CH_3)ClGe(acac)_2$ in $CDCl_3$-CCl_4, 0.27 to 0.64 M; and $(C_6H_5)ClGe(acac)_2$ in $CDCl_3$-CCl_4, 0.22 to 0.48 M; at a temperature below and above coalescence. In the case of $(C_6H_5)ClSn(acac)_2$ in $CHBr_3$ two concentrations were used, 0.2414 and 0.3808 M, at several temperatures in the range 23 to 72°. The order of the kinetics for $(C_6H_5)ClSi(acac)_2$ in $CDCl_3$-CCl_4 was checked at five concentrations in the range 0.09 to 0.31 M at only one temperature. In all cases, attempts were made to keep the highest concentration at least a factor of two greater than that of the lowest concentration. This procedure was used for the purpose of exaggerating any effects of a process that may be other than first order and possibly dependent upon concentration. For a more detailed discussion of the check of the order of kinetics of configurational rearrangements see Section III.

III. RESULTS AND DISCUSSION

A. Stereochemistry and Bonding

1. Tin Complexes

There is no longer any doubt that the stereochemistry of $(CH_3)_2Sn(acac)_2$ in the solid state is trans (35). Unfortunately, the structure in solution is still open to question. The large value of the dipole moment (static) of 2.95 D for $(CH_3)_2Sn(acac)_2$ was suggested (41) as describing a structure basically of the cis type in which the C-Sn-C bond angle may have a value in the 90-110° range. Raman studies (38) in solution and in the solid state, however, rule out a cis structure in solution, and a trans → cis isomerization upon passing from the solid state to solution. The observed moment (38) may arise entirely from atomic polarization in which the C-C-C moieties of the two acetylacetonate rings undergo dynamic "flapping" to give a cisoid arrangement of the rings about the SnO_4 plane in the overall trans molecular structure of the complex. Yet dielectric loss measurements (42) indicate that although the atomic polarization contribution to the dipole moment is high (115 cm^3) there is a significant contribution from the orientation polarization (63 cm^3), with implications that the molecule is definitely polar and cis in solution. A distorted cis (or trans) structure, where 180° > C-Sn-C angle > 90°, as well as the existence of cis-trans equilibria are not precluded by

polarization and dielectric loss measurements. Regularities observed in μ static would indicate (42) that the trans form is either absent or always present in the same proportion along with the cis form. Such a possibility appears to be ruled out by the nearly identical values (38) of the polarizability tensor for the symmetric SnC_2 stretching vibration at 510 cm^{-1} in the solution and solid state Raman spectrum of the dimethyltin complex.

In the case of compounds of the type $X_2M(acac)_2$ ($X = CH_3$ or C_6H_5; and M = Sn, Ge or Si) which are monomeric and six-coordinate one might expect to observe two possible nmr spectra. If the spectrum contains two peaks, one in the acetylacetonate-methyl region and one in the acetylacetonate ring proton region it may be presumed that the R group substituents are equivalent, indicating D_2h symmetry or a trans structure such as is presented in structure II (Figure 4A). However, should two acac-CH_3 resonances be observed in the methyl region and a single resonance in the acetylacetonate ring proton region be evident then it may be presumed that the R group substituents are nonequivalent and consequently the complexes assume a cis configuration having C_2 symmetry, structure I (Figure 4A). This observation of course, depends on the fact that the chemical shifts are sufficiently large in order to separate the two signals. Should there be configurational rearrangements in the chelate rings, the dynamic process may time-average the environments of the two sites of the cis isomer (Figure 4A, I) such that the nmr spectrum

Figure 4A.- Structural configurations of complexes of the type $XYM(acac)_2$ (see text).

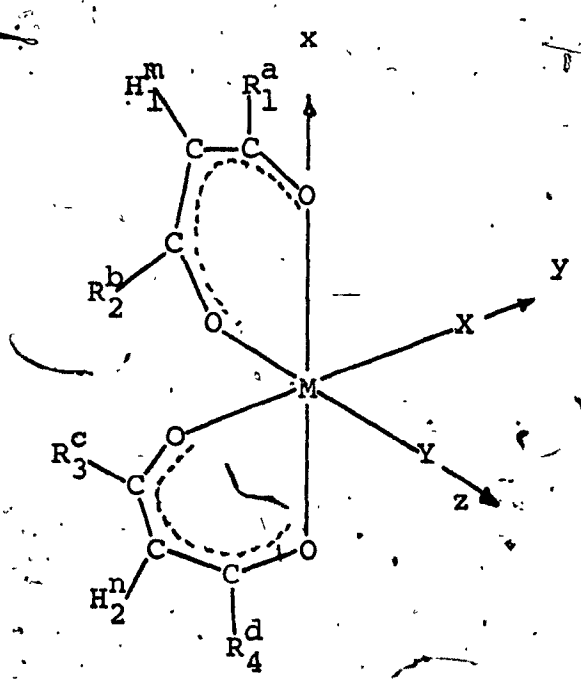

CIS

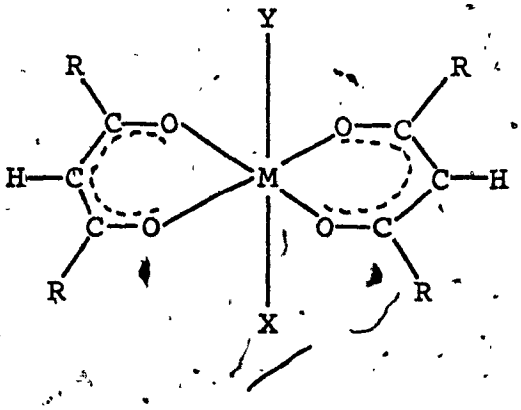

TRANS

WHEN

I. $A(C_2)$ (2R, 1 ring H)	X = Y	II. D_{2h} (1R, 1 ring H)
III. $A(C_1)$ (4R, 2 ring H)	X ≠ Y	IV. C_{2v} (1R, 1 ring H)

of the cis complex qualitatively resembles that of the trans complex.

In the case of the cis isomer there exist two possible configurations: a Δ isomer and a Λ isomer. These isomers can be defined as follows; the two ligating atoms of a chelate ring define a line. Two such lines for the pair of chelate rings define a helix. One line is the axis of the helix and the other is the tangent of the helix at the common normal for the skew lines. The tangent describes a right-handed (Δ) or a left-handed (Λ) helix with respect to the axis and thereby defines the configuration, (107). This is illustrated in Figure 4B.

Our attempts at determining the stereochemical nature of $(CH_3)_2Sn(acac)_2$ in solution using the variable-temperature nmr technique were unsuccessful. Only a single, relatively sharp methyl proton resonance ($W_{1/2}$ = 3.13 Hz at -77°; 0.97 Hz at 26°; in $CDCl_3$-CCl_4 solutions), a single acetylacetonate ring proton signal, and a single Sn-CH_3 methyl resonance were observed. These observations are consistent with (a) the dimethyltin complex having the trans structure in solution, (b) the complex being cis in solution, but only a time-averaged methyl resonance being observed because of a rapid intra- or intermolecular exchange process (1), or (c) both cis and trans forms existing in some proportion but with degenerate chemical

Figure 4B.- Explanation of Δ and Λ isomers:
(i) and (ii); Two skew lines AA and BB which are not orthogonal define a helical system. In the figure, AA is taken as the axis of a cylinder whose radius is determined by the common normal NN of the two skew lines. The line BB is a tangent to the above cylinder at its crossing point with NN and defines a helix upon this cylinder by being the tangent to it at this crossing point. (i) and (ii) illustrate a right- and left-handed helix. (iii) and (iv); These figures show a pair of nonorthogonal skew lines in projection upon a plane parallel to both lines. The fully drawn line BB is above the plane of the paper, the dotted line AA below this plane. (iii) corresponds to (i) above and defines a right-handed helix. (iv) corresponds to (ii) above and defines a left-handed helix. (v) and (vi) show a bis-bidentate complex redrawn so as to become associated with the above figures and thus become designated as Δ and Λ.

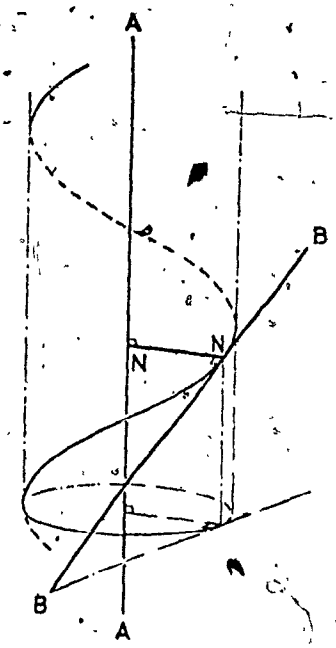

(i) Δ

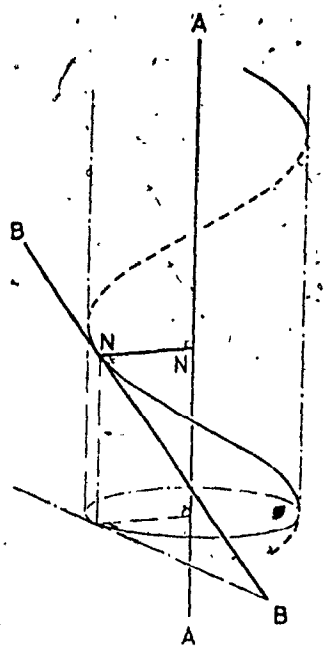

(ii) Λ

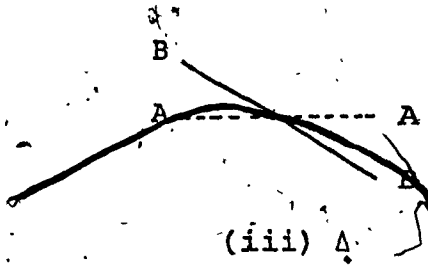

(iii) Δ

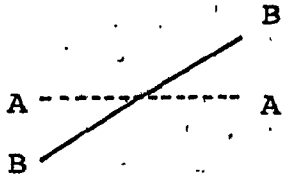

(iv) Λ

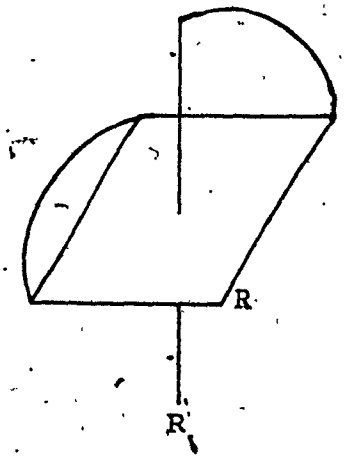

(v) Δ

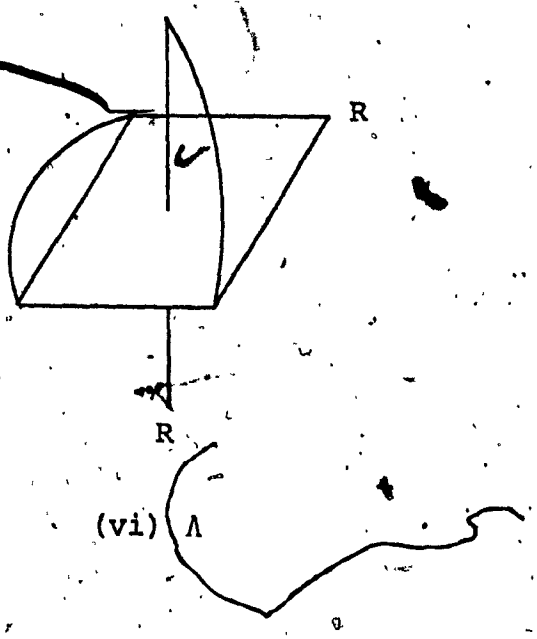

(vi) Λ

shifts. It is, indeed, difficult to determine which process is occurring even with the voluminous evidence available.

The structure of $(C_6H_5)_2Sn(acac)_2$ in the solid state has been shown to be cis (33,39); however, the structure in solution has been the subject of some controversy. Room temperature nmr spectra (12), dipole moment studies (13) and vibrational spectral results (13) suggest a trans structure. On the other hand, more recently, detailed dipole moment studies (41), atomic polarization measurements (42) and dielectric relaxation studies (44) support the cis configuration in solution although a mixture of cis and trans isomers was not precluded. We have conducted our own variable temperature nmr studies and have obtained more conclusive results (Figure 5). The room temperature spectrum of $(C_6H_5)_2Sn(acac)_2$ in $CDCl_3$ reveals a single, sharp line at $\delta = 2.0$ (the acetylacetonate-CH_3 protons), a sharp line, six times less intense, at $\delta = 5.4$ (the acetylacetonate ring proton resonance), and a complex multiplet at δ = 7.1-7.7 ppm (the phenyl proton). In the low temperature region, the spectra reveal a single, sharp acetylacetonate ring proton resonance, an acetylacetonate methyl doublet with components of equal intensity, and a broadened phenyl group complex multiplet. At intermediate temperatures, the acetylacetonate ring proton resonance remains sharp, whilst the two methyl resonances broaden and merge to a single, broad line (ca. -42° Varian) which then sharpens with further increase in temperature. This

Figure 5.- Nmr spectra for the acetylacetonate methyl region as a function of temperature for cis-$(C_6H_5)_2Sn(acac)_2$ in deuteriochloroform. Temperatures shown are based on the Varian graph.

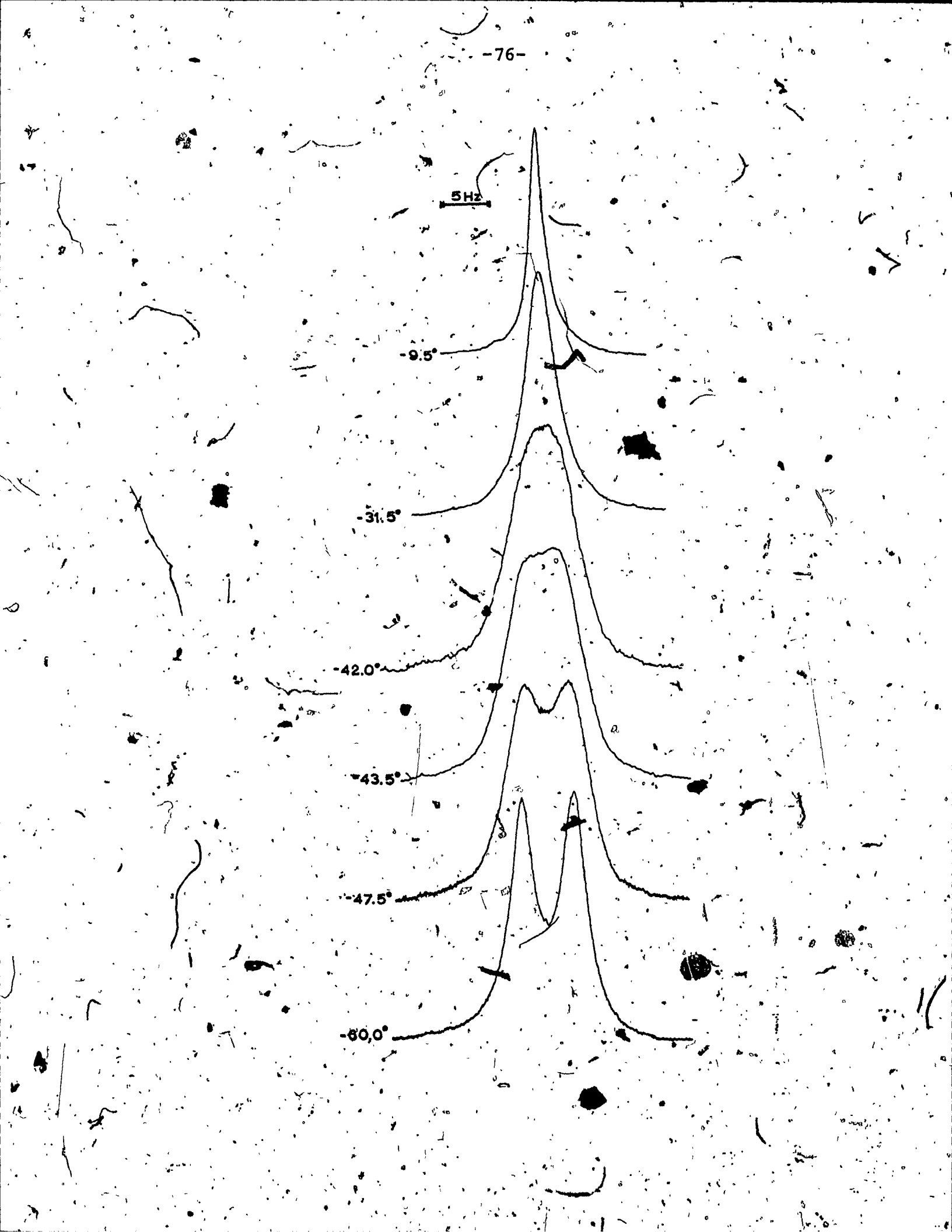
5Hz
-9.5°
-31.5°
-42.0°
-43.5°
-47.5°
-60.0°

process represents the classical coalescence behavior of two nonequivalent nuclei rapidly exchanging between two sites (94). In the low temperature region, the spectra demonstrate that $(C_6H_5)_2Sn(acac)_2$ adopts the cis structure (C_2 symmetry); the trans isomer would have yielded only one methyl resonance. Coalescence of the two methyl signals is attributed to a rate process which rapidly exchanges the methyl protons between the two nonequivalent sites of the cis isomer (87).

Variable-temperature nmr spectra of methylchloro- and phenylchlorotin acetylacetonate complexes are presented in Figures 6 and 7, respectively. The geometries and expected signal multiplicities for these two complexes are shown in Figure 4A as structures III and IV. Observation of four acac-CH_3 resonances in the variable-temperature spectra is consistent with these complexes existing in solution in the cis configuration, at least at low temperatures. In an earlier report (28), the methyl quartet and ring proton doublet in the spectrum of $(C_6H_5)XSn(acac)_2$ (X = Cl or Br) were incorrectly attributed to a trans configuration. Observations analogous to those reported here for $(CH_3)ClSn(acac)_2$ and shown explicitly in Figure 6 were interpreted (45) in terms of (a) a cis configuration at -30°, (b) a trans structure at 20°, and (c) in the intermediate temperature range 0 to 15°, to a cis $\rightleftharpoons$ trans isomerization reaction (the -CH- proton region consisted of

Figure 6.- Nmr spectra for the acetylacetonate ring proton region and methyl region as a function of temperature for cis-$(CH_3)ClSn(acac)_2$ in deuteriochloroform. Dashed lines refer to resonances attributed to the trans isomer (see text).

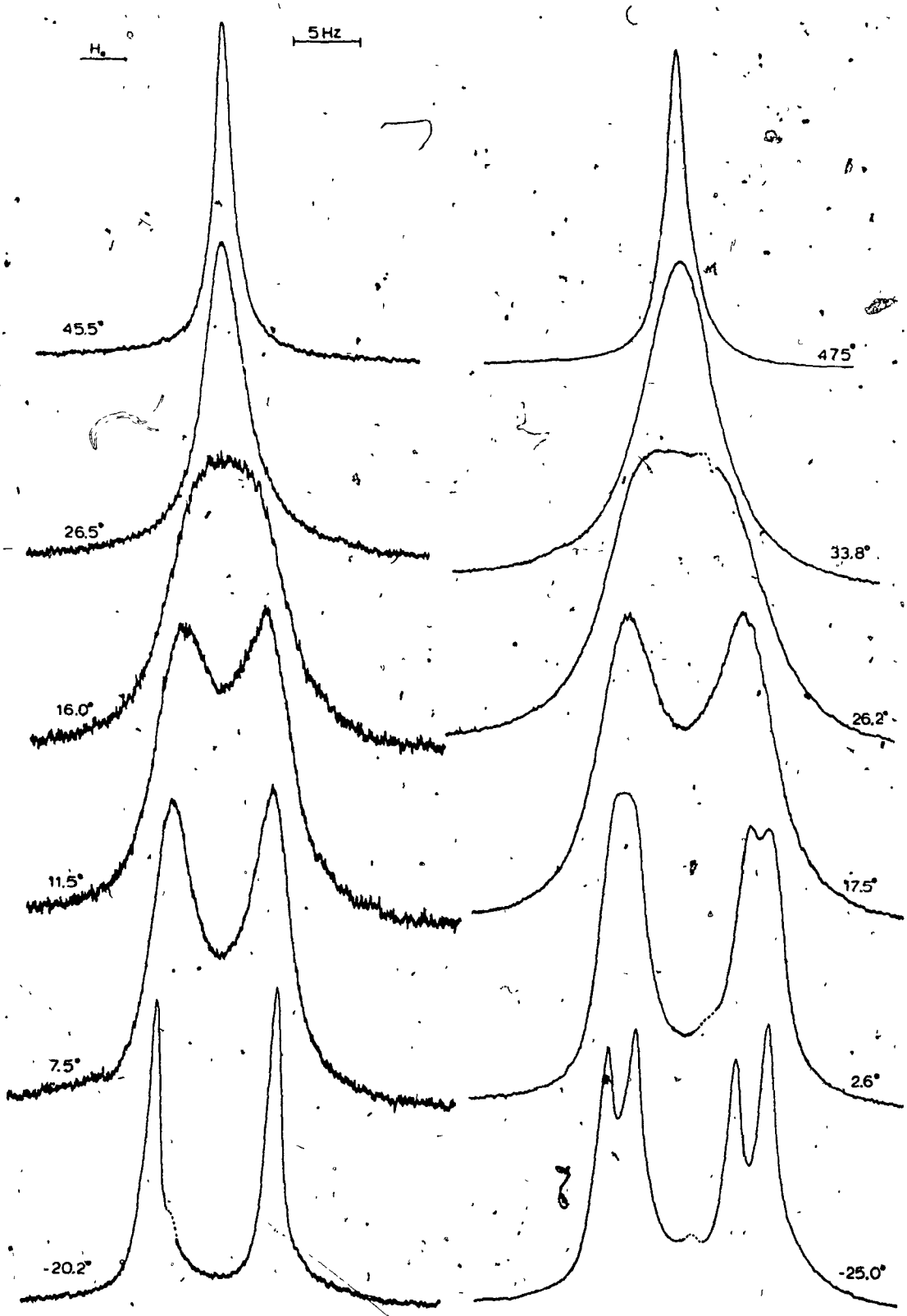
5 Hz
H_o
45.5°
26.5°
16.0°
11.5°
7.5°
-20.2°
47.5°
33.8°
26.2°
17.5°
2.6°
-25.0°
-CH=(acac)
($CDCl_3$)
$-CH_3$(acac)
($CDCl_3$)

Figure 7.- Nmr spectra for the acetylacetonate ring proton (in bromoform) and methyl region (in deuteriochloroform) as a function of temperature for cis-$(C_6H_5)ClSn(acac)_2$. Temperatures shown for the methyl spectra are based on the Varian graph. Dashed lines refer to resonances attributed to the trans isomer (see text).

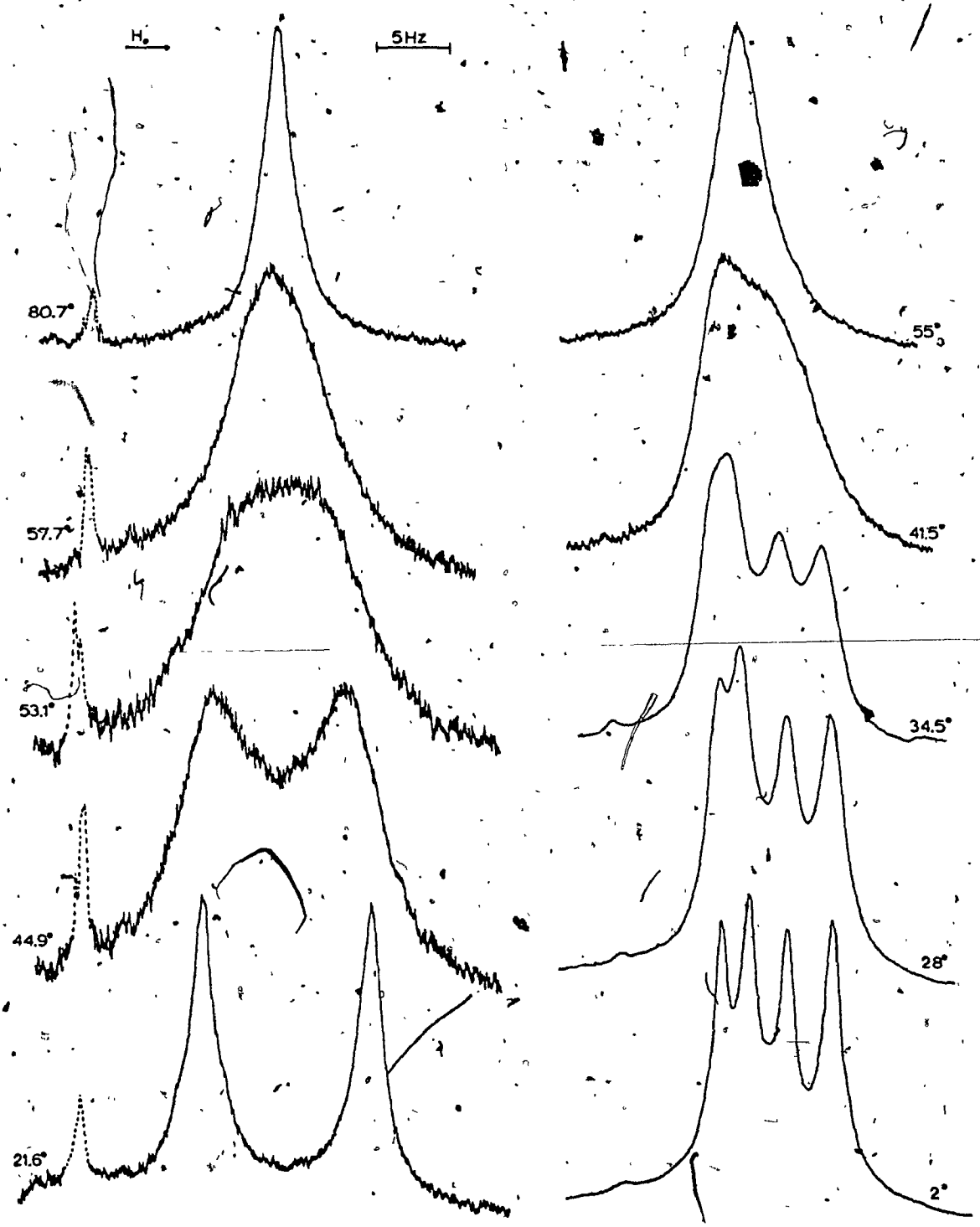
H₀
5Hz
80.7°
57.7°
53.1°
44.9°
21.6°
55°
41.5°
34.5°
28°
2°
-CH=(acac)
(CHBr3)
-CH3(acac)
(CDCl3)

three resonance lines). In accord with the latter, we also observed a distinct -CH= doublet and an additional weak signal at -20.2° (shown as a dashed line in Figure 6). A small resonance is also observed between the lowfield and upfield doublets in the acetylacetonate methyl region. These two signals are ascribed to the existence of a small amount of trans isomer, but obliteration of the -CH= resonance of the trans form with increase in temperature is probably the result of masking by the broadening of the more intense -CH= resonance of the cis isomer and not to a cis-trans equilibration reaction (vide infra). In the high temperature region, signals from the cis and trans isomers appear to have identical chemical shifts.

Similarly, spectra of the phenylchlorotin complex reveal (Figure 7, dashed lines) an additional small -CH= signal (δ5.65 ppm; $CDCl_3$; ca. 37°) and a slightly perceptible methyl resonance. Again we attribute these low intensity signals to the trans structure since other possible impurities, which include 2,4-pentanedione, sodium acetylacetonate, and occluded dichloromethane, all reveal different chemical shifts when added to a solution of the $(C_6H_5)ClSn(acac)_2$ complex. Integration of the -CH= resonances at four selected temperatures between high and low temperature regions shows that the phenylchlorotin complex exists in solution as ∿95% cis and ∿5% trans. It is important to note that the signals due to the trans isomer (Figure 7)

remain unchanged and thus no cis-trans equilibration occurs at least at temperatures below 81°.

Much has been said about the bonding scheme in six-coordinate tin(IV) complexes. On the basis of tin-methyl spin-spin coupling in trans-$(CH_3)_2Sn(acac)_2$, McGrady and Tobias (12) have proposed that the bonds in the C-Sn-C moiety are essentially sp_z hybrids while the $5p_x$ and $5p_y$ orbitals are used to accomodate the four "highly ionic" tin-oxygen bonds in the equatorial plane. Schlemper (11,36) contends that the equatorial σ bonds to the acetylacetonate ligands are of the three-center four-electron type, using the tin p_x and p_y orbitals. Some admixture from $5d_z2$ and $5d_x2-y2$ has also been suggested (15,25). Using the Holmes-Kaesz (95) correlation of the amount of s-character in a Sn-C bond with tin proton coupling constants and the values of $J(^{117}Sn-CH_3)$ and $J(^{119}Sn-CH_3)$, 119.2 and 124.6 Hz, respectively, for $(CH_3)ClSn(acac)_2$ it appears that the Sn-C bond has ∿ 56% s-character. The small, long-range $Sn-CH_3(acac)$ coupling constant of 2.2 Hz (90) also would indicate a certain degree of s-character in the Sn-O bonds. Indeed, if the s-character is maximized along the $Sn-CH_3$ bond in $(CH_3)ClSn(acac)_2$, a stronger tin-oxygen bond trans to $Sn-CH_3$ is predicted. No crystal structure of this compound has yet been reported. Also, it is not clear how much d-orbital involvement the H-K treatment can tolerate in a bonding scheme of Sn(IV) compounds, nor is

a near lack of s-character in the equatorial plane understood. The possible breakdown of the H-K correlation in six-coordinate tin complexes cannot be overlooked.

2. Germanium and Silicon Complexes.

The six-coordinate nature of $RClSi(acac)_2$ (R = CH_3 and C_6H_5) is confirmed by infrared spectroscopic evidence (60); there are no carbonyl stretching bands above 1600 cm^{-1}, indicating that both carbonyl oxygens are bound (96) to the central atom. The complexes $RClGe(acac)_2$ (R = CH_3 and C_6H_5) and $(C_6H_5)_2Ge(acac)_2$ are similarly six-coordinate. Variable temperature nmr spectra of the methyl and ring proton region for the phenylchlorogermanium complex are presented in Figure 8; those for the silicon analog are illustrated in Figure 9. Observation at low temperatures of four methyl proton signals, (the lowfield doublet unresolved in Figure 9 at the lowest accessible temperature, -80°) and two acetylacetonate ring proton resonances for both the phenylchlorogermanium and phenylchlorosilicon acetylacetonates is consistent with these complexes adopting the cis diastereomeric form. In addition, a small, but perceptible resonance is likewise observed in the methyl and ring proton spectral regions. This signal (dashed lines in Figures 8 and 9) is attributed to a small amount ($\leq$ 5%) of the trans-$(C_6H_5)ClM(acac)_2$ complexes. This is similar to the effect observed

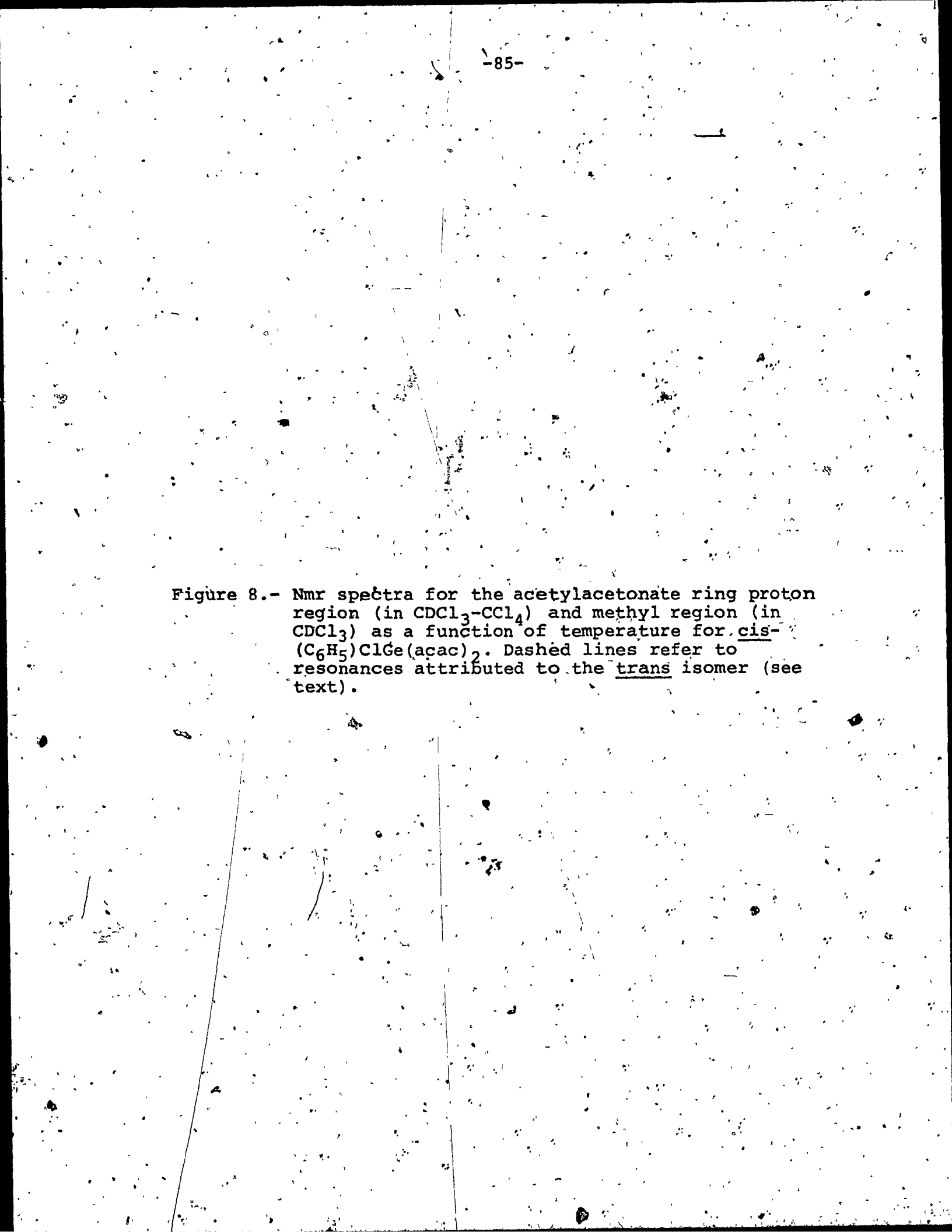

Figure 8.- Nmr spectra for the acetylacetonate ring proton region (in $CDCl_3$-CCl_4) and methyl region (in $CDCl_3$) as a function of temperature for cis-$(C_6H_5)ClGe(acac)_2$. Dashed lines refer to resonances attributed to the trans isomer (see text).

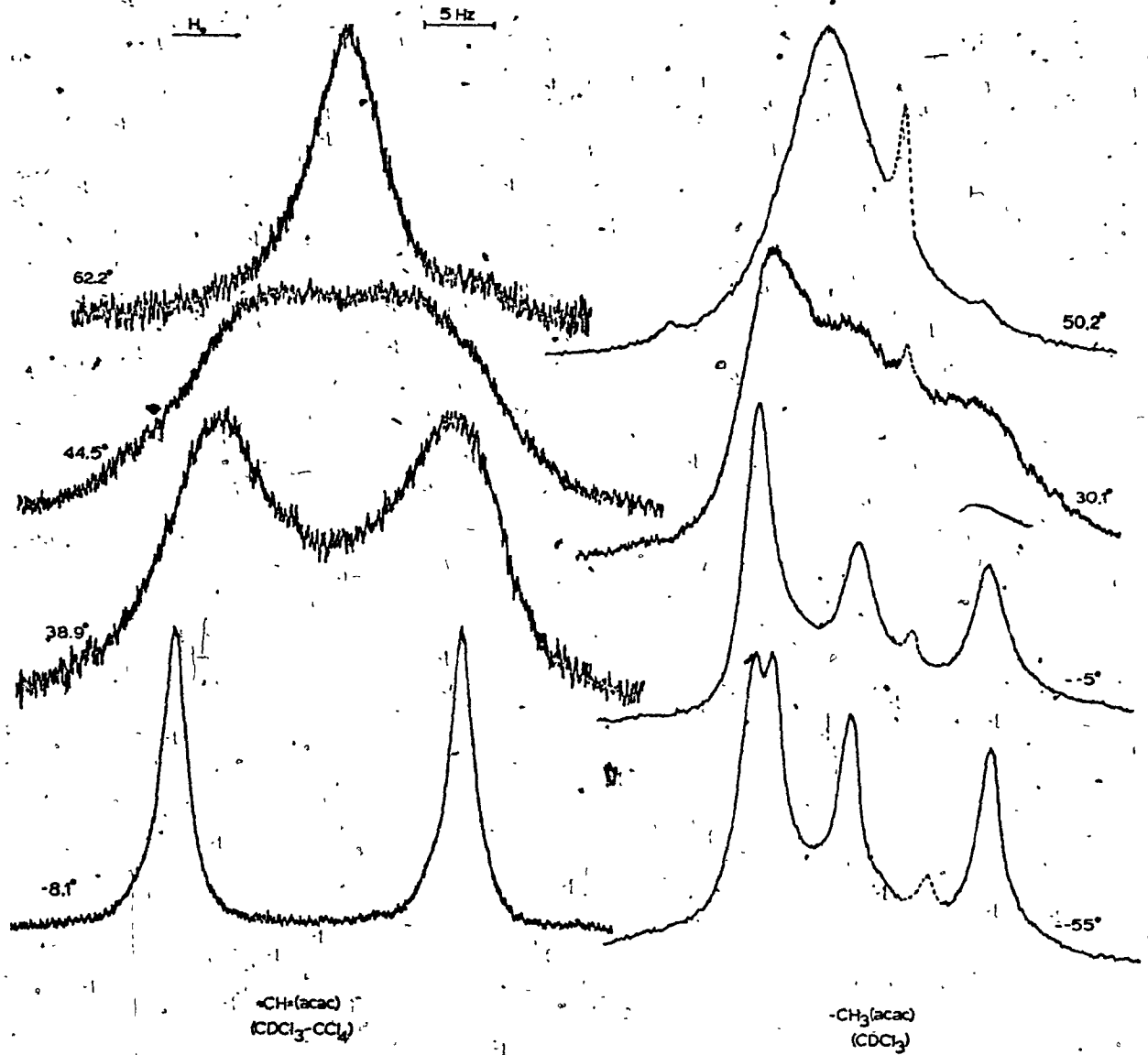
H
5 Hz
62.2°
50.2°
44.5°
30.1°
38.9°
-5°
-8.1°
-55°
=CH-(acac)
(CDCl3-CCl4)
-CH3(acac)
(CDCl3)

Figure 9.— Nmr spectra of the acetylacetonate ring proton region (in $CDCl_3$–CCl_4) and methyl group region (in CH_2Cl_2) as a function of temperature for the cis-$(C_6H_5)ClSi(acac)_2$ complex. Dashed lines refer to resonances attributed to a small amount of the trans isomer (see text).

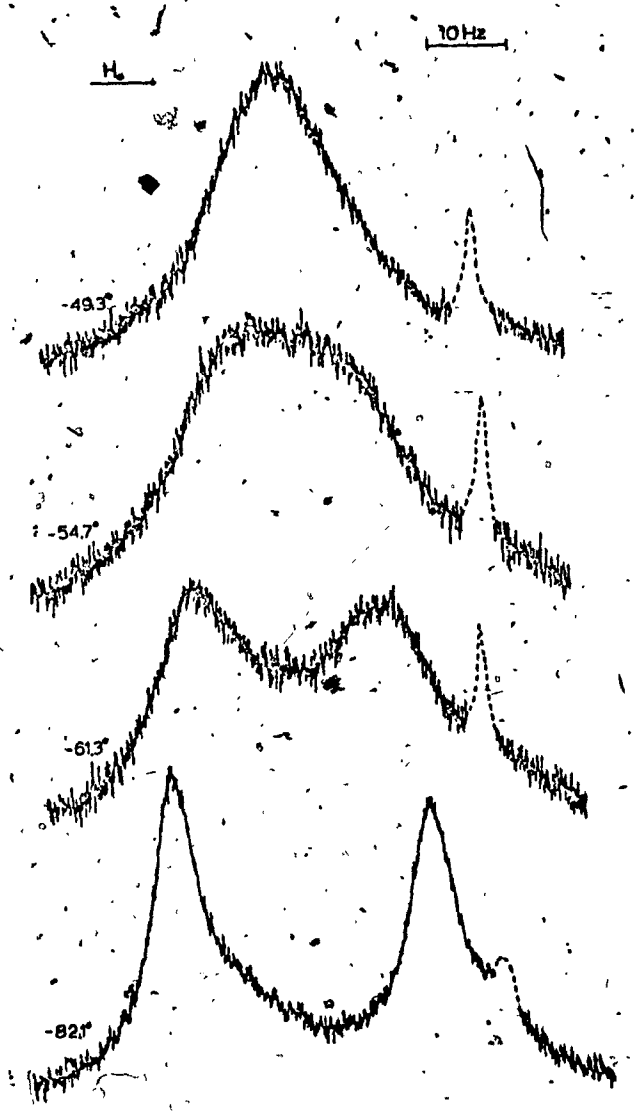

$-CH(acac)$
$(CDCl_3CCl_4)$

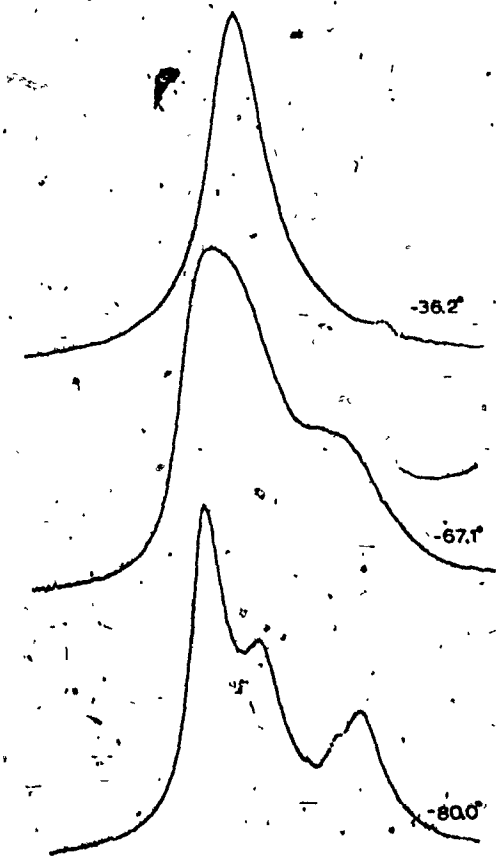

$-CH_3(acac)$
(CH_2Cl_2)

for the $(C_6H_5)ClSn(acac)_2$ complex (vide supra).

Variable temperature nmr spectra for $(CH_3)ClGe(acac)_2$ at several selected temperatures between -76° and 23°C are reproduced in Figure 10. At ambient temperatures the proton spectrum consists of single, sharp ring proton ($W_{1/2}$ = 0.74 Hz) and methyl proton resonances. Below room temperature, line broadening is observed. The methyl resonance begins to split into two lines at ca. -29°, and at ca. -54° the upfield line splits again to give a total of four lines in the low temperature region (the downfield doublet is unresolved, probably owing to chemical shift degeneracy of the two components). The ring proton spectrum reveals a doublet at -61.7°; with increasing temperature the two components broaden and collapse at -13.3°. Line broadening is ascribed to an environmental averaging process which exchanges ring protons and methyl groups between the respective two and four nonequivalent sites of the cis diastereomer. An additional observation in the -CH= proton spectrum is a slightly perceptible resonance in the highfield side of the upfield component. This resonance is attributed (vide supra) to a small amount (probably not more than 5%) of the trans isomer; the corresponding methyl signal is apparently masked by the more intense signals of the cis diastereomer.

Variable temperature nmr spectra of the methyl-

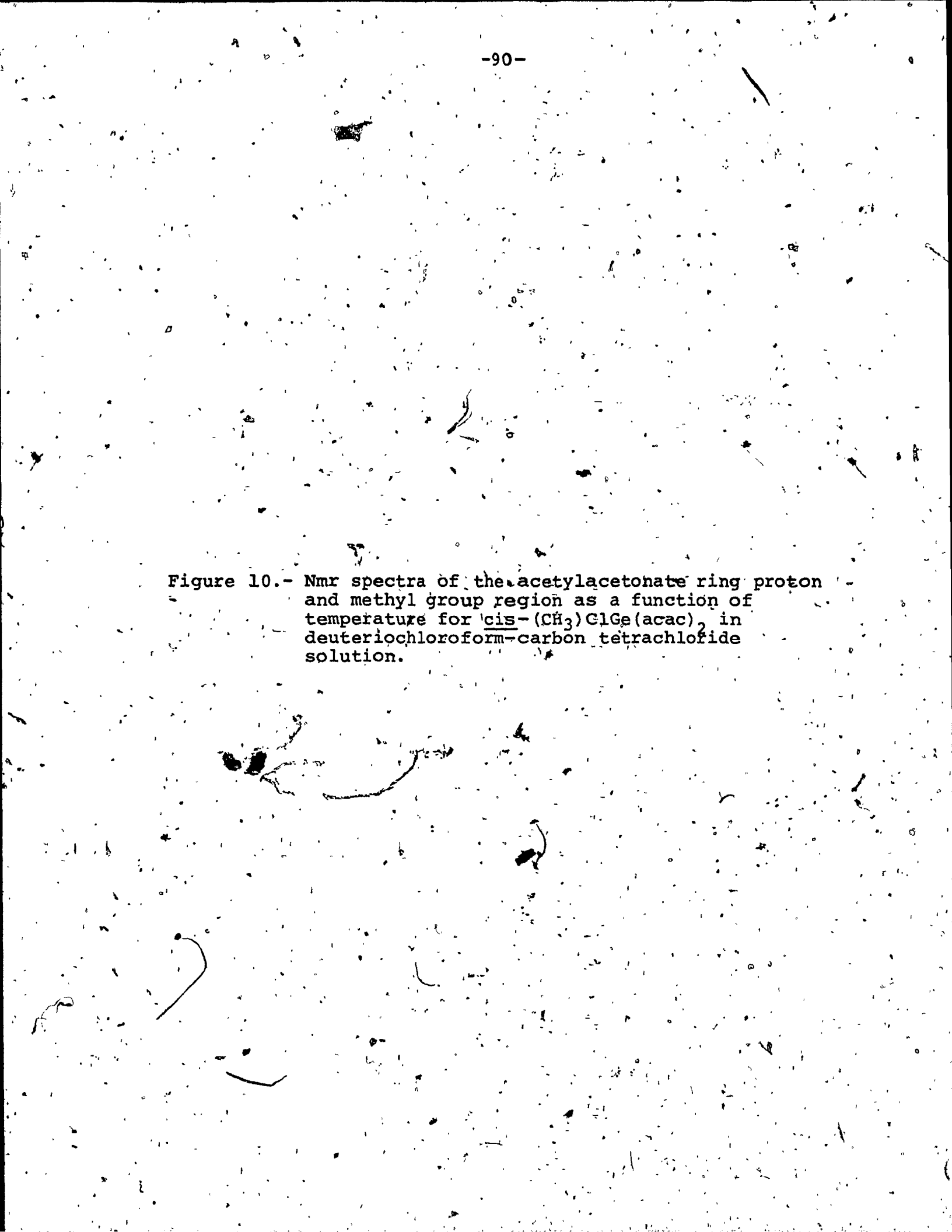

Figure 10.- Nmr spectra of the acetylacetonate ring proton and methyl group region as a function of temperature for cis-$(CH_3)ClGe(acac)_2$ in deuteriochloroform-carbon tetrachloride solution.

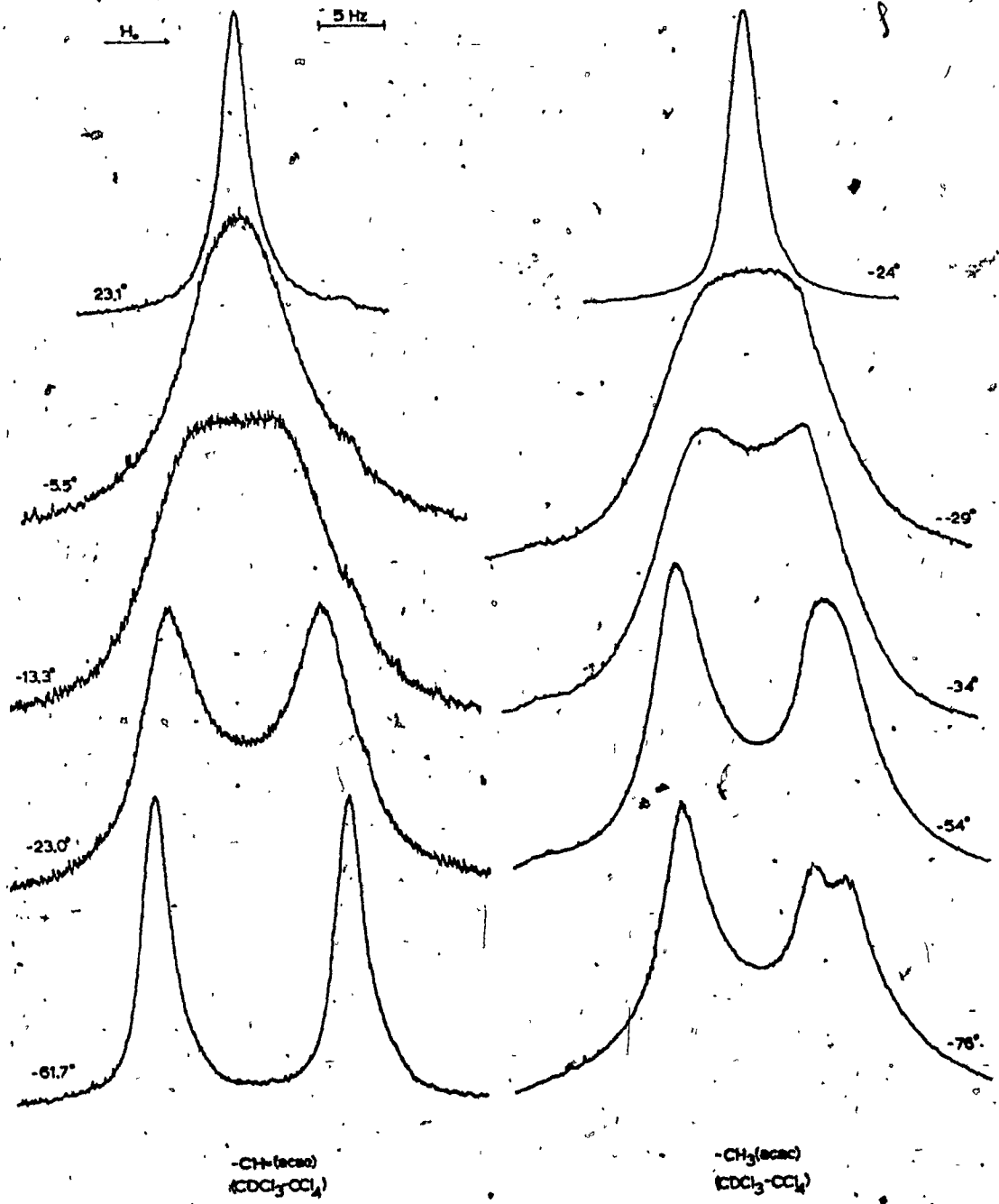
H₀
5 Hz
23.1°
-5.5°
-13.3°
-23.0°
-61.7°
-24°
-29°
-34°
-54°
-76°
-CH=(acac)
(CDCl₃-CCl₄)
-CH₃(acac)
(CDCl₃-CCl₄)

chlorosilicon acetylacetonate complex in chloroform-d-carbontetrachloride solution (0.457M) reveal two methyl proton signals (lowfield resonance more intense), and a single, broad line ($W_{1/2}$ = 1.10 Hz at 28°, 3.95 Hz at -68°, and 7.45 Hz at -76°) for the ring proton -CH- . These observations are also suggestive that the compound adopts the cis structure, at least at low temperatures.

Our efforts with the diphenylgermanium complex proved less successful. Spectra (in $CDCl_3$-CCl_4; 0.243 M) revealed a single methyl ($W_{1/2}$ = 4.12 Hz at -80.6°) and a single -CH- proton signal ($W_{1/2}$ = 3.90 Hz at -80.6°). An unequivocal assignment of sterochemistry in solution is precluded by the above data; linewidths of CH_3 and -CH- proton resonances are nearly the same (for the cis isomer, one ring proton and two methyl signals are expected). However, we believe that the complex probably exists in the cis form on the basis of the following evidence. The analogous diphenyltin complex is unequivocally cis in solution (vide supra). Further, phenylchlorogermanium acetylacetonate is more labile (vide infra) than the corresponding tin complex. Thus, it is not unreasonable to expect that $(C_6H_5)_2$-$Ge(acac)_2$ be more labile than $(C_6H_5)_2Sn(acac)_2$. For the latter complex, T_c for methyl signals is $\sim$-40° and $\delta\nu$ at -60° is about 3.5 Hz (vide supra). It is not surprising then that coalescence behavior for the germanium compound has not been observed.

B. Kinetics of the Environmental Averaging Process

1. Transverse Relaxation Times

In order to determine τ_a and τ_b, the lifetimes of a nucleus at sites A and B, respectively, of an exchanging system it is necessary to determine the transverse relaxation times T_{2a} and T_{2b} in the absence of exchange.

In the slow exchange limit the observed full linewidth, in Hz, at one-half maximum amplitude is defined by the equation

$$1/\pi T_2 = 1/\pi T_2^{\circ} + 1/\pi T_2' + (1/\pi\tau)_{exch}$$

where $1/\pi T_2$ is the observed linewidth; $1/\pi T_2^{\circ}$, the contribution from field inhomogeneity; $1/\pi T_2'$, the natural linewidth; and $(1/\pi\tau)_{exch}$, the contribution due to exchange broadening. In the absence of exchange, the exchange term vanishes with the result that the observed linewidth is determined by the natural linewidth and the inhomogeneity contribution. Similarly, in the fast exchange limit the contribution to the linewidth from the exchange term becomes negligible, and a narrow lineshape is observed (86). Therefore, theoretically, if T_2 is independent of temperature, then the linewidth at one-half maximum amplitude of a complex at the slow exchange limit would be equal to that at the fast exchange limit and probably at any temperature in between. In our case T_2 was found to be temperature dependent as is evidenced from viscosity broadening in the region of slow exchange (e.g. $W_{1/2}$ is 1.39 Hz at -20.0° and 1.56 Hz at

-44.6° for $(CH_3)ClSn(acac)_2$ in $CDCl_3$ solution; for (C_6H_5)-$ClSn(acac)_2$ in $CDCl_3$, $W_{1/2}$ is 1.08 Hz (-16.3°) and 1.27 Hz (-42.6°); for $(C_6H_5)ClGe(acac)_2$ in $CDCl_3$-CCl_4, $W_{1/2}$ at 13.2° is 2.37 Hz for the lowfield line and 2.55 Hz for the highfield line, but at -53.9° the corresponding values are 2.68 and 2.75 Hz) and from differences in $W_{1/2}$ in the slow and in the fast exchange regions (e.g., $W_{1/2}$ is 0.8 Hz at 35° but 2.50 Hz at ca. -70° for $(C_6H_5)_2Sn(acac)_2$ in CH_2Cl_2; also for $(CH_3)ClGe(acac)_2$ in $CDCl_3$-CCl_4, $W_{1/2}$ at 55.6° is 0.74 Hz, while at -70.2° $W_{1/2}$ is 2.32 Hz (lowfield line) and 2.54 Hz (highfield line), and at -80.7° the corresponding values are 8.58 and 9.33 Hz).

This phenomenon has been recognized by Gutowsky and Holm (78) and Allerhand and Gutowsky (97) who acknowledge that this dependence is a possible source of systematic error. To illustrate the results of presuming T_2 to be independent of temperature we did the following; A transverse relaxation time T_2 was chosen from what was believed to be the fast exchange limit for $(C_6H_5)_2Sn(acac)_2$ in CH_2Cl_2. This corresponded to a value of $T_2 = 0.397$ ($W_{1/2}$ at 31° is 0.80 Hz, and $T_2 = 1/(\pi \times W_{1/2})$). This value was then considered a constant and subsequently used in the determination of the lifetimes at each temperature. The results of a plot of Log k vs 1/T are presented in Figure 11b (Table XIV). As is apparent from the graph, as the temperature progresses away from coalescence there is

Table XIV.- Log k's Calculated for $(C_6H_5)_2Sn(acac)_2$ Using Various Transverse Relaxation Times.

Temperature °C	T_2 0.397	T_2 $Zr(acac)_2Cl_2$	T_2 $(CH_3)_2Sn(acac)_2$
-56.8	0.624	0.557	0.392
-53.8	0.661	0.615	0.496
-51.7	0.668	0.630	0.502
-48.8	0.756	0.746	0.646
-48.4	0.791	0.778	0.681
-46.8	0.863	0.853	0.795
-45.0	0.852	0.845	0.785
-42.3	0.904	0.903	0.858
-38.6	0.957	0.958	0.934
-37.4	1.038	1.037	1.043
-35.1	1.085	1.082	1.097
-30.5	1.251	1.247	1.246
-24.8	1.393	1.378	1.415
-17.5	1.532	1.497	1.552
-9.5	1.688	1.623	1.704
-6.0	1.786	1.699	1.807
3.0	1.941	1.805	1.997

Figure 11.- Graph of Log k vs 1/T for a) $(CH_3)ClSn(acac)_2$ whereby log k was calculated using program NICKA and NLINGH (half-solid circles are NICKA results, open circles are NLINGH results ($\delta\nu$ fixed) and open squares are NLINGH results ($\delta\nu$ variable).
b) $(C_6H_5)_2Sn(acac)_2$ whereby log k was calculated using program NICKA with different T_2's (solid circles are T_2's from $(CH_3)_2Sn(acac)_2$, open triangles are from a constant T_2 (0.397), open circles are from T_2's from $Zr(acac)_2Cl_2$.

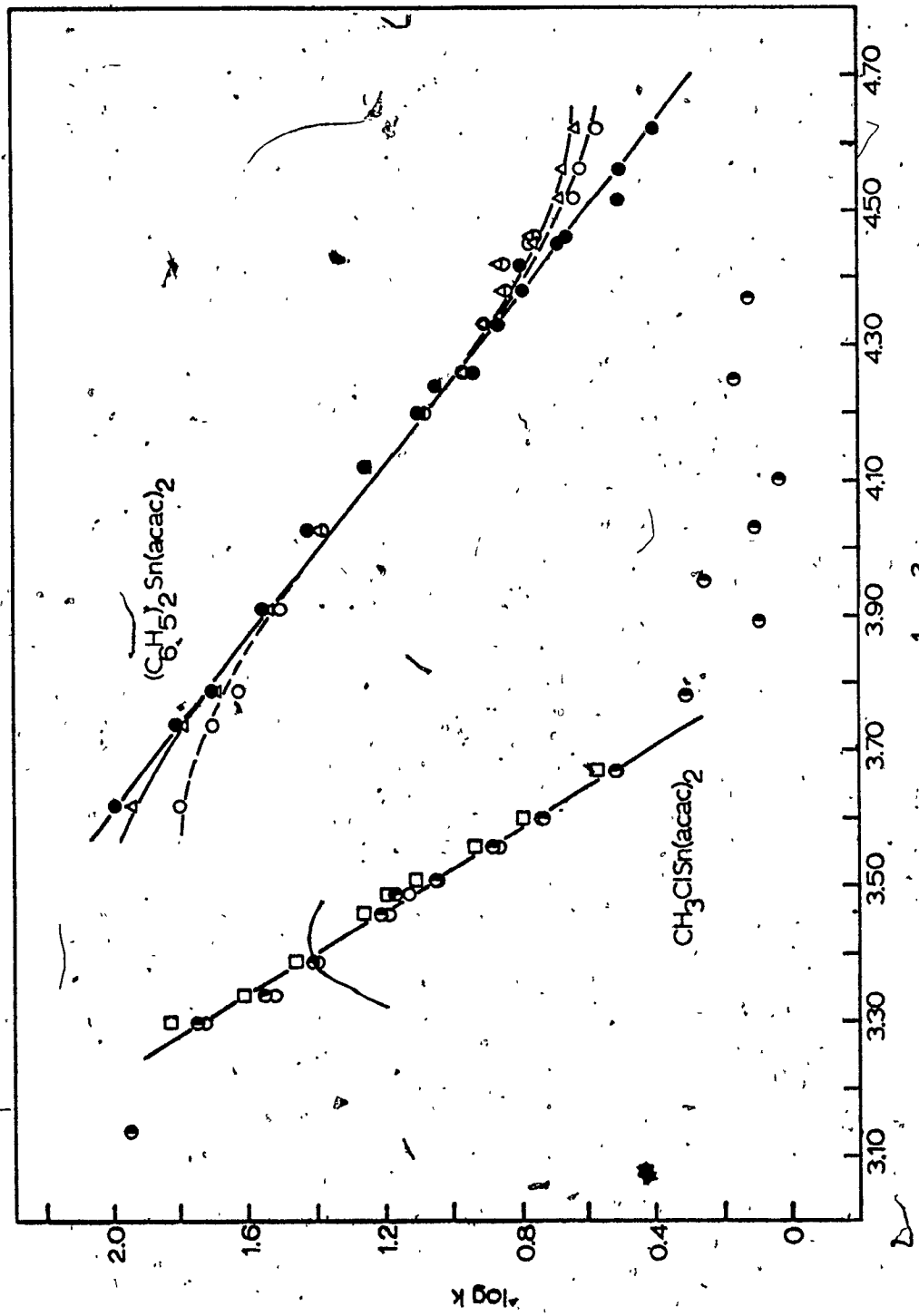
$(C_6H_5)_2Sn(acac)_2$
$CH_3ClSn(acac)_2$
$-\log k$
$\frac{1}{T} \times 10^3$
2.0
1.6
1.2
0.8
0.4
0
3.10
3.30
3.50
3.70
3.90
4.10
4.30
4.50
4.70

considerable deviation from linearity making the need for correction of the T_2 necessary at the individual temperatures. Therefore, a single value of T_2 may not be appropriate and a correction would have to be made for the temperature dependence.

A more appropriate technique is that used by Fay and coworkers (32,87) whereby an isostructural complex, $Zr(acac)_2Cl_2$, was chosen. The linewidths from this compound were then determined at a series of temperatures, from which the corresponding T_2's were obtained. Although only a single methyl resonance was observed for $Zr(acac)_2Cl_2$ in solution, Pinnavaia and Fay assigned a cis configuration to this complex on the basis of chemical shifts (98), infrared and Raman (99) data. The single resonance was attributed to a rapid exchange process which time averages the methyl group environments. Owing to this very rapid exchange it is believed that the changes which occur in the linewidth in the temperature range of interest reflect only the temperature dependence of T_2 (87,100). We subsequently used the T_2's obtained from $Zr(acac)_2Cl_2$ in CH_2Cl_2 (87) to determine the lifetimes at each temperature for $(C_6H_5)_2Sn(acac)_2$ in CH_2Cl_2. The results of the plot of Log k vs 1/T are presented in Figure 11b (Table XIV). Again, as the temperature progressed away from coalescence there was some deviation from linearity, however, this was a much improved situation over that of the constant T_2. The activation parameters are

E_a = 6.0 ± 0.3 kcal/mole and $\Delta S^{\ddagger}$ = -30 ± 1 eu. Although these were acceptable results it was believed that a compound more analogous to our case might be even more appropriate. The compound with the most valid characteristics was $(CH_3)_2Sn(acac)_2$. This complex exhibits one peak in the acetylacetonate-methyl region and one peak in the ring proton region of the nmr spectrum. It is assumed to have a trans structure (see section I); however, even if it did assume the cis configuration, the change in linewidths is sufficiently small ($W_{1/2}$ = 1.51 Hz at -59.4°; 0.85 Hz at -9.7° in CH_2Cl_2) over a large range of temperature (Figure 3, Table X to XII) that the exchange is probably so rapid that the change in linewidths only reflects the change in T_2, similar to the $Zr(acac)_2Cl_2$ case. The results of using the T_2's from the linewidths of the dimethyltin chelate to calculate the lifetimes for $(C_6H_5)_2Sn(acac)_2$ in CH_2Cl_2 are illustrated in Figure 11b (Table XIV). The straight line produced yields an even better Arrhenius plot than that using the zirconium complex; consequently the T_2's from $(CH_3)_2Sn(acac)_2$ in the appropriate solvent were used for all calculations of all the complexes studied in this work (this includes the germanium and silicon complexes for which the analogous dimethyl complexes were not available. It was assumed that the dimethyltin complex was sufficiently isostructural to be acceptable).

In the nmr spectrum of $(CH_3)_2Sn(acac)_2$ there is a peak in the acac-CH_3 region and one peak in the ring proton region of which the former is about six times more intense than the latter. When determining the rate parameters for $(C_6H_5)_2Sn(acac)_2$ the T_2's used for the calculation were obtained from the linewidths of the methyl resonance of the dimethyltin complex appropriate for the data collected on the diphenyl complex. Similarly, the same T_2 data were used in the calculation of the rate parameters of the methylchloro and phenylchloro complexes; however, the kinetic data for these complexes were collected in the ring proton region of the nmr spectrum. The reason for not utilizing T_2 data from the ring proton region of the dimethyltin complex was due to a poor relative solubility of this compound. Consequently, this produced such a weak signal in the ring proton region that when the signal was sufficiently amplified, in order to be read with some degree of accuracy, it became noisy leading to unreliable results. This, however, brings up the question of our being justified in using only the methyl region T_2's. Would the ring proton T_2's yield different lifetimes? To illustrate the effect we chose the data from $(CH_3)ClSn(acac)_2$ in $CDCl_3$. Lifetimes were obtained using T_2's from both regions of the dimethyltin complex nmr spectra. These data were then plotted as Log k vs 1/T (Figure 12) and are tabulated in Table XV. As is evident, the results are equivalent using either technique and are well within experimental error.

Table XV.- Comparison of Lifetimes of Environmental Averaging Processes for $(CH_3)ClSn(acac)_2$ in $CDCl_3$ Obtained by Using T_2's from the Methyl and Ring Proton Regions of $(CH_3)_2Sn(acac)_2$.

Temperature °C	$2\tau \times 10^1$ (T_2 from acac-CH_3 region) sec	$2\tau \times 10^1$ (T_2 from acac-CH region) sec
-0.5	3.106	2.912
4.5	1.699	1.650
7.5	1.326	1.318
11.5	0.883	0.877
13.5	0.684	0.684
16.0	0.622	0.623
21.5	0.373	0.376
26.5	0.275	0.280
29.5	0.167	0.173

Figure 12.- Graph of Log k vs 1/T for $(CH_3)ClSn(acac)_2$ where Log k was calculated using T_2's obtained from the acetylacetonate methyl region and the ring proton region of $(CH_3)_2Sn(acac)_2$.

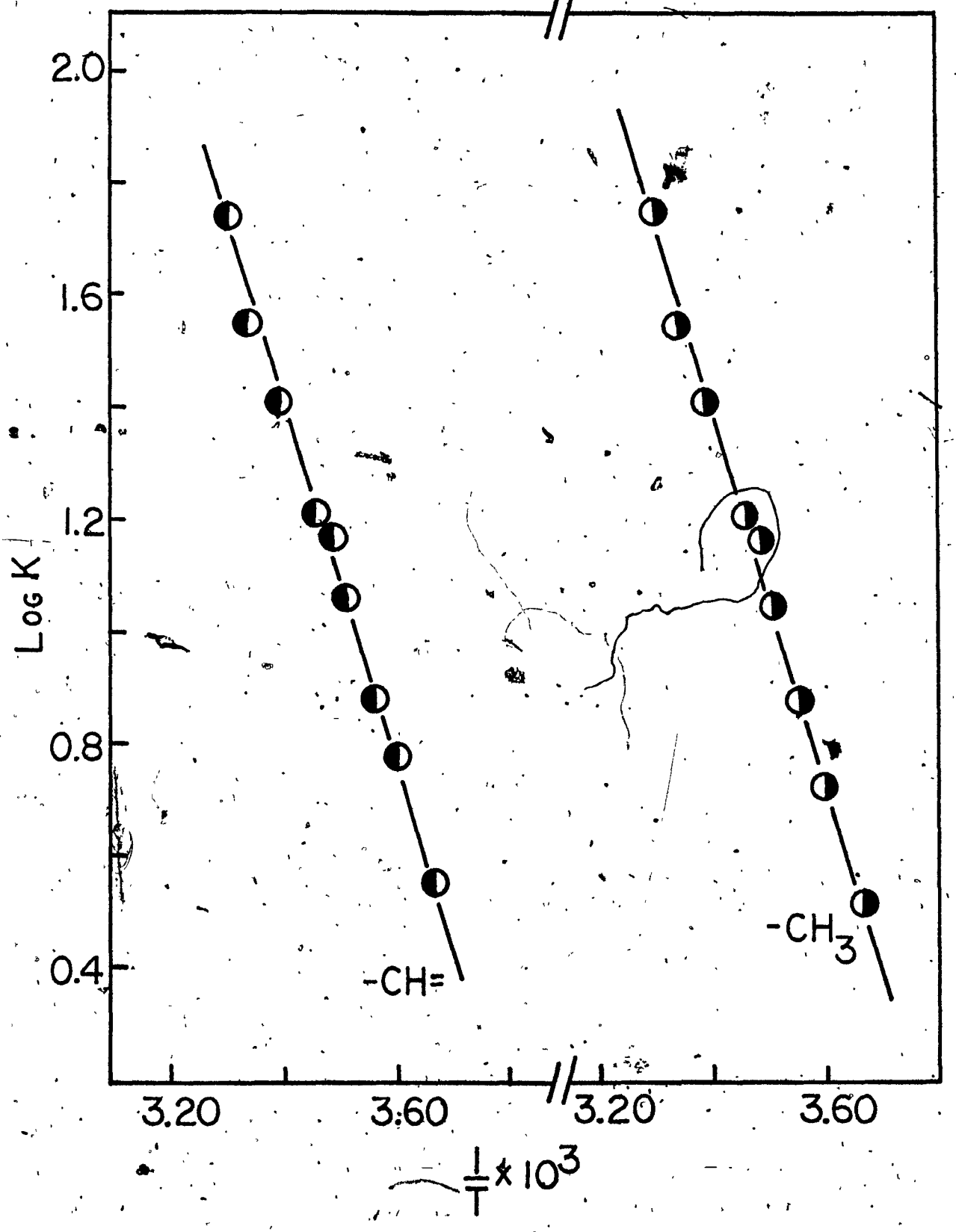
2.0
1.6
1.2
0.8
0.4
Log K
-CH=
-CH3
3.20
3.60
3.20
3.60
1/T x 10^3

This being the case, we felt justified in using T_2's from the methyl region of the dimethyltin complex to calculate lifetimes from the ring proton regions of interest.

2. Activation Parameters

From the definition of τ (equation 8), and from the fact that $\tau_a = \tau_b$ for a two-site exchange process, $k = 1/2\tau$, where k is the first-order rate constant for exchange. The temperature dependence of the rate constant can be adequately represented by the Arrhenius equation, to which the rate data were fitted by least squares analysis. Each activation energy was determined from the slope of a linear plot of Log k vs 1/T (Figures 13-15) via the Arrhenius relationship

$$\ln k = \ln A - \frac{E_a}{RT}$$

where A is the pre-exponential factor and ln A corresponds to the intercept of the plot at $1/T = 0$. Activation entropies at 25° were estimated from the relation

$$\Delta S^{\ddagger} = R\left[\ln A - \ln \frac{RT}{Nh}\right] + R$$

obtained by equating the Arrhenius and transition state theory pre-exponential factors (101):

$$\ln k = \ln \frac{RT}{Nh} + \frac{\Delta S^{\ddagger}}{R} - \frac{E_a}{RT} + 1$$

where $E_a = RT + \Delta H^{\ddagger}$.

Figure 13.- Log k *vs* 1/T least squares plots for acetylacetonate methyl group exchange in $(C_6H_5)_2Sn(acac)_2$ in the indicated solvents. $k = 1/2\tau$ is the first-order rate constant for the configurational rearrangement process.

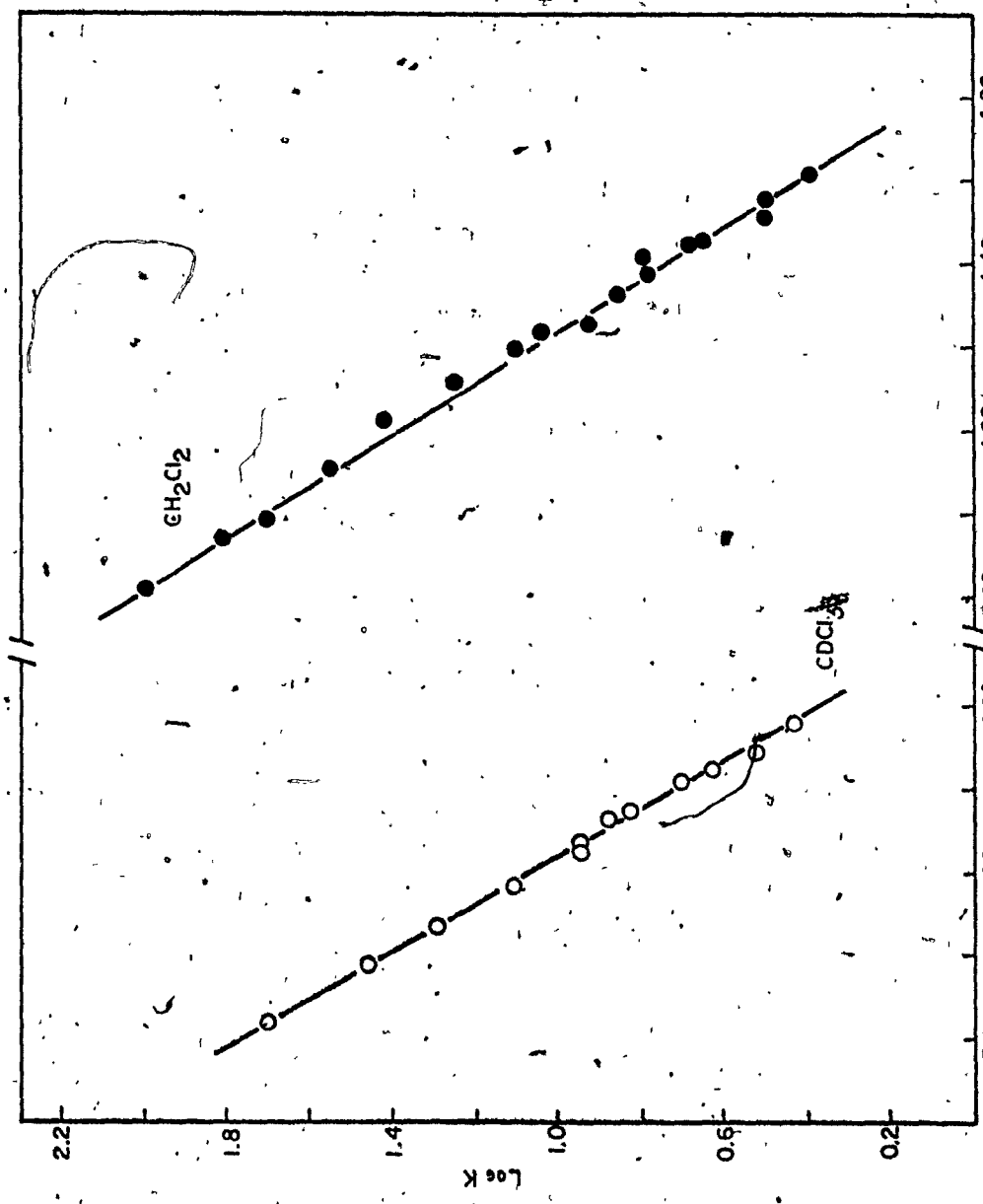
CH_2Cl_2
$CDCl_3$
Log K
2.2
1.8
1.4
1.0
0.6
0.2
3.80
4.00
4.20
4.40
4.60
4.80
$\frac{1}{T} \times 10^3$

Figure 14.- Log k vs 1/T least squares plots for acetylacetonate ring proton exchange in $RClSn(acac)_2$ ($R = CH_3$, C_6H_5) in the indicated solvents. $k = 1/2\tau$, is the first-order rate constant for the configurational rearrangement process.

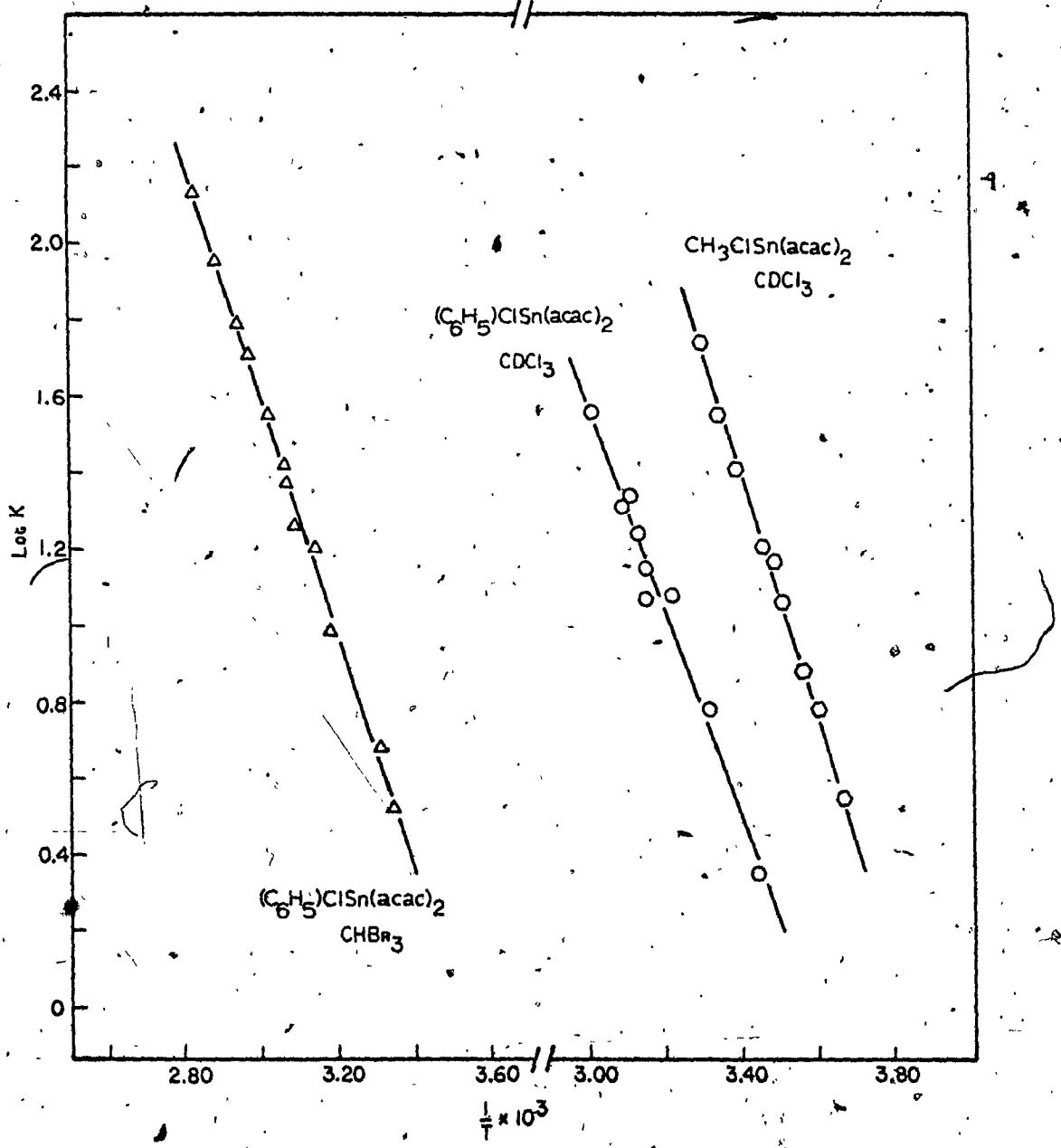
2.4
2.0
1.6
1.2
0.8
0.4
0
Log K
$CH_3ClSn(acac)_2$
$CDCl_3$
$(C_6H_5)ClSn(acac)_2$
$CDCl_3$
$(C_6H_5)ClSn(acac)_2$
$CHBr_3$
2.80
3.20
3.60
3.00
3.40
3.80
$\frac{1}{T} \times 10^3$

Figure 15.- Log k *vs* 1/T least squares plots for acetylacetonate ring proton exchange in $(C_6H_5)ClM(acac)_2$ (M = Ge, Si) and $(CH_3)ClGe(acac)_2$ complexes in $CDCl_3$-CCl_4 solutions. $k = 1/2\tau$ is the first-order rate constant for the environmental averaging process. For the methylchlorogermanium complex k refers to the second order rate constant for exchange (see text).

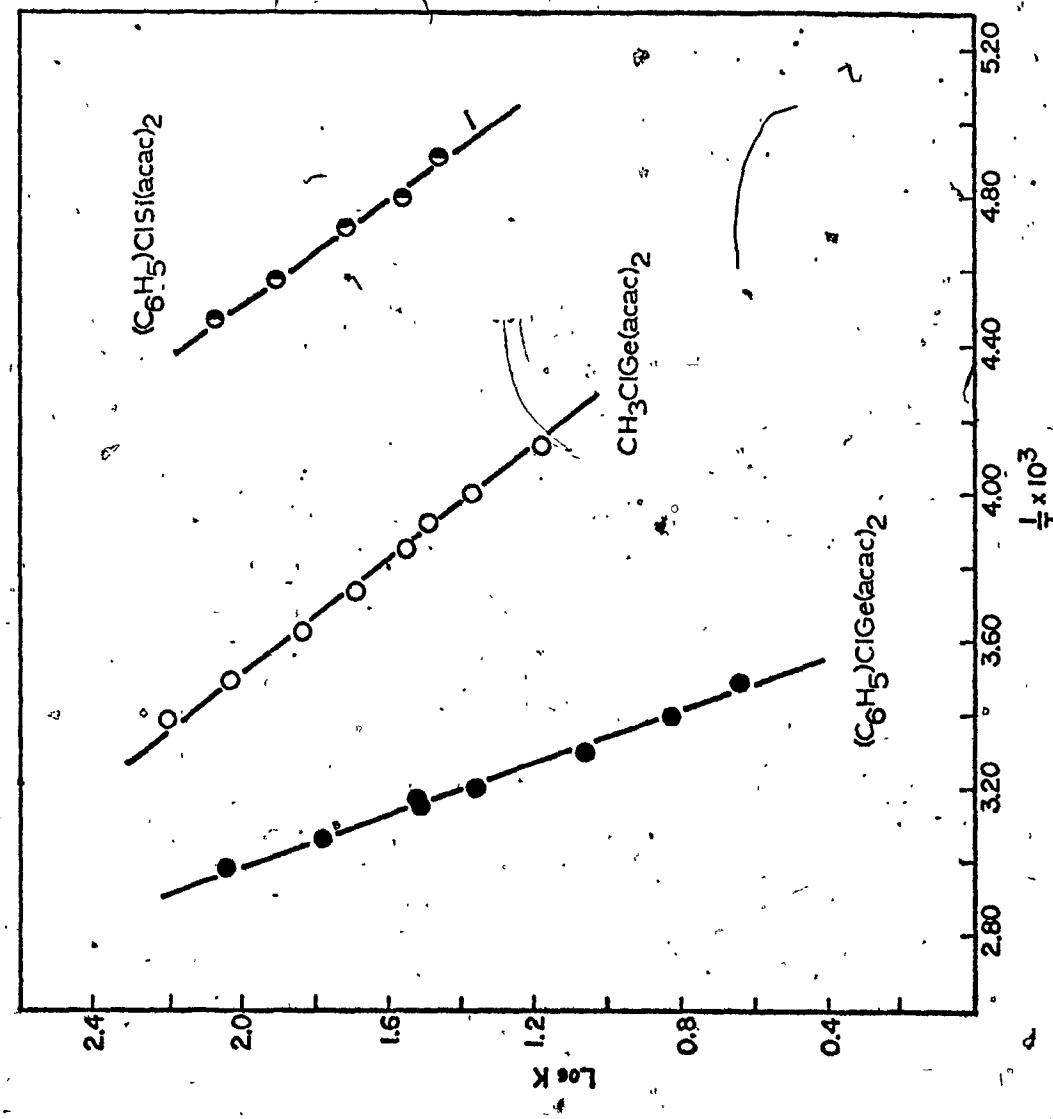
$(C_6H_5)ClSi(acac)_2$
$CH_3ClGe(acac)_2$
$(C_6H_5)ClGe(acac)_2$
Log K
$\frac{1}{T} \times 10^3$
2.4
2.0
1.6
1.2
0.8
0.4
2.80
3.20
3.60
4.00
4.40
4.80
5.20

In order to compare the relative labilities of the complexes, the activation parameters were calculated at 25° and/or at T_c using the data from Tables XVI-XVII. Also included for comparison purposes are the values for the exchange processes in $Cl_2Sn(acac)_2$ and $Cl_2Ge(dpm)_2$ (30). Values of the activation parameters for the complexes of interest are subject to appreciable systematic errors owing to the temperature dependence of the transverse relaxation times throughout the temperature range at which kinetic data are reported. These errors were compensated for and are discussed later. Errors in the activation parameters of Tables XVI and XVII represent the random scatter of the data points in Figures 13-15. Also, a reasonable uncertainty in T_2 appears to lead to systematic errors of the order of ± 1 kcal/mole in the activation energy and ± 4 eu in the activation entropy (32). A number of features can be noted from Tables XVI and XVII. The rate of configurational rearrangement in the tin(IV) acetylacetonates decreases in the order $(C_6H_5)_2Sn$ > $(CH_3)ClSn$ > $(C_6H_5)ClSn$ > Cl_2Sn. Interestingly, the rate of intermolecular exchange of acetylacetonate ligands in the systems $RR'Sn(acac)_2$-Hacac decreases in the order $(CH_3)_2Sn$ > $(C_6H_5)_2Sn$ > $(CH_3)ClSn$ > Cl_2Sn (102). Evidently, replacement of a chloride in $Cl_2Sn(acac)_2$ with a phenyl or a methyl group leads to a significant increase in the lability of the acetylacetonate complexes. Substitution of the two chloro groups increases the lability further. A similar

Table XVI.- Arrhenius and Eyring Activation Parameters for Configurational Rearrangements in Organotin(IV) β-ketoenolate Complexes.

Parameters	$(C_6H_5)_2Sn(acac)_2$		$(CH_3)ClSn(acac)_2$	$(C_6H_5)ClSn(acac)_2$		$Cl_2Sn(acac)_2$ [c]
	$CDCl_3$	CH_2Cl_2	$CDCl_3$	$CDCl_3$	$CHBr_3$	$1,1,2,2\text{-}C_2H_2Cl_4$
T_c [a], °C	-38.0	-37.4	17.0	46.0	53.1	82
E_a, kcal/mole	8.1 ± 0.3 [b]	7.4 ± 0.3	14.6 ± 1.1	12.7 ± 2.0	14.7 ± 0.8	16.0 ± 0.4
log A	8.49 ± 0.31	7.87 ± 0.26	12.29 ± 0.81	9.96 ± 1.38	11.25 ± 0.52	10.92 ± 0.23
$\Delta H^{\ddagger}_{25}$, kcal/mole	7.5 ± 0.3	6.8 ± 0.3	14.1 ± 1.1	12.2 ± 2.0	14.1 ± 0.8	-
$\Delta S^{\ddagger}_{25}$, e.u.	-21.7 ± 1.4	-24.5 ± 1.2	-4.3 ± 3.7	-15 ± 6	-9.1 ± 2.4	-10.6 ± 1.0
$\Delta G^{\ddagger}_{25}$, kcal/mole	13.95 ± 0.09	14.11 ± 0.08	15.32 ± 0.05	16.61 ± 0.12	16.81 ± 0.07	-
k_{25}, sec^{-1}	369 ± 58	281 ± 37	36 ± 3	4.1 ± 0.9	2.9 ± 0.4	0.15
$\Delta G^{\ddagger}_{T_c}$, kcal/mole	12.60 ± 0.02	12.59 ± 0.02	15.29 ± 0.04	16.93 ± 0.08	17.06 ± 0.04	-
k_{T_c}, sec^{-1}	9.5 ± 0.3	10.3 ± 0.4	17 ± 1	17 ± 2	25.0 ± 1.4	-

[a] ±1°. [b] Random errors estimated at the 95% confidence limit. [c] Reference 30.

Table XVII.- Arrhenius and Eyring Activation Parameters at 25° for Environmental Averaging in Organogermanium(IV) and Organosilicon(IV) β-ketoenolate Complexes in $CDCl_3$-CCl_4 Solutions.

Parameters	$(CH_3)ClGe(acac)_2$	$(C_6H_5)ClGe(acac)_2$	cis-$Cl_2Ge(dpm)_2$ [c]	$(C_6H_5)ClSi(acac)_2$
E_a, kcal/mole	6.0 ± 0.3 [a]	12.8 ± 1.2	25.2 ± 1.4	6.4 ± 1.0
log A	6.65 ± 0.28	12.3 ± 0.8	13.00 ± 0.67	8.3 ± 1.0
$\Delta H^{\ddagger}$, kcal/mole	5.5 ± 0.3	12.2 ± 1.2	-	5.8 ± 1.0
$\Delta S^{\ddagger}$, e.u.	-30 ± 1	-13 ± 4	-1.1 ± 3.0	-22 ± 5
$\Delta G^{\ddagger}$, kcal/mole	14.43 ± 0.05	16.12 ± 0.07	-	12.5 ± 0.4
k,	160 $M^{-1}sec^{-1}$ [b]	9.4 sec^{-1}	3 X 10^{-6} sec^{-1}	4.2 X 10^{3} sec^{-1}
T_c, °C [d]	-13.3	44.5	197.0	-54.7

[a] Random errors estimated at the 95% confidence level.

[b] Second order rate constant; Concentration = 0.548 M.

[c] In diphenylmethane-m-dimethoxybenzene; Although this is a different solvent than in the other cases, solvent effects are not expected to contribute more than ca. 1-2 kcal/mole to E_a (cf. reference 117). Also the nature of the β-diketonate ligand, dpm vs acac does not appear to have significance in the value of E_a (cf. reference 30).

[d] ±1°.

phenomenon is exhibited in the germanium(IV) and silicon-(IV) acetylacetonate complexes. The rate of configurational rearrangement of the germanium(IV) acetylacetonate complexes decreases in the order $(C_6H_5)_2Ge$ > $(CH_3)ClGe$ > $(C_6H_5)ClGe$ > Cl_2Ge whereas for the silicon(IV) acetylacetonate complexes the order appears to be $(CH_3)ClSi$ > $(C_6H_5)ClSi$. This is the same order as in the tin complexes and definitely confirms the order of labilities. It is, therefore, not surprising, considering the greater labilizing effect of the methyl groups vs the phenyl groups on coordinated acetylacetonate ligands, that our efforts to observe coalescence behaviour in the $(CH_3)_2Sn(acac)_2$ complex proved unsuccessful. Although the activation energy, within experimental error, is independent of methyl and phenyl groups in $RClSn(acac)_2$, the activation energy of the diphenyltin complex is substantially lower, by ca. 6 kcal/mole, and the entropy of activation is also lower.

If the activation parameters of the $(C_6H_5)ClM(acac)_2$ (M = Sn,Ge,Si) complexes are compared there appear some noteworthy features. The rate of environmental averaging of -CH- protons in these three complexes increases as the metal varies in the order Sn ≈ Ge << Si. The energy of activation varies according to the series Sn ≈ Ge >> Si, E_a for the phenylchlorosilicon complex being about 6 kcal/mole smaller. This is unexpected if the rearrangement process occurs via a metal-oxygen bond rup-

ture mechanism (vide infra) since metal-oxygen bond strength increases (for gaseous diatomic molecules) in the order Sn-O (125 kcal/mole) < Ge-O (159 kcal/mole) < Si-O (188 kcal/mole)(98). Of significance is the energy of activation (25.2 ± 1.4 kcal/mole) in the environmental averaging of terminal t-butyl groups in the complex $Cl_2Ge(dpm)_2$, where the favored mechanism for the rearrangement process is rupture of a germanium-oxygen bond (30). Further, as has already been noted above, replacement of a chloro group in the dichlorogermanium complex by an aryl or alkyl group appears to have a dramatic influence on the stereochemical nonrigidity of these germanium chelates (3×10^{-6} sec^{-1} for the dichloro complex; 9.4 sec^{-1} for the phenylchlorogermanium complex). The difference of ca. 12-13 kcal/mole in the activation energies of these two complexes may probably be ascribed to different mechanisms for the exchange process.

Since both the phenylchlorotin and phenylchlorogermanium complexes have nearly identical activation parameters, it does not seem unreasonable to expect both $(CH_3)ClSn(acac)_2$ and $(CH_3)ClGe(acac)_2$ to have similar activation parameters. In the case of the former complex, the activation energy is 8.6 kcal/mole larger. This difference cannot be attributed to differences in electronic effects of the metal in view of similarities in the data of the phenylchloro complexes; however, it is not unexpected since

rearrangements in the tin complexes are intramolecular but intermolecular in the methylchlorogermanium complex (vide infra).

The activation parameters of $(C_6H_5)_2Sn(acac)_2$ appear to be nearly independent of solvent, while E_a for the phenylchlorotin complex in bromoform is 2 kcal/mole larger than in deuteriochloroform, but owing to the experimental uncertainty in measurements taken using the latter solvent any discussion of possible solvent effects is tenuous. An added observation is that at the coalescence temperature the $RClSn(acac)_2$ complexes are slightly more labile than the diphenyltin complex. The activation energy reported here for $(C_6H_5)ClSn(acac)_2$ does not agree with the low value of 3 kcal/mole reported by Kawasaki and Tanaka (28).

Recently, a report (103) on the study of intermolecular acetylacetonate ligand exchange between $(C_6H_5)_2Sn(acac)_2$ and $(CH_3)_2Sn(acac)_2$ complexes has indicated that the rate of exchange was first order in $[(C_6H_5)_2Sn(acac)_2]$, and the rate determining step was identified as rupture of one Sn-O bond in the diphenyltin complex; E_a = 7.5 ± 1.5 kcal/mole, $\Delta S^{\ddagger}$ = -33 ± 5 eu., k_{25} = 3.8 sec^{-1} ($CDCl_3$ solution). The activation energy for exchange of methyl groups in $(C_6H_5)_2Sn(acac)_2$ in deuteriochloroform solution (Table XVI) is 8.1 ± 0.3 kcal/mole, $\Delta S^{\ddagger}$ = -21.7 ± 1.4 eu

and $k_{25} = .369\ sec^{-1}$. The activation energy for the two processes is nearly identical within experimental error.

3. Determination of the Order of the Kinetics of Configurational Rearrangements

The phenomenon of broadening and collapse of -CH- and CH_3 proton resonances into a single sharp line in the high temperature limit is ascribed to a configurational rearrangement process in the chelate rings which exchanges acetylacetonate ring protons and methyl groups between the two and four, respectively, non-equivalent sites in the cis C_1 isomer; exchange of methyl groups in the diphenyl complex occurs between the two non-equivalent sites of the cis C_2 isomer. To describe this exchange process, one first-order rate constant is required in the case of the C_2 isomer (methyl groups) and C_1 isomer (-CH- protons); six independent first-order rate constants will define the methyl group exchange process in the C_1 methylchloro and phenylchloro complexes. In order to confirm the order of the kinetics of the configurational rearrangements, concentration dependence studies were undertaken. In the cases of $(C_6H_5)_2Sn(acac)_2$ and $(CH_3)ClSn(acac)_2$, solutions of five different concentrations of each complex in $CDCl_3$ were made up in the ranges 0.04 M to 0.12 M and 0.16 to 0.52 M, respectively. The mean residence times of these two complexes were then determined at a temperature below and above coalescence. For $(C_6H_5)ClSn(acac)_2$ in $CHBr_3$

solution only two concentrations were used to obtain lifetimes at several temperatures in the range 23° to 72°C. The results are presented in Table XVIII.

In order to determine the mean residence times of the various concentrations of a compound at any one temperature, the procedure used was as follows. Initially $\delta\nu$ in the absence of exchange is obtained for the temperature at which the concentration dependence study was carried out. This $\delta\nu$ is determined from the plot of $\delta\nu_e$ vs temperature obtained from the investigation of the variable temperature dependence of $\delta\nu$ (e.g., for $(C_6H_5)_2Sn(acac)_2$, $(CH_3)ClSn(acac)_2$ and $(C_6H_5)ClSn(acac)_2$, the desired data are presented in Figure 1). With the value of $\delta\nu$ and the appropriate T_2, a set of calculated lineshape parameters were obtained using program NICKA on the Sir George Williams University CDC Cyber 70-72 computer. The experimental lineshape parameters from each spectrum of the concentration dependence study were then compared to the calculated lineshape parameters at the corresponding temperature; then, the mean lifetimes were determined (the detailed procedure is described in Section II). If the rearrangement process were, for instance, a bimolecular process τ would then be dependent on the complex concentration. On the other hand, in a first-order process, the mean lifetime is independent of concentration since Rate = k[complex]. As is evident from Table XVIII, for the organo-

Table XVIII.- First-Order Check on the Kinetics of Configurational Rearrangements of Organotin(IV) Chelates.

$(C_6H_5)_2Sn(acac)_2$ in $CDCl_3$

Conc., M	τ(-50.4°) sec	τ(-39.4°) / sec
0.0405	0.101	0.057
0.0658	0.100	0.052
0.0838	0.102	0.047
0.1040	0.096	0.083
0.1209	0.099	0.058

$(CH_3)ClSn(acac)_2$ in $CDCl_3$

Conc., M	τ(22.4°) sec	τ(10.1°) sec
0.1602	0.025	0.045
0.2836	0.024	0.043
0.3396	0.023	0.048
0.4259	0.024	0.045
0.5231	0.023	0.043

$(C_6H_5)ClSn(acac)_2$ in $CHBr_3$

Temp., °C	2τ, sec	
	0.2414 M	0.3808 M
23.0	0.36	0.37[a]
36.3	0.12	0.13
37.2	0.16	0.12
49.4	0.048	0.050
53.6	0.037	0.038
63.1	0.020	0.020
71.9	0.011	0.012

[a] Obtained by interpolation at the appropriate temperatures from log k vs 1/T of Figure 14.

tin chelates the lifetimes are independent of concentration and therefore the rearrangement process for these complexes is first-order.

In the cases of $(C_6H_5)ClGe(acac)_2$ and $(CH_3)ClGe(acac)_2$, five concentrations of the former complex were made up in $CDCl_3$-CCl_4 in the range 0.22 to 0.48 M and four concentrations of the latter complex were made up in the range 0.27 to 0.52 M. The mean lifetimes were determined at two temperatures (for the phenylchloro complex + 30 and + 55.3° and for the methylchloro complex -31.5 and -2.2°) one below and one above coalescence; however, the method of determination of the lifetimes for these complexes had to be altered from the method described above for the tin complexes. This was necessitated by the resulting inconsistent variation of mean lifetimes with concentration on using program NICKA. Mean lifetimes showed neither first-order nor second-order trends.

For $(C_6H_5)ClGe(acac)_2$ the lifetimes were first determined using the same technique as was used for the tin complexes. The results are presented in Table XIX.

Except for a few fluctuations at both 30.0 and 55.3° the lifetimes would indicate a first-order process. However, these fluctuations are sufficiently large to make it difficult to arrive at a definite conclusion. Since changes in $\delta\nu$ reflect changes in τ, it follows that if τ

Table XIX.- Variation of Mean Lifetimes with Concentration for $(C_6H_5)ClGe(acac)_2$.

	Conc. M	$\delta\nu$ exp Hz	τ (30.0°) X 10^2 sec	τ (55.3) X 10^3 sec
(A)	0.4818	18.10	3.0	5.6
(B)	0.4331	18.69	4.0	6.0
(C)	0.3527	19.40	4.1	6.4
(D)	0.2970	19.35	3.4	5.8
(E)	0.2191	19.81	3.9	6.7

is independent of concentration then $\delta\nu$ should also be independent of concentration. A plot of $\delta\nu$ vs concentration for $(C_6H_5)ClGe(acac)_2$ at +30.0° (Figure 16a) indicates that $\delta\nu$ varies with concentration and consequently, the mean lifetimes ought to be also dependent. It is, therefore, incorrect to assume a priori that the $\delta\nu$ in the absence of exchange obtained from the plot of $\delta\nu$ vs temperature obtained from studies of the temperature dependence of the chemical shift (Figure 2) is constant at all concentrations of the phenylchlorogermanium complex. In fact, a different $\delta\nu$ may be required for each concentration. An alternative procedure was then devised in order to determine the appropriate values of $\delta\nu$ at a particular concentration. It was assumed that lines drawn through the different $\delta\nu$ values of Table XIX when these $\delta\nu$'s are plotted against tempera-

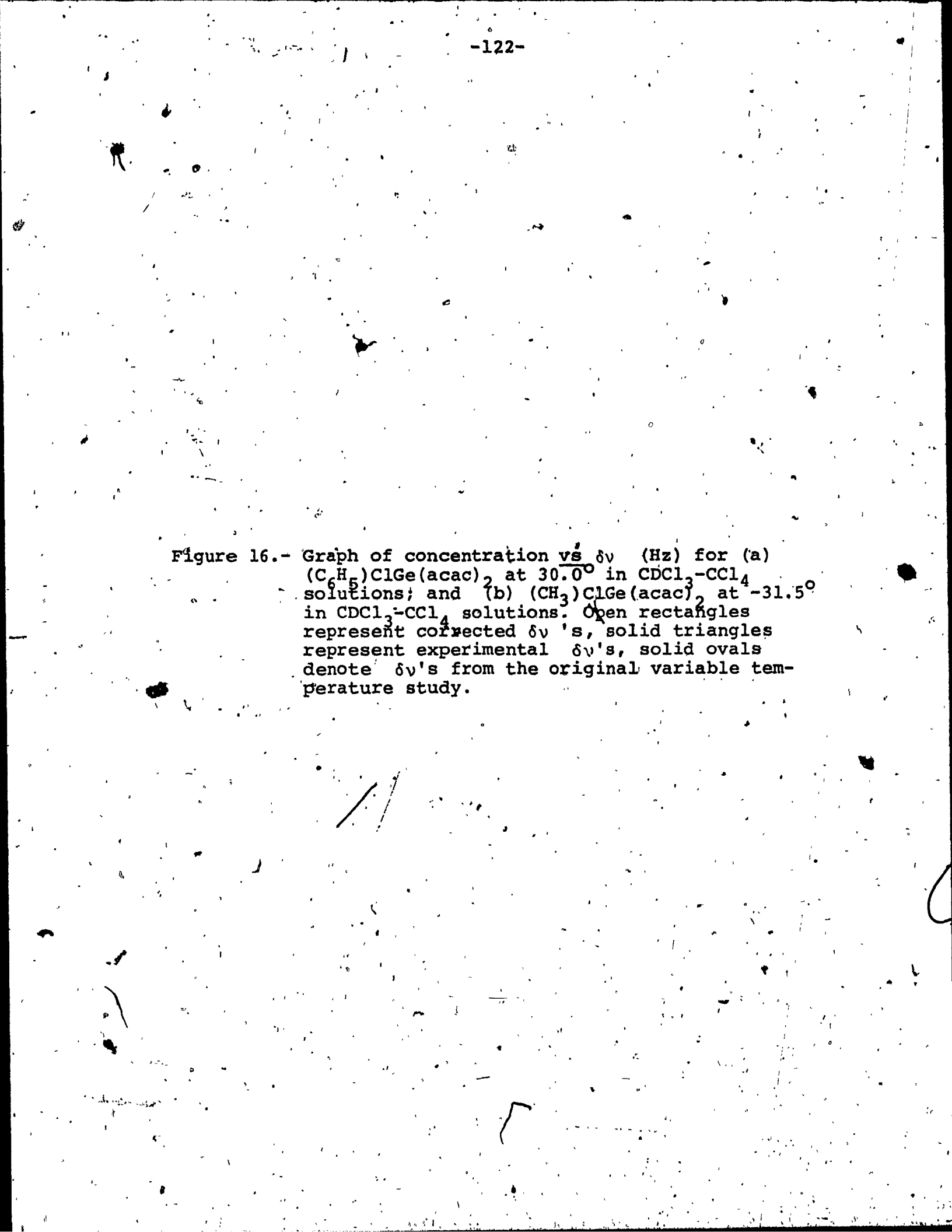

Figure 16.- Graph of concentration vs $\delta\nu$ (Hz) for (a) $(C_6H_5)ClGe(acac)_2$ at 30.0° in $CDCl_3$-CCl_4 solutions; and (b) $(CH_3)ClGe(acac)_2$ at -31.5° in $CDCl_3$-CCl_4 solutions. Open rectangles represent corrected $\delta\nu$'s, solid triangles represent experimental $\delta\nu$'s, solid ovals denote $\delta\nu$'s from the original variable temperature study.

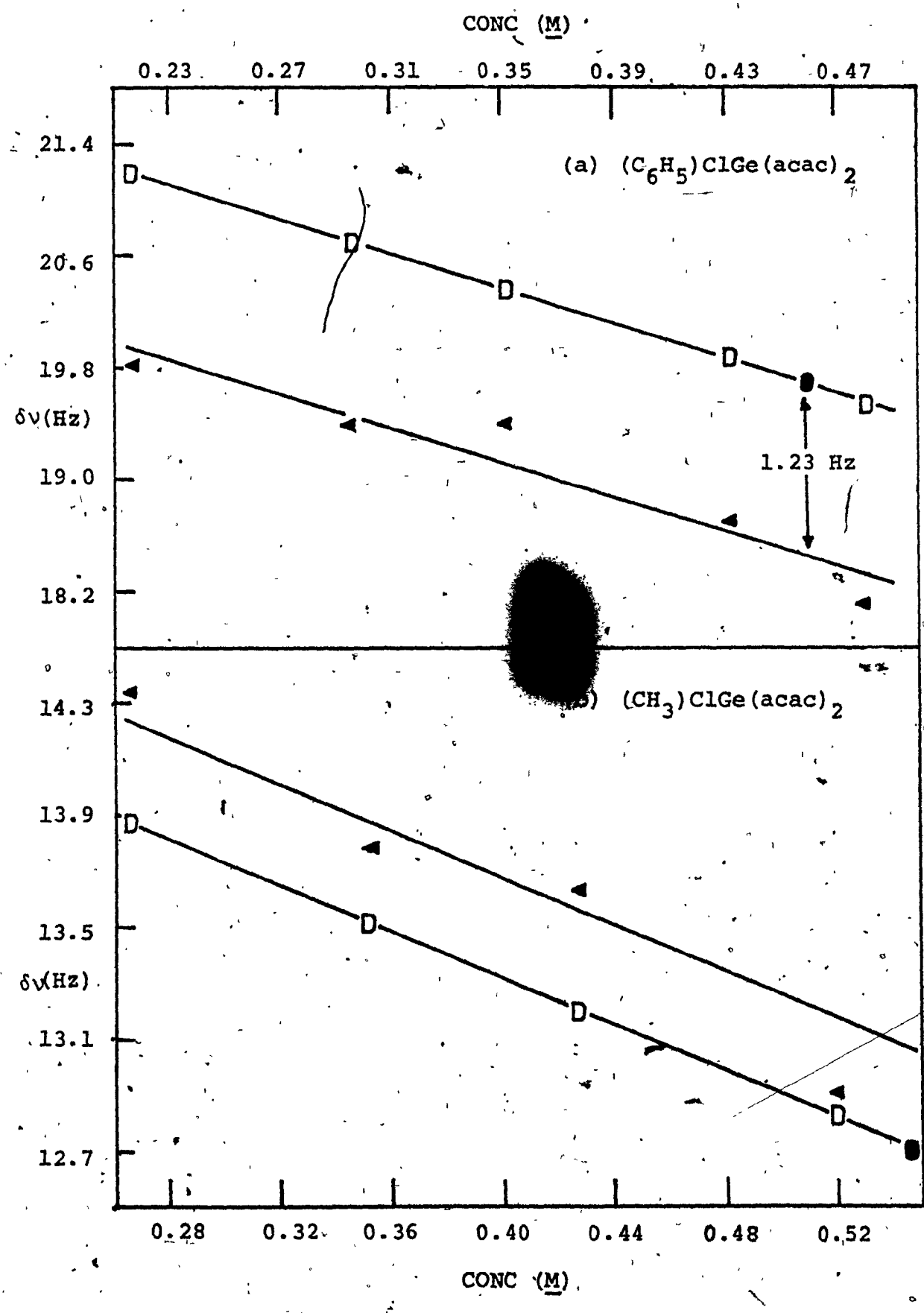
CONC (M)
0.23
0.27
0.31
0.35
0.39
0.43
0.47
21.4
20.6
19.8
δν(Hz)
19.0
18.2
(a) $(C_6H_5)ClGe(acac)_2$
D
1.23 Hz
14.3
13.9
13.5
δν(Hz)
13.1
12.7
$(CH_3)ClGe(acac)_2$
0.28
0.32
0.36
0.40
0.44
0.48
0.52
CONC (M)

ture have the same slope as that in Figure 2 for (C_6H_5)-ClGe(acac)$_2$. Consequently, the $\delta\nu$s obtained from the concentration dependence study had to be corrected. This was accomplished by positioning the $\delta\nu$ obtained from the plot of $\delta\nu_e$ vs temperature from the study of the temperature dependence of the chemical shift (these are at conc. = 0.4603 M, $\delta\nu$ = 19.67 Hz at 30.0° and 19.09 Hz at 55.3°) on the plot of $\delta\nu$ vs concentration (Figure 16a). Then a line was drawn through this point (19.67 Hz) which had the same slope as that of the concentration dependence study. A constant difference of 1.23 Hz (19.67- 18.44 Hz (Figure 16a)) is obtained. The position of the new $\delta\nu$ values for each concentration was then determined on the newly drawn line. The new values are presented in Table XX. Owing to the lack of a $\delta\nu$ value at 55.3° it was necessary to extrapolate the plot up to this temperature, again assuming that the slope (Figure 16a) of the lines at this temperature was the same as that of the 30.0° plot. A $\delta\nu$ of 19.09 Hz was obtained from the data of the original variable temperature study. A line is then drawn through this value of $\delta\nu$(19.09) parallel to the corrected line at 30.0° (Table XX). The constant difference between these two lines is 0.58 Hz (19.67 - 19.09 Hz). The corrected values at 55.3° are presented in Table XXI.

The new $\delta\nu$'s obtained for 30.0° and 55.3° were then submitted to program NICKA to obtain a new set of mean

Table XX.- Corrected Values of $\delta\nu$ for $(C_6H_5)ClGe(acac)_2$ at 30.0°

Solution	$\delta\nu$[a] Hz	(+) Const.	New $\delta\nu$ Hz
A	18.31	1.23	19.54
B	18.61	1.23	19.84
C	19.07	1.23	20.30
D	19.44	1.23	20.67
E	19.92	1.23	21.15

[a] Calculated from the least squares line.

Table XXI.- Corrected Values of $\delta\nu$ for $(C_6H_5)ClGe(acac)_2$ at 55.3°.

Solution	$\delta\nu$[a] Hz	(-) Const.	New $\delta\nu$ Hz
A	19.54	0.58	18.96
B	19.84	0.58	19.27
C	20.30	0.58	19.72
D	20.67	0.58	20.09
E	21.15	0.58	20.57

[a] $\delta\nu$ obtained from the corrected 30.0° line.

lifetimes; these are presented in Table XXII. The results in Table XXII indicate that the lifetimes at both temperatures are independent of concentration. However, it is possible that the above technique in obtaining a τ value is not justifiable. Therefore, another method was implemented using the curve fitting program NLINGH to access τ values at the different concentrations. The $\delta\nu$'s were allowed to vary in NLINGH for the data at 30.0°, but the $\delta\nu$'s at 55.3° were kept fixed for reasons already discussed in Section II. Values of τ from NLINGH are presented in Table XXIII. Upon comparing the results from programs NLINGH and

Table XXII.- Mean Lifetimes for $(C_6H_5)ClGe(acac)_2$ Obtained from Program NICKA Using Corrected $\delta\nu$'s.

Concentration M	$\tau(30.0^\circ) \times 10^2$ sec.	$\tau(55.3^\circ) \times 10^3$ sec.
(A) 0.4818	3.0	5.7
(B) 0.4331	3.9	5.9
(C) 0.3527	4.0	6.0
(D) 0.2970	3.3	5.3
(E) 0.2191	3.6	5.9

Table XXIII.- Mean Lifetimes for $(C_6H_5)ClGe(acac)_2$ Obtained by Using Program NLINGH.

Concentration M	τ (30.0°) X 10^2 sec	τ (55.3°) X 10^3 sec
(A) 0.4818	2.8	5.3
(B) 0.4331	4.2	5.8
(C) 0.3527	3.5	6.0
(D) 0.2970	3.0	4.9
(E) 0.2191	3.5	6.2

NICKA it can be seen that the results are nearly the same within experimental error. Thus our earlier technique in getting τ is justifiable. The above τ values for (C_6H_5)-$ClGe(acac)_2$ are essentially independent of concentration and it is concluded, therefore, that the rearrangement process is first-order.

For $(CH_3)ClGe(acac)_2$ in $CDCl_3$-CCl_4 solutions a similar technique was used to obtain $\delta\nu$ values as used for the phenylchloro complex. Residence times were initially determined using the values from the original variable temperature study (Figure 2) (these are at conc. = 0.5478 M, $\delta\nu$ = 12.70 Hz at -31.5° and $\delta\nu$ = 10.76 Hz at -2.2°) using program NICKA. These data are presented in Table XXIV.

Table XXIV.- Mean Lifetimes for $(CH_3)ClGe(acac)_2$ Obtained from Program NICKA.

	Concentration M	$\delta\nu_{exp}$ Hz	$\tau(-31.5^{\circ})$ X 10^2 sec	$\tau(-2.2^{\circ})$ X 10^2 sec
(A)	0.5212	12.91	5.5	1.7
(B)	0.4283	13.63	8.1	2.5
(C)	0.3522	13.78	8.2	3.2
(D)	0.2671	14.34	12.7	2.8

In this case the lifetimes vary with concentration. Also a plot of $\delta\nu$(experimental) vs concentration at -31.5° (Figure 16b) shows that $\delta\nu$ is concentration dependent. As in the last case a $\delta\nu$ was obtained from the original variable temperature study at the appropriate temperature and concentration. A line was then drawn through the point (12.70 Hz) for the -31.5° data parallel to the line for the data of the concentration dependence study (Figure 16b). For the data at -31.5° the constant difference between the two lines is 0.14 Hz (Figure 16b at conc. = 0.5478 M. 12.84 - 12.70 Hz). The new $\delta\nu$'s are presented in Table XXV. Similarly, for the data at -2.2° the same technique was used, but since there are no $\delta\nu$'s available at this temperature the slope is parallel to that at -31.5°, the constant difference between the two lines is 1.94 Hz (12.70 - 10.76 Hz). The corrected $\delta\nu$'s are

Table XXV.- Calculation of Corrected $\delta\nu$ for $(CH_3)ClGe(acac)_2$ at -31.5°.

Solution	$\delta\nu$[a] Hz	(-) Const.	New $\delta\nu$ Hz
A	13.98	0.14	12.84
B	13.47	0.14	13.33
C	13.88	0.14	13.74
D	14.33	0.14	14.19

[a] Calculated from the least squares line.

presented in Table XXVI. The new $\delta\nu$'s were then submitted to program NICKA to calculate a new set of mean lifetimes (Table XXVII). At this point the difference in the lifetimes, especially at -31.5°, indicates concentration dependence. Therefore, to further confirm this phenomenon, the lifetimes were also determined using the computer digitization NLINGH technique. The results are presented in Table XXVIII. A typical series of matches of experimental and calculated spectra using program NLINGH for $(CH_3)ClGe(acac)_2$ at -2.2° is illustrated in Figure 17. Figure 17a exhibits experimental spectra at several concentrations while Figure 17b shows the comparison between the experimental spectra (solid circles) and the computer-fitted spectra (solid triangles; open circles represent good fit).

Table XXVI.- Calculation of Corrected $\delta\nu$ for $(CH_3)ClGe(acac)_2$ at -2.2°.

Solution	$\delta\nu$[a] Hz	(-) Const.	New $\delta\nu$ Hz
A	12.84	1.94	10.90
B	13.33	1.94	11.39
C	13.74	1.94	11.80
D	14.19	1.94	12.25

[a] These are the corrected $\delta\nu$'s at -31.5°

Table XXVII.- Mean Lifetimes for $(CH_3)ClGe(acac)_2$ Obtained by Using Program NICKA.

Concentration M	$\tau(-31.5^{\circ}) \times 10^2$ sec	$\tau(-2.2^{\circ}) \times 10^2$ sec
(A) 0.5212	5.5	1.6
(B) 0.4283	7.9	2.2
(C) 0.3522	7.8	2.4
(D) 0.2671	12.2	2.4

Figure 17.- Acetylacetonate ring proton spectra as a function of concentration for $(CH_3)ClGe(acac)_2$ in $CDCl_3$-CCl_4 solutions at -2.2°; (a) experimental spectra; (b) comparison of experimental and calculated nmr spectra; solid circles represent experimental points, solid triangles represent calculated points, and open circles denote perfect fit of experimental and calculated points.

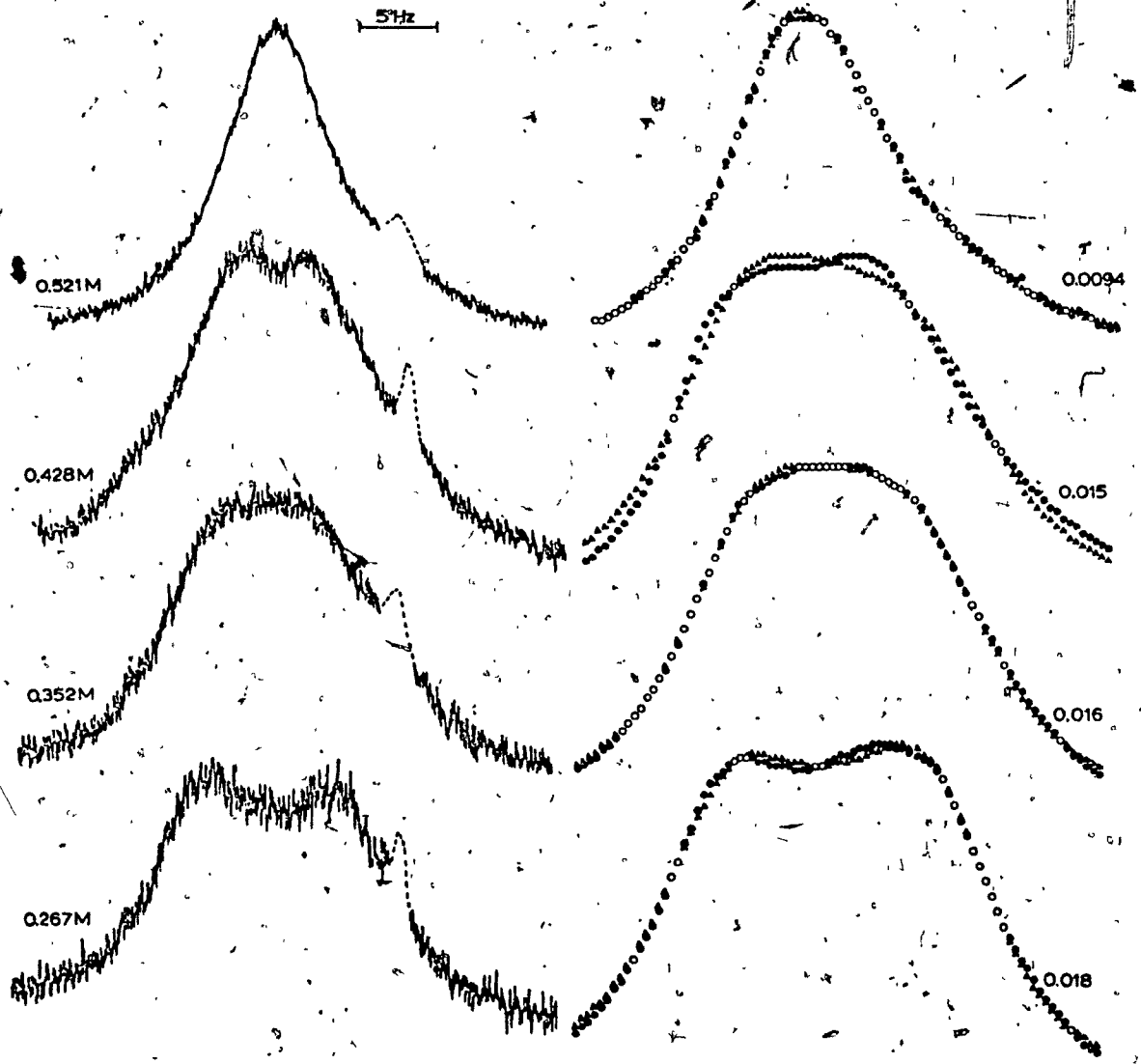
5Hz
0.521M
0.428M
0.352M
0.267M
0.0094
0.015
0.016
0.018
(a)
(b)

Table XXVIII.- Mean Lifetimes for $(CH_3)ClGe(acac)_2$ Obtained by Using Program NLINGH.

Concentration M	$\tau(-31.5^{o}) \times 10^2$ sec	$\tau(-2.2^{o}) \times 10^2$ sec
(A) 0.5212	4.8	0.94
(B) 0.4283	6.3	1.5
(C) 0.3522	7.2	1.6
(D) 0.2671	9.7	1.8

From the results presented above it becomes evident that environmental averaging of -CH- protons for $(CH_3)ClGe(acac)_2$ is concentration dependent and follows second-order kinetics. This dependence is also exhibited in Figure 18 which shows linear plots of τ_A vs $\left[(CH_3)ClGe(acac)_2\right]^{-1}$ at -31.5^{o} and -2.2^{o}. Thus, the rate of environmental averaging may be written as; Rate $= k\left[(CH_3)ClGe(acac)_2\right]^2$; since $\tau_a^{-1} = \left[(CH_3)ClGe(acac)_2\right]^{-1} \times$ Rate $= k\left[(CH_3)ClGe(acac)_2\right]$. From the slope of the linear plot at -31.5^{o} of Figure 18, $k = 19\ \underline{M}^{-1}sec^{-1}$, which is in good agreement with $k = 16\ \underline{M}^{-1}sec^{-1}$ obtained from the log k vs 1/T plot (Figure 15).

The original variable temperature study for $(C_6H_5)ClSi(acac)_2$ involved data from both below and above coalescence; however, for the purposes of the concentra-

Figure 18.- Plots of the mean lifetime τ_A as a function of $\left[(CH_3)ClGe(acac)_2\right]^{-1}$ at the indicated temperatures.

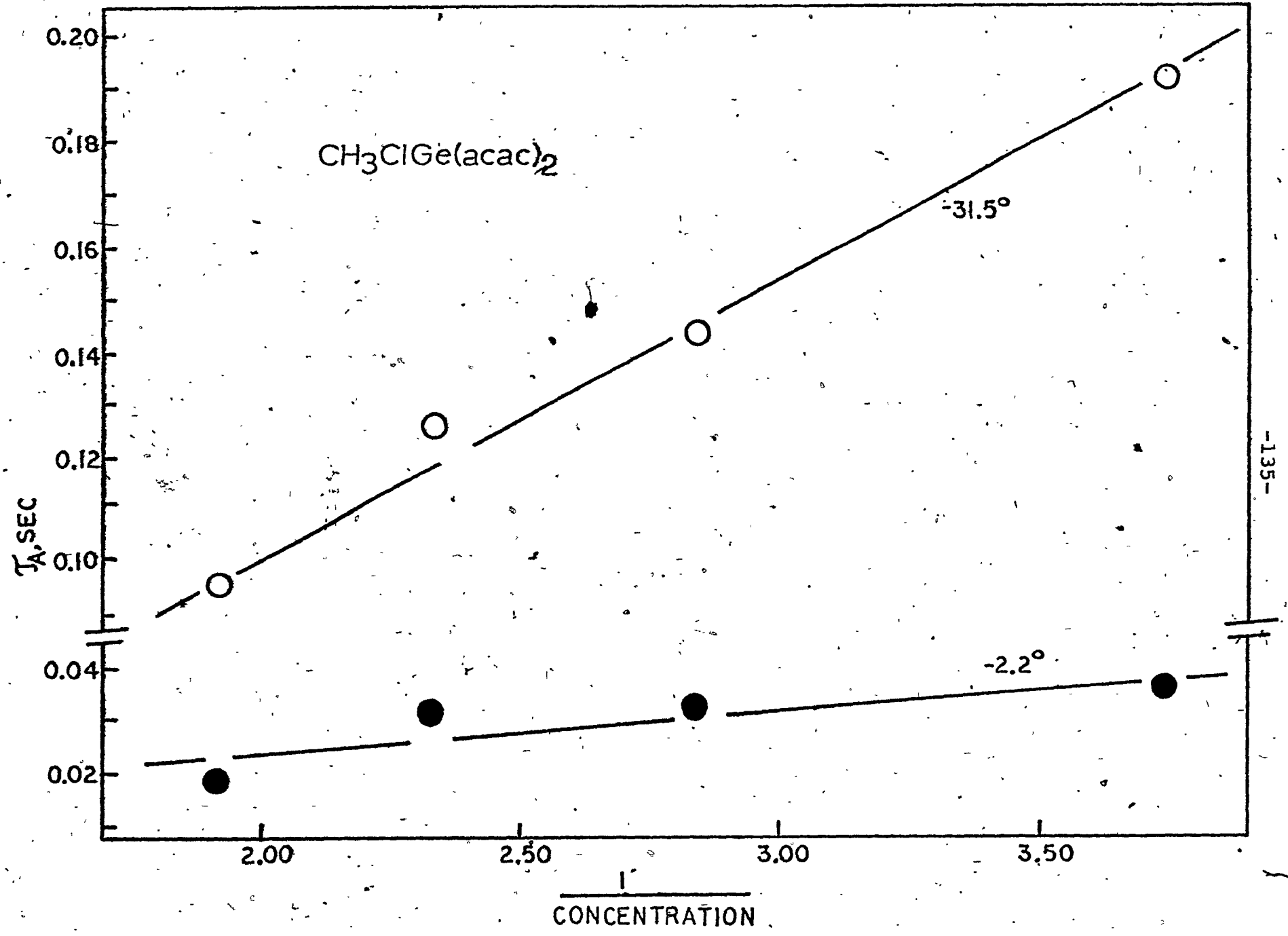
0.20
0.18
0.16
0.14
0.12
0.10
0.04
0.02
τ_A, SEC
$CH_3ClGe(acac)_2$
-31.5°
-2.2°
2.00
2.50
3.00
3.50
1/
CONCENTRATION

tion dependence study and because of solubility limitations, only one temperature below coalescence (-70°C) was studied. In this case, as in the case of the variable temperature chemical shift study (Figure 2), the spectra were digitized and curve-fitted with program NLINGH as described earlier. For these data the $\delta\nu$'s were allowed to vary and find their own values. The results are presented in Table XXIX. An attempt was made to use program NLINGH keeping the $\delta\nu$'s fixed, however, this procedure led to poor spectral fits. Mean lifetimes are independent of concentration and the rearrangement process for $(C_6H_5)ClSi(acac)_2$ is first-order.

Table XXIX.- Mean Lifetimes for $(C_6H_5)ClSi(acac)_2$ Obtained by Using Program NLINGH.

Concentration M	$\tau(-70.0^{\circ})$ X 10^2 sec
0.3096	1.4
0.2798	1.6
0.2178	1.5
0.1567	1.5
0.09496	1.3

4. Comparison of Results from Programs NLINGH and NICKA

As has been previously described (Section II), two methods were used to determine lifetimes for the complexes in this work. A method mainly used for the tin and germanium compounds was one whereby parameters were manually determined from the various spectra. These parameters were then compared with a calculated normalized digital spectrum which was produced by program NICKA on the Sir George Williams University CDC Cyber 70-72 computer. The results of this comparison produced the appropriate lifetimes. On the other hand, many of these spectral parameters were not available in the case of $(C_6H_5)ClSi(acac)_2$, and consequently, another technique was utilized. Here, the experimental spectra were digitized by the Hewlett-Packard 2114A computer. The experimental spectra were then internally fitted with program NLINGH on the Sir George Williams University CDC Cyber 70-72 computer. This program also produced the appropriate lifetimes. As is inevitable when using two different techniques to obtain similar results there may occur variations between these results. We wished to assure ourselves that the results we obtained from the two programs were indeed comparable and consistently valid. Also, we wished to assure ourselves that the activation parameters obtained for $(C_6H_5)ClSi(acac)_2$ were not an artifact of the

particular method used. In order to test this, a compound was chosen for which we could calculate lifetimes by both methods. The compound chosen was $(CH_3)ClSn(acac)_2$. The lifetimes at each temperature were calculated using both the NICKA technique and the NLINGH technique. The results were then plotted as Log k vs 1/T as illustrated in Figure 11 and tabulated in Table XXX. In the data using the NICKA technique there is a great variation of points at the two extremes of the temperature range. This variation illustrates the consequences of attempting to obtain rate data too far from coalescence where spectral parameters are insensitive to changes in the rate phenomena and consequently, true mean lifetimes become difficult to estimate. These anomalous data were not used for the NLINGH calculation as it would not have been any more fruitful. Nevertheless, a linear plot (the dark line in the plot is the least squares line of the NICKA method) is obtained in the optimum region. When the same spectra were submitted for calculation by NLINGH the results are almost equivalent to those produced by NICKA. The data were calculated with NLINGH allowing the program a) to find its own $\delta\nu$'s and b) giving it fixed $\delta\nu$'s. Both of these approaches yielded similar results. In fact they lie on the same least squares line drawn for the NICKA results.

The data would thus seem to indicate that within experimental error the results from both the NICKA and

Table XXX.- Results of the Comparison of Programs NICKA and NLINGH

Temperature °C	NLINGH $2\tau \times 10^1$ sec ($\delta\nu$ var.)	NLINGH $2\tau \times 10^1$ sec ($\delta\nu$ fixed)	NICKA $2\tau \times 10^1$ sec
-44.5	-	-	7.545
-37.6	-	-	6.880
-29.3	-	-	9.336
-25.0	-	-	7.870
-20.2	-	-	5.968
-15.9	-	-	8.101
-8.6	-	-	4.382
-0.5	2.700	3.043	2.850
4.5	1.600	1.808	1.650
7.5	1.159	1.351	1.318
11.5	0.783	0.892[a]	0.877
13.5	0.651	0.747[a]	0.684
16.0	0.554	0.640[a]	0.623
21.5	0.344	0.396	0.389
26.5	0.243	0.302	0.284
29.5	0.149	0.186	0.182
45.5	-	-	0.112
54.7	-	-	0.041

[a] Gave a poor fit.

NLINGH techniques are equivalent and both methods can be used interchangeably, as it should be. This also reassures the validity of each technique as they both use different approaches to yield similar results. Therefore, these two methods effectively check each other.

5. Methyl Proton NMR Region

A feature of mechanistic significance concerns the four methyl signals in Figures 6 to 10. The components of the lower field and higher field doublets in the (CH_3)-$ClSn(acac)_2$ spectra (Figure 6) appear to broaden and collapse simultaneously with increasing temperature to yield a single doublet at 4.5°. As the temperature is further increased, the components of this doublet broaden and the doublet finally coalesces at 21.5°. The methyl proton resonances in $(C_6H_5)ClSn(acac)_2$ (Figure 7), (CH_3)-$ClGe(acac)_2$ (Figure 10), $(C_6H_5)ClGe(acac)_2$ (Figure 8), and $(C_6H_5)ClSi(acac)_2$ (Figure 9) undergo similar coalescence phenomena except that in the latter three complexes the methyl spectra are poorly resolved. It is also noted that the -CH- proton signals undergo broadening and coalescence in the same temperature range as the methyl resonances, so that whatever the mechanism responsible for the nmr coalescence behavior, both the ring protons and methyl groups are exchanged between their respective nonequivalent sites by the same physical process.

The magnitude of the $Sn-CH_3$ proton coupling to the lowfield component of the two cis methyl signals in $X_2Sn(acac)_2$ (X = Cl, Br, or I) has been observed to be larger than to the upfield component (24,34). This has led to the assignment (24) of the lower field resonance to the unique pair of CH_3 groups in the nonequivalent site trans to the halo groups. Also the lowfield and highfield methyl resonances of $Cl_2Sn(acac)_2$ are shifted upfield by 0.62 and 0.54 ppm (24), respectively, on going from deuteriochloroform to benzene solvent. A solvation model with benzene molecules in tangential contact with the surface of the complex (104) and clustered about the C_2 axis of $X_2Sn(acac)_2$ predicts that methyl groups trans to X groups will exhibit the larger upfield shift. Hence, the lower field methyl signal has been associated with acetylacetonate methyl groups trans to X groups (24). Moreover, the methyl groups trans to the methoxy groups in dimethoxybis(N,N,N',N'-tetramethylmalonamidato)titanium(IV) were assigned to the lower field resonance by Weingarten and coworkers (105) on the basis of the more rapid loss of rotation of the $N(CH_3)_2$ group trans to the monodentate methoxy ligands. We have not been successful in estimating the magnitudes of $J(Sn-CH_3)$ to the four nonequivalent methyls owing to the broadness of the resonances and to the expected low values of J (≈ 2-3 Hz(90)). However, at 11.7° the solvent shift on passing from deuteriochloroform

to benzene, $\Delta^{CDCl_3}_{C_6H_6}$, is 0.50 ppm for the unresolved (at 500 Hz sweep width) lowfield doublet in the $(C_6H_5)ClSn(acac)_2$ spectra while that of the higher field doublet is 0.41 and 0.46 ppm, respectively, for the downfield and upfield component. In the methylchlorotin spectra at 13.8°. $\Delta^{CDCl_3}_{C_6H_6}$ of the lowfield doublet (unresolved at this temperature) is 0.43 ppm, that of the upfield doublet is 0.36 ppm (the tin-methyl proton signal suffers a diamagnetic downfield shift by 0.19 ppm on going from deuteriochloroform to benzene). Accordingly, we assign the lowfield doublet to the unique acetylacetonate methyl groups trans to, and equatorial with, the monodentate ligands in the phenylchloro and methylchloro complexes which are represented in the case of the tin chelates in Figures 6 and 7 and for the germanium and silicon chelates in Figures 8 to 10. Coalescence of the four methyl signals to a single resonance in the spectra of both complexes is attributed to a configurational rearrangement process which time-averages the methyl proton environments among the four nonequivalent sites of the cis isomers. The only complex which yielded sufficiently resolved spectra that could be used for analysis was $(CH_3)ClSn(acac)_2$ (Figure 6). Initially, an attempt was made to obtain activation parameters for the methyl proton system using the two-site exchange program NICKA. To accomplish this, the coalescence phenomena of the lowfield (A-B) and upfield (C-D) doublet

(see Figure 6) were treated as two separate two-site exchange processes from -10.1 to 3.0°. (see Table XXXI). Above ca. 4°, the methyl spectrum consists only of a doublet (AB-CD) also undergoing line-broadening and coalescence with increase in temperature to yield a single, sharp line (ABCD) in the high temperature limit. Using this technique, of course, involved certain assumptions: a) the doublet AB exchanges independently of doublet CD and, b) peaks AB and CD exchange between each other without considering the exchange that might be occurring under each of the individual envelopes. Assuming this to be the situation the spectral and kinetic parameters are presented in Table XXXI. As is apparent, the activation parameters obtained here are far from even similar to those presented in Table XVI. Therefore, it would seem that the assumptions made above for utilizing this technique may not be valid in this case.

Considering that exchange may be occurring among all four methyl sites it was necessary to use a multisite exchange computer simulation-curve fitting program DNMR3 (106), adapted for the Sir George Williams University CDC Cyber 70-72 computer (see Appendix). This program simulates a given exchange matrix and produces the resulting calculated spectrum within given parameters. These include, the rate constant, fractional populations of each site, transverse relaxation time, T_2, in the absence of exchange,

Table XXXI.- Spectral and Exchange Parameters for the Acetylacetonate Methyl Region of $(CH_3)ClSn(acac)_2$ Using Program NICKA.

Temperature	A-B Doublet		C-D Doublet	
°C	δν Hz	τ X 10^2 sec	δν Hz	τ X 10^2 sec
-10.1	1.91	104.	2.22	88.8
-6.8	1.86	86.1	2.15	77.3
-2.3	1.80	66.6	2.06	75.5
1.3	1.76	56.8	1.98	53.3
2.6	1.74	46.8	1.95	45.0
3.0	1.73	49.1	1.94	47.3
	AB - CD Doublet			
17.5	9.38	9.09		
22.6	9.08	7.69		
26.2	8.86	5.96		
33.8	8.41	4.06		
47.5	7.59	2.10		

Activation Parameters

	E_a (kcal/mole)	$\Delta S^{\ddagger}$ (e.u.)	k_{25} (sec^{-1})
A - B Doublet	8.5 ± 1.4	-28 ± 5	6.4
C - D Doublet	7.3 ± 3.6	-33 ± 13	5.5
AB - CD Doublet	9.3 ± 1.2	-24 ± 4	16

chemical shifts from an arbitrary zero point of the experimental spectrum, description of the exchange matrix, and the description of the desired plot parameters (i.e. frequency range, scale, height). The program then produces a plot of the calculated spectrum. In our case, the plots generated by DNMR3 were first written on magnetic tape by the CDC computer; the actual hard-copy plot was obtained on a Complot digital plotter (model DP-1-5) interfaced with a Hewlett-Packard 2114A computer and tape drive. This plot was then manually superimposed upon the experimental spectrum to assess closeness of fit. If any corrections were necessary a new set of values of the rate constant were given to program DNMR3. This technique was used with the four-site methyl proton spectra of $(CH_3)ClSn(acac)_2$ in the range 17.5° to 47.5°C (Figure 19). The initial problem, of course, was to decide on which exchange matrix to use. Various pathways may be described when going from the initial matrix, (1234)*, to a final matrix, eg., 2134, 1243 or any combination of 1234. Each exchange may represent a different mechanism, although it is possible that two final

---

* This matrix designation describes the four possible sites where exchange could take place for the compounds of interest. Program DNMR3 allows for up to eight possible exchange sites but this number was not required here.

Figure 19.- Computer calculated spectra of the acetylacetonate methyl region of $(CH_3)ClSn(acac)_2$ in the range 17.5° to 47.5°C using program DNMR3.

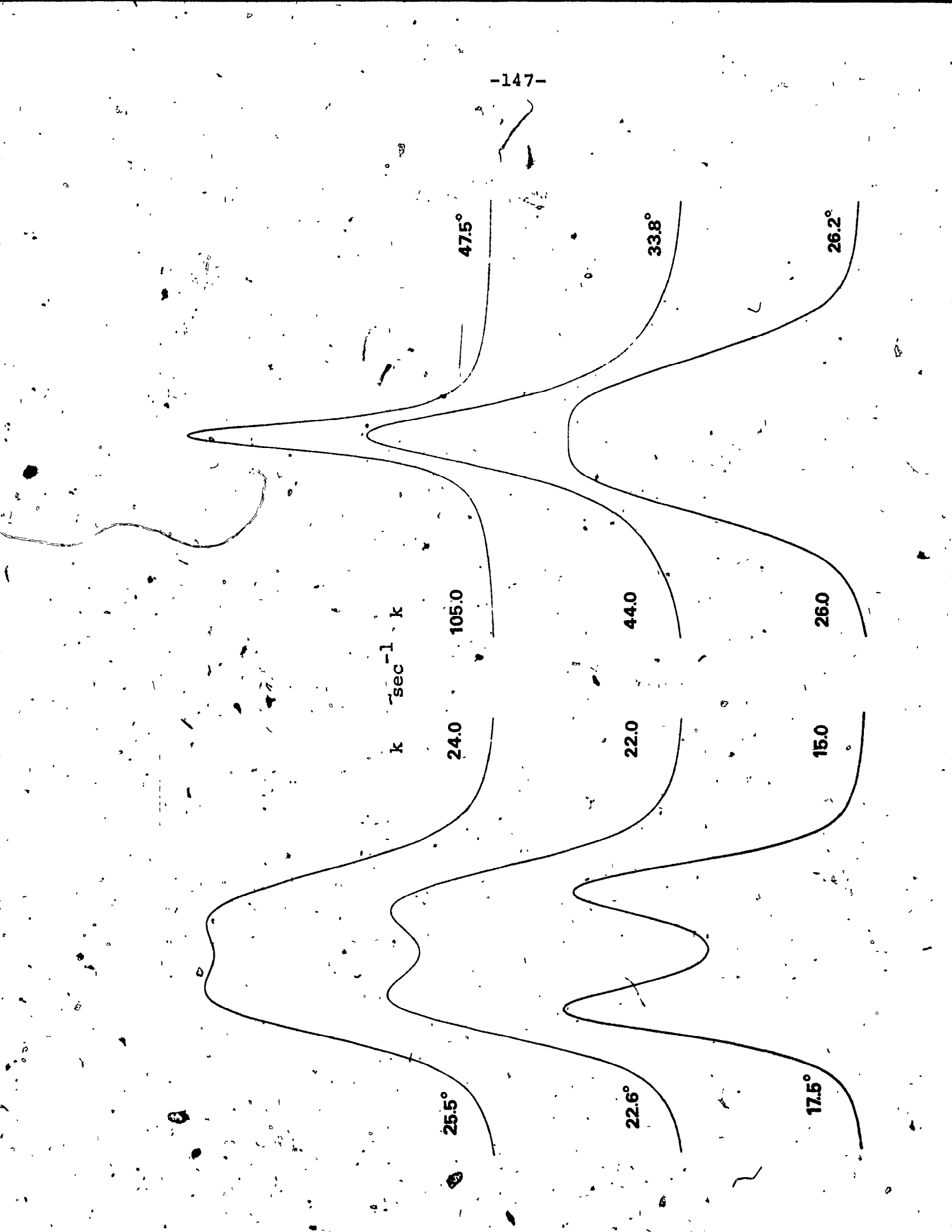
47.5°
33.8°
26.2°
k sec⁻¹ k
105.0
44.0
26.0
k
24.0
22.0
15.0
25.5°
22.6°
17.5°

pathways described by 1234 → 4321 and 1234 → 3412 might be equivalent, but produce different spectra. It is also possible that under various conditions of chemical shifts and rate constants different pathways may yield identical spectra. Nonetheless, all exchange matrices were evaluated to determine the most reasonable pathway for $(CH_3)ClSn(acac)_2$. Pathways where only two or three sites interchanged (e.g., final matrices 1234 or 1423) were eliminated entirely. Only exchange matrices leading to random scrambling of the four methyl sites are consistent with the experimentally observed coalescence behaviour (but see reference 113). Out of the possible six random-scrambling matrices, four matrices, namely 4123, 2341, 3142 and 2413 produced identical spectra (Figure 19) which were also good matches to the experimental spectra. The random scrambling matrices 3421 and 4312 did not yield spectra identical to those from the above four under the same input parameters. Most probably these latter two matrices are not encountered among the possible physical pathways. The above procedure does not take into consideration the possibility that additional intermediate exchange processes occur, consequently it may be oversimplifying the processes that do take place. With this matching technique a rate constant was determined at each temperature. A linear least-squares plot of Log k vs 1/T for the best spectral fit yielded the following activation parameters: E_a = 12.0

± 1.0 kcal/mole, log A = 10.2 ± 0.7, $\Delta H^{\ddagger}_{298}$ = 11.4 ± 1.0 kcal/mole, $\Delta S^{\ddagger}_{298}$ = -13.8 ± 3.4 eu, $\Delta G^{\ddagger}_{298}$ = 15.55 ± 0.03 kcal/mole, k_{298} = 25 sec^{-1}. Only the overall rate constant for exchange between the four sites is reported. Rate constants for exchange between any two sites were not accessible with this method of computer fitting. Differences between the above values and those presented in Table XVI are probably the result of using different T_2 values and the rather poor fit in the region of the signals below one-quarter of the maximum height. Considering these limitations values of activation parameters are in reasonable agreement.

6. Mechanisms of Environmental Averaging

Various mechanisms that can lead to averaging of ring proton and methyl group environments in neutral β-ketoenolate complexes of the type $M(dik)_2X_2$ have been discussed in some detail (1). The following processes could interchange the R group substituents between the two environments: (a) dissociation of a monodentate ligand to give a five-coordinate intermediate; (b) complete dissociation of a diketonate ligand to yield a four-coordinate intermediate; (c) momentary rupture of one metal-oxygen bond to give a trigonal bipyramidal (TBP) transition state with the dangling ligand in the axial or equatorial positions, or a square pyramidal (SP) transition state with a

basal or axial dangling ligand, and (d) twist motions of the ligands to give an idealized trigonal prismatic (TP) intermediate.

In the discussion of rearrangement mechanisms it should be noted that only slight variations in the bond angles and bond distances are necessary in order to form intermediates of differing geometry. For example, a twist about a C_3 axis of an ideal ML_6 octahedral complex to give a D_{3h} transition state must be accompanied by an increase in the M-O bond length in order to compensate for the increased steric repulsion in the transition state. Similarly, after rupture of one M-L bond of an ML_6 complex slight rearrangements can lead to either of two ML_5 intermediates. That is, the vacant coordination site permits relaxation of the bond angles (<LML) from the octahedral values. Such minor changes and also migration of bound ligand atoms to vacant sites are quite probable and may occur <u>via</u> pathways of low energy. Rearrangement of two different ML_5 transition states is illustrated below.

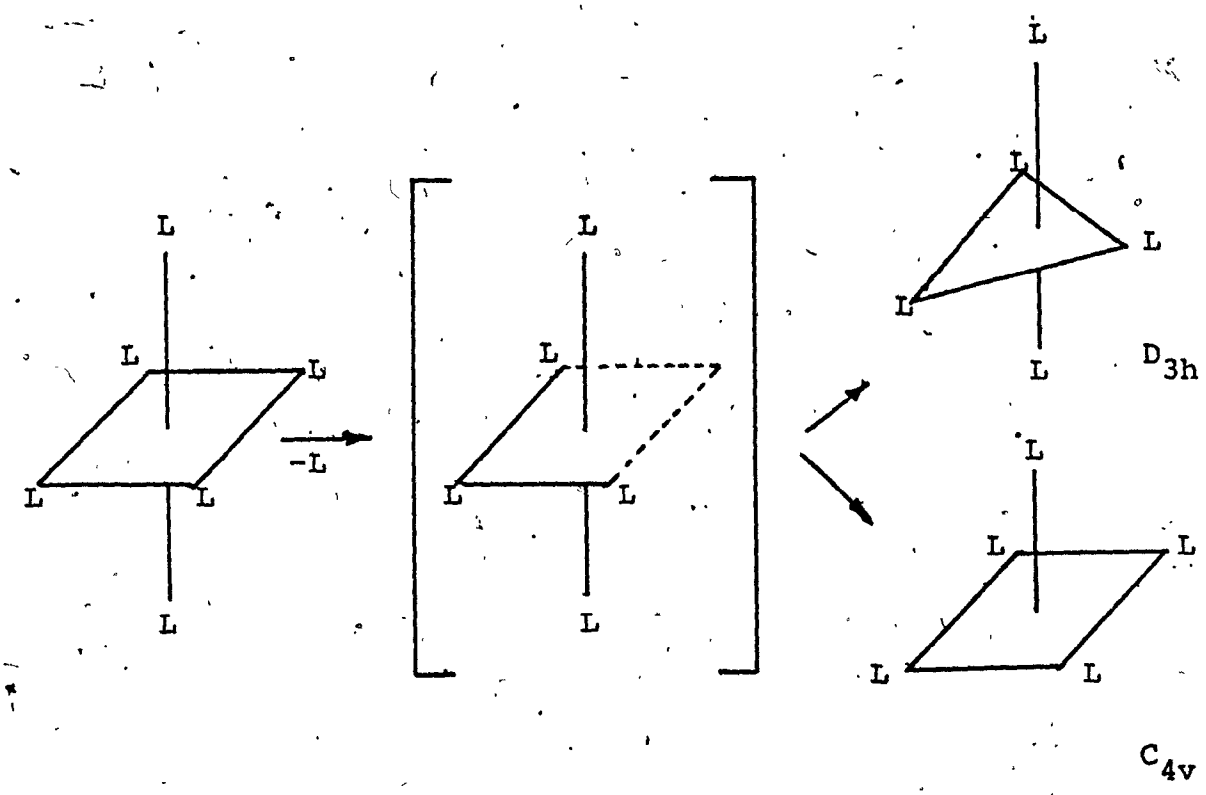

We now look at the above-mentioned four possible physical processes that could lead to environmental averaging of -CH- and/or CH_3 groups. (a) Configurational rearrangements in $M(dik)_2X_2$ or $M(dik)_2XY$ can result from dissociation of a monodentate ligand such as a methyl, phenyl, or halogen group

$$M(dik)_2XY \longrightarrow M(dik)_2X^+ + Y^- \qquad 9$$

If this were the case and if the dissociated ion became part of the bulk dissociated ion concentration then there can form a five-coordinated intermediate complex. As is illustrated in Figure 20 the remaining coordinated halogen,

Figure 20.- Possible five-coordinate intermediates as a result of methyl, phenyl or halide dissociation.

TBP Intermediates

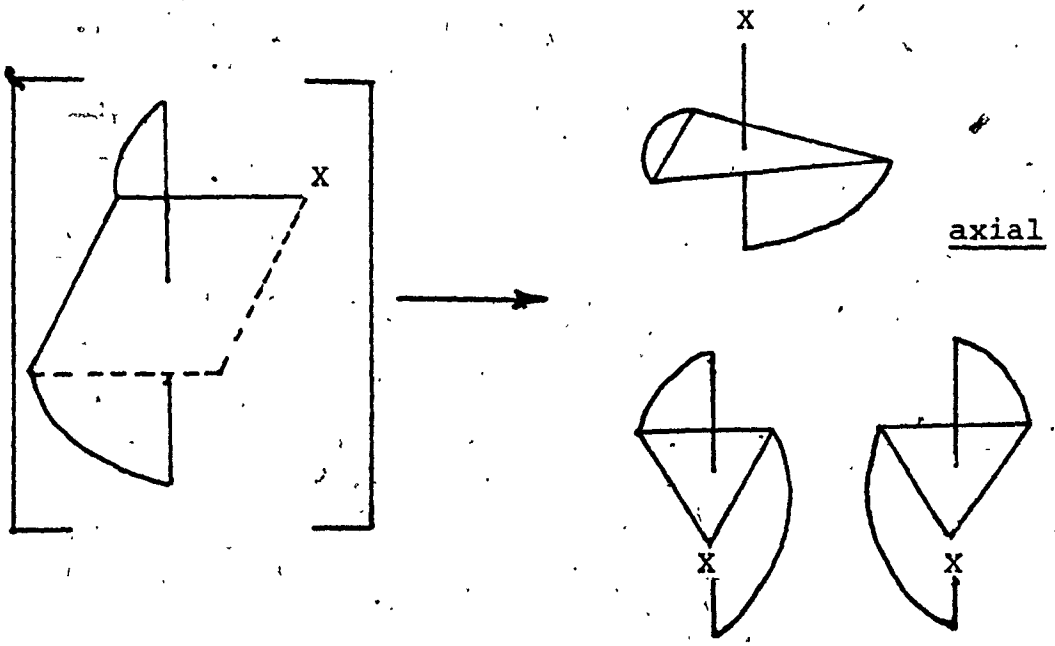

SP Intermediates

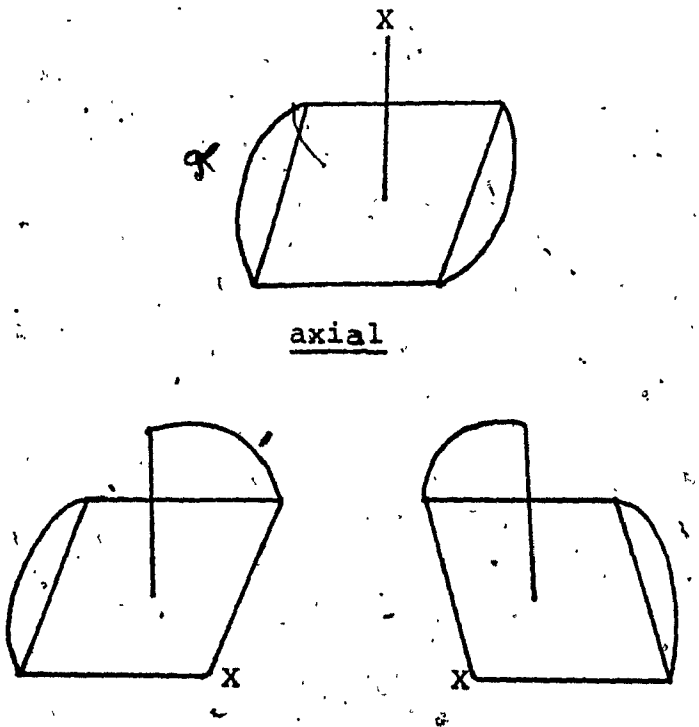

alkyl, or aryl group may occupy equatorial or axial positions in both the TBP and SP intermediates. Those intermediates lacking a mirror plane exist as enantiomeric pairs (107). Dissociation of a methyl or phenyl group in a medium such as CH_2Cl_2, $CDCl_3$, or $CHBr_3$ is not likely owing to a high bond dissociation energy (of the order of ca. 100 kcal/mole (108)); also, an equimolar mixture of $(C_6H_5)_2Sn(acac)_2$ and $(CH_3)_2Sn(acac)_2$ in $CDCl_3$ (or $CHBr_3$) yields no nmr resonances attributable to the mixed complex $(C_6H_5)(CH_3)Sn(acac)_2$. However, equimolar mixtures of $X_2Sn(acac)_2$ and $Y_2Sn(acac)_2$ in 1,1,2,2-tetrachloroethane yield an equilibrium mixture containing the parent complexes as well as the mixed complex $XYSn(acac)_2$ (X = Y = F, Cl, Br, or I), but halide exchange appears to be slow compared to methyl group exchange (30). In addition, ^{36}Cl exchange between $Cl_2Sn(acac)_2$ and tetraethylammonium chloride is slow ($k_{15} = 0.0018\ M^{-1}sec^{-1}$) (109). In the case of the germanium complexes it was found that $Ge(dpm)_2I_2$ (30) was ca. 8 to 13% more dissociated than the corresponding tin complex. However, a dissociative mechanism was discounted (30) because the rate of dissociation was much slower than methyl group exchange. Chloride exchange is also expected to be slower than methyl group exchange in $RClM(acac)_2$ (M = Sn, Ge or Si) complexes; (b) It is possible that enviromental averaging proceed via bidentate ligand dissociation:

$$M(dik)_2XY \longrightarrow M(dik)XY^+ + dik^- \qquad 10$$

However, available evidence argues against this mechanism. Tin-ring proton coupling in both methylchlorotin and phenylchlorotin complexes is observed before (∿2.5-3 Hz) and after (∿2 Hz) (90) coalescence: $J(Sn-CH_\gamma)$ is too small to be observed during coalescence. These data suggest that acetylacetonate ligands remain attached to the tin atom, at least through one oxygen, even though Sn-O bond breaking may be fast (110). Faller and Davison (23) have also noted retention of $J(Sn-CH_3)$ and $J(Sn-CH_\gamma)$ in dynamic nmr studies of $Cl_2Sn(acac)_2$. Additional support for rejecting complete dissociation of an acetylacetonate ligand comes from a recent report (102) that the rate of intermolecular exchange of acetylacetonate ligands between $(CH_3)ClSn(acac)_2$ and Hacac in acetylacetone solvent is a hundred fold slower, $k_{25} = 0.03\ sec^{-1}$ (extrapolated; cf. Table XVI). Such exchange causes collapse of the individual resonances of the free and complexed ligand as the rate of exchange increases. Exchange between $(CH_3)ClSn(acac)_2$ and Hacac is also slow in chlorobenzene solvent. No appreciable exchange was observed even at ∿110° (at ambient temperatures, $W_{1/2}$ for -CH= of $(CH_3)ClSn(acac)_2$ is 0.5 Hz and of Hacac (enol) $W_{1/2}$ is 0.6 Hz; at ca. 110° the corresponding values are 0.9 Hz and 1.3 Hz (116)). Of importance is the fact that in the exchange of acetylacetonate ligands between $(C_6H_5)_2Sn(acac)_2$ and $(CH_3)_2Sn(acac)_2$, the rate controlling step does not involve complete dissociation

of a given bidentate ligand (103).

The proposal by Harrod and Taylor (111), that molecular rearrangements could occur via migration of a monodentate anionic ligand across the surface of the cationic complex and followed by collapse of the tightly bound ion-pair to a neutral six-coordinate species, cannot be evaluated with the data presented here. This mechanism does not appear to be an attractive one for configurational rearrangements in $X_2Sn(acac)_2$ and $X_2Ti(acac)_2$ (X = Cl, Br, F, or I) complexes (30). It is, therefore, concluded that the rate of exchange of chelate ligands with bulk ligands is much slower than the rate of intramolecular environmental averaging and that this type of dissociative mechanism (equation 10) does not appreciably contribute to the exchange.

Two other mechanisms which may lead to environmental averaging of -CH- and/or CH_3 groups in $XYM(acac)_2$ are the intramolecular pathways (c) the cleavage of a single metal-oxygen bond in the heterochelate ring chelate (112) and (d) a number of variations of mechanisms involving twisting (or non-bond rupture) about real or imaginary C_3 axes of the six coordinate complex carried out singly or in a stepwise manner. A permutational analysis of a neutral bidentate six-coordinate chelate of the type $XYM(acac)_2$ (M = Sn, Ge, Si; AA = a bidentate ligand, e.g. acac) has

been carried out (113). This analysis allows for the mathematical description of all the possible permutations of nuclei without having to specify how atoms move from one position to another. From such a description it is possible to deduce actual configurational changes (diastereomerization and/or enantiomerization) and proton nmr observable site interchanges. Also, the most probable physical pathway which produces a particular permutation may be inferred provided the observed site interchanges are unique to that one permutation; however, the pathway need not be unique to this particular permutation. From experimental observations reported here evolve the following constraints on the mechanism of the exchange process; i) configurational rearrangement in $RClM(acac)_2$ (M = Sn, Ge, Si; R = phenyl or methyl) complexes proceed via a mechanism which simultaneously exchanges -CH- protons and methyl groups between the two and four, respectively, nonequivalent sites of the cis isomer to yield singlets under conditions of fast exchange, and, ii) although not observed for the complexes reported here, rearrangements most probably occur with inversion of configuration($\Delta \rightleftarrows \Lambda$).

Momentary rupture of a metal-oxygen bond in $XYM(acac)_2$ yields two chiral and two achiral TBP-axial intermediates, four chiral TBP-equatorial intermediates, and two chiral SP-axial intermediates. These are illus-

trated in Figure 21*. The consequences of reattachment of the dangling ligand end to the central metal ion via the above intermediates are presented in Figure 22. Reattachment of the dangling end to the metal ion in TBP-axial intermediates leads to inversion of the molecular configuration but does not exchange ring protons and methyl groups between the appropriate sites according to constraint (i). TBP-equatorial transition states afford retention of the molecular configuration, contrary to constraint (ii), and lead to environmental averaging of only two of the four methyl group environments without exchange of ring protons (cf. Figure 22a). Rupture of the metal-oxygen bond a in the isomer cis-Λ(abcd;m) followed by attack of the dangling ligand end at the four basal positions in the SP-axial intermediates (formed and decaying through a primary process (1) leads to rearrangements identical to those from rupture of any one of the remaining three M-O bonds. Reactions involving SP-axial transition states (Figure 22b) are improbable because, in theory, they could provide a route for Λ ⇌ Δ interconversion and for simultaneous exchange of ring protons and methyl groups according to constraints (i) and (ii)-if the attack of the dangling end

---

*The four nonequivalent sites in a complex such as XYM(acac)$_2$ are labeled as follows: the site trans to the ligand Y is always b, the one trans to X is labeled c. Sites c and d are always connected with the same ring; similarly for sites a and b. Thus if R_1 is in site c, then R_2 is in site d, etc.. Site m for the ring proton H_1 is the site cis to X; site n is cis to Y.

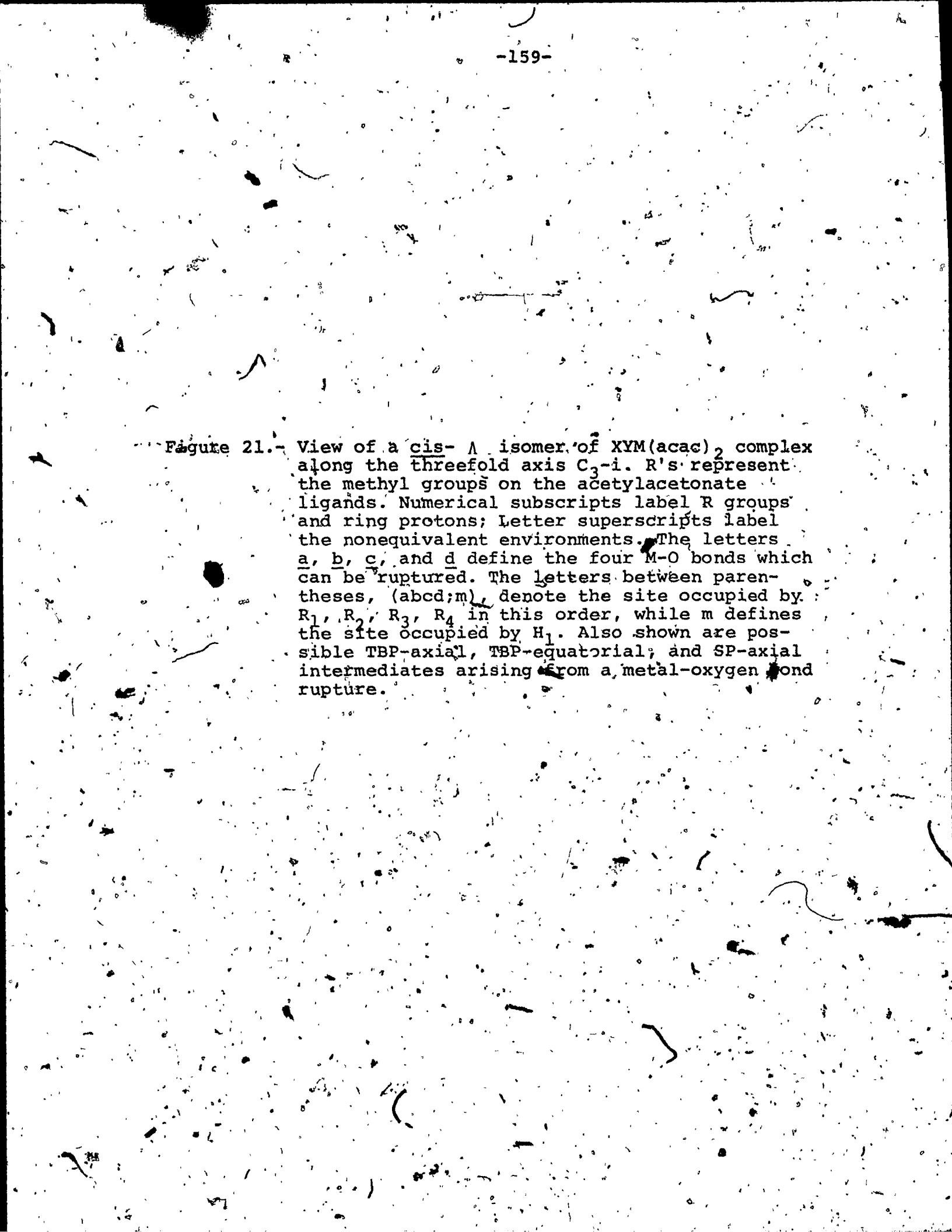

Figure 21.- View of a cis- Λ isomer of XYM(acac)$_2$ complex along the threefold axis C_3-i. R's represent the methyl groups on the acetylacetonate ligands. Numerical subscripts label R groups and ring protons; Letter superscripts label the nonequivalent environments. The letters a, b, c, and d define the four M-O bonds which can be ruptured. The letters between parentheses, (abcd;m), denote the site occupied by R_1, R_2, R_3, R_4 in this order, while m defines the site occupied by H_1. Also shown are possible TBP-axial, TBP-equatorial, and SP-axial intermediates arising from a metal-oxygen bond rupture.

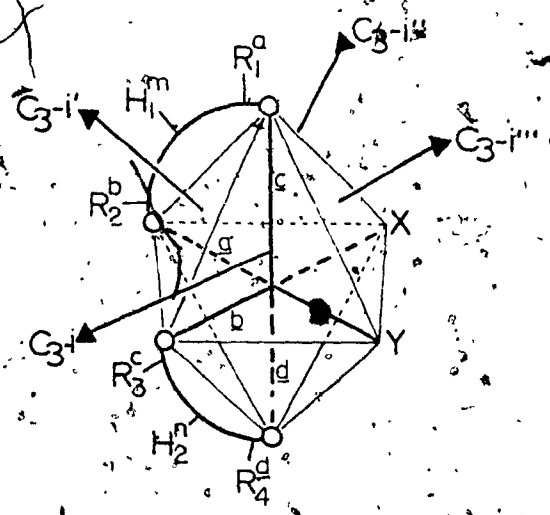

cis-Λ(abcd;m)

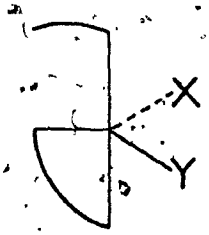

1d

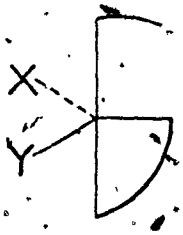

1l

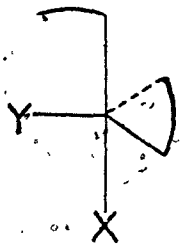

2

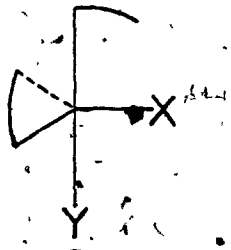

3

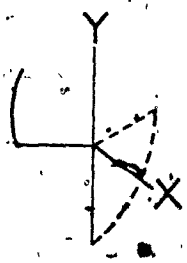

4d

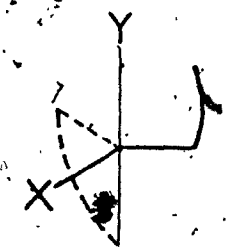

4l

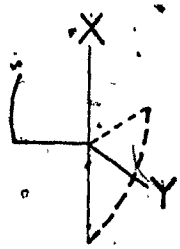

5d

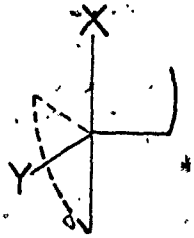

5l

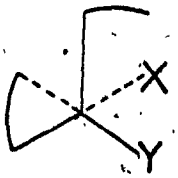

6d

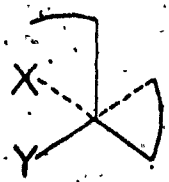

6l

Figure 22.- (a) Example of configurational rearrangements proceeding through TBP-axial and TBP-equatorial intermediates derived from rupture of the metal-oxygen bond a; (b) Example of rearrangements occurring via a SP-axial intermediate derived from rupture of the metal-oxygen bond a in the isomer cis-Λ (abcd;m) and decaying to products through a primary process (see text); (c) Configurational rearrangements for the isomer cis-Λ (abcd;m) proceeding through prismatic intermediates obtained by rotations about the indicated imaginary threefold axes of the complex. Note that rotations about C_3-i'' axis may also provide a path to yield the trans isomer (see text).

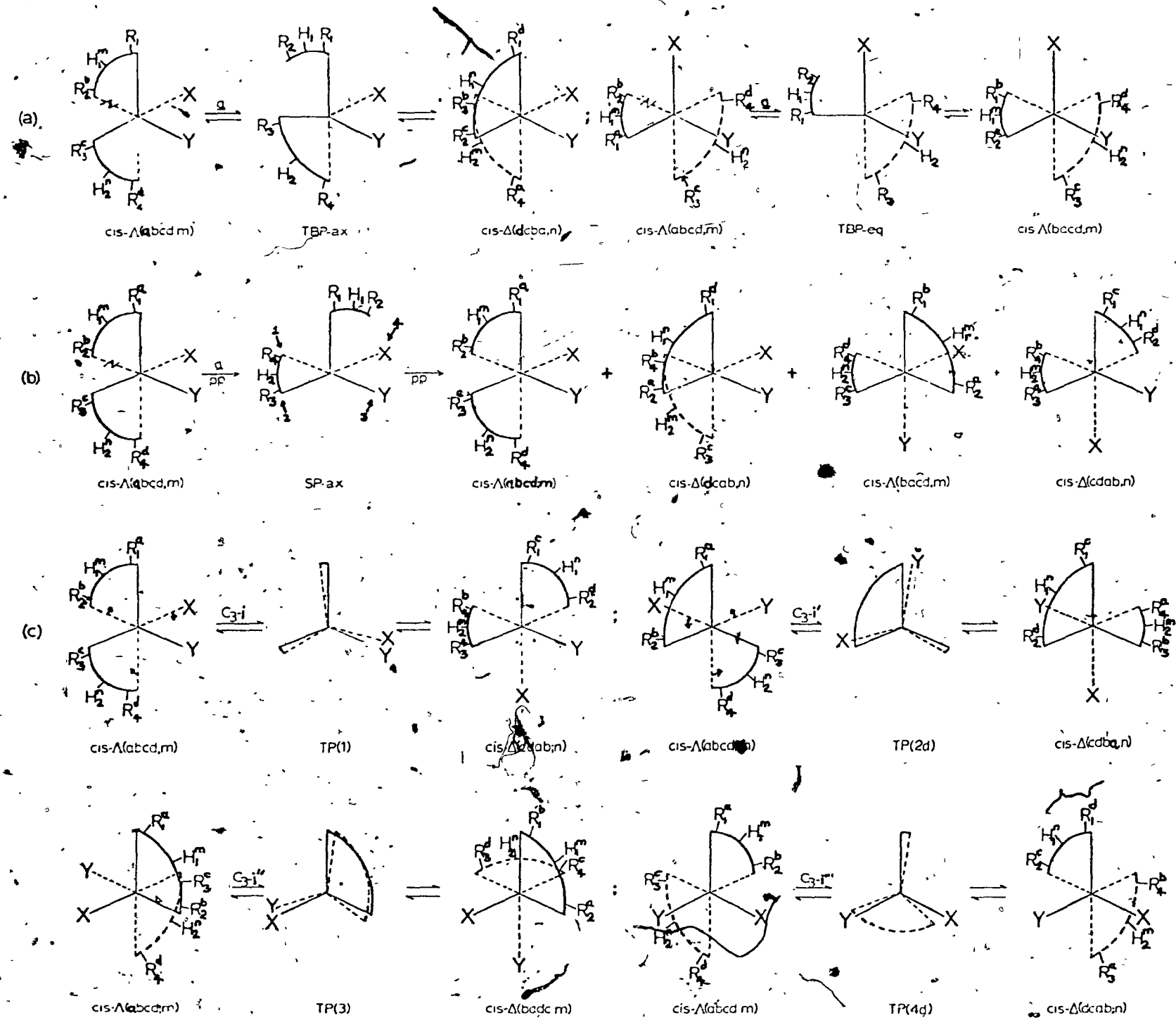
(a)
a
cis-Λ(abcd,m)
TBP-ax
cis-Δ(dcba,n)
cis-Λ(abcd,n)
TBP-eq
cis Λ(bacd,m)
(b)
a
pp
pp
cis-Λ(abcd,m)
SP-ax
cis-Λ(abcd,n)
cis-Δ(dcab,n)
cis-Λ(bacd,m)
cis-Δ(cdab,n)
(c)
C3-i
C3-i'
cis-Λ(abcd,m)
TP(1)
cis-Δ(cdab,n)
cis-Λ(abcd,n)
TP(2d)
cis-Δ(cdba,n)
C3-i''
C3-i''
cis-Λ(abcd,m)
TP(3)
cis-Δ(badc m)
cis-Λ(abcd m)
TP(4d)
cis-Δ(dcab;n)

occurs at just one (or possibly two) basal positions. Such a case would, of necessity, require implausible discrimination by the attacking ligand end between the four ligand atoms in the basal plane of the SP transition state. Although, a priori, attack is not expected to be equally probable at all four basal positions, especially since the atoms at these positions are so different (Cl, O, C), neither is it expected that exclusive preferential attack will occur at any one specific basal position since, for example, cis-Δ-(cdab;n) is obtained by attack at one of the two basal oxygens in breaking bonds a and b (cf. Figure 22b). SP intermediates with basal dangling ligands are kinetically equivalent to TBP-axial intermediates, and thus are not considered as possible routes to the observed configurational changes. The TBP pathway has also been analyzed in terms of the eight transition states undergoing pseudorotation (pr) about each of the three metal-ligand equatorial bonds. TBP-axial intermediates 1d and 1ℓ undergo pseudorotation to yield TBP-equatorial intermediates which, upon reattachment of the dangling ligand, either produces $\Lambda \rightleftarrows \Delta$ interconversion without methyl group exchange, contrary to constraint (i), or produce methyl group exchange with no $\Lambda \rightleftarrows \Delta$ interconversion, contrary to constraint (ii). Pseudorotation of TBP-equatorial intermediates leads to a mixture of TBP-axial and -equatorial intermediates. The configurational consequences

from these upon reattachment of the ligand end onto the central metal ion is inconsistent either with constraint (i), or with constraint (ii), or is inconsistent with both. In addition, configurational changes proceeding through pseudorotated TBP transition states are not likely in view of the extensive ligand motion involved in such processes.

Another possible pathway for configurational rearrangements in $XYM(acac)_2$ complexes but which does not necessitate metal-ligand bond rupture is twist motions about the four threefold axes of the octahedral framework. These twist motions, carried out for the cis-Λ(abcd;m) isomer, are illustrated in Figure 22c. Rotations about the imaginary threefold axes of the complex (Figure 21) are thought to occur by keeping one triangular face of the octahedron fixed (solid lines in Figure 22c) while the opposite face (dashed lines) is rotated clockwise by 60° about C_3-i to produce the idealized trigonal prismatic achiral transition state TP1. Further rotation through 60° in the same direction yields the isomer cis-Λ(cdab;n). Rotations about C_3-i' and C_3-i''' give the same net configurational changes, cis-Δ(cdba;n), consistent with constraints (i) and (ii). Twists about C_3-i'' produce the achiral TP3 intermediate which upon further rotation provides for $\Lambda \rightleftarrows \Delta$ interconversion as well as exchange of methyl groups but does not time-average the ring proton

environments, (cis- Δ(badc;m)) contrary to constraint (i). Rotations about C_3-i'' also provide a path for cis-trans isomerization since the bidentate ligands do not span opposite triangular faces. It is concluded, therefore, on the basis of the above analysis, that configurational rearrangements in $RClM(acac)_2$ (R= CH_3, C_6H_5; M = Sn, Ge, Si, except for $(CH_3)ClGe(acac)_2$ vide infra) complexes occur via twist motions about the C_3-i' and/or C_3-i''' axes (nearly identical stereochemically), though twists about C_3-i(cis-Δ (cdab;n)) cannot be precluded for reasons noted earlier.

There have been various sources of support for twist mechanisms, some of which come from direct evidence such as the coalescence behavior of nmr spectra owing to the resolution of the nonequivalent nuclei, distortion of the structure of crystalline complexes and the relationship of optical inversion to proton exchange (113). Where direct evidence has been unobtainable in determinations of the specific pathway for configurational rearrangements, mechanisms have generally been inferred from the magnitudes of the frequency factors (or entropy of activation) and/or the activation energy. Negative activation entropies (low frequency factors) have long been argued as support for a twist mechanism. However, it may be misleading to make claims about mechanisms on the basis of activation parameters alone, especially on the basis of activation

entropies. This is borne out by a literature survey (1) which revealed that $\Delta S^{\ddagger}$ values fall in the range -24 to +20 eu for about 40 compounds where rearrangements have been thought to occur via a bond rupture process, while in about 11 compounds, $\Delta S^{\ddagger}$ falls within -23 to +10 eu for rearrangements thought to occur via a twist mechanism. Significant is the value of -33 eu, the activation entropy for the intermolecular ligand exchange between $(C_6H_5)_2Sn(acac)_2$ and $(CH_3)_2Sn(acac)_2$, where the mechanism has been established to be a tin-oxygen bond rupture process (103). It appears that there has not yet been enough cases studied for which mechanisms have been definitely established to permit the use of activation entropies, or frequency factors, as reliable indicators of mechanism (114). Also, although twisting motions may in principle be expected to give rise to low frequency factors, low frequency factors do not necessarily imply twisting processes. Entropies of activation reported in this work (Tables XVI - XVII) are neither inconsistent with a bond breaking process, nor with a twist mechanism. Nevertheless, there are some trends which are in evidence between the data from the various tin, germanium and silicon complexes which may possibly lend some support to a twist mechanism.

From a comparison of the different $(C_6H_5)ClM(acac)_2$ complexes (M = Sn, Ge, Si) the observed relative order of the activation energy E_a is Sn ≈ Ge>> Si.

Although the bond strengths* for the Sn-O, Ge-O and Si-O bonds are not available for these or related complexes, the expected relative order of bond strengths is Si-O > Ge-O > Sn-O. This is also the expected relative order of the activation energies for these complexes for rearrangements occurring through TBP and SP intermediates. Also, the very large activation energy (25.2 kcal/mole) found for rearrangements in $Cl_2Ge(dpm)_2$ as opposed to the values obtained (12.8 kcal/mole) for $(C_6H_5)ClGe(acac)_2$ is suggestive of a different mechanism for environmental averaging in the two instances. For the former complex, evidence has been presented in support of a bond rupture path (30).

More important is the comparison between values of activation parameters from the intermolecular exchange process in the diphenyltin- dimethyltin system (103) with those from the intramolecular process in diphenyltin acetylacetonate in the hope that a mechanism may be deduced for the latter process. If the same mechanism were operative in both processes, namely a bond rupture mechanism, it is difficult to understand reasons for a larger entropy of activation (11 eu larger) and the greater lability (100-fold) in the environmental averaging of

---

* Homolytic bond dissociation energy (kcal/mole) in diatomic metal oxides is; 188 (Si-O), 157 (Ge-O), and 125 (Sn-O) (108).

terminal methyl groups in the diphenyltin complex, especially since the species in solution in both studies are so related, unless, of course, different mechanisms were operative. It is concluded that intramolecular rearrangements in $(C_6H_5)_2Sn(acac)_2$ also proceed through TP transition states; for every 100 twists ($k_{25} = 3.69$ sec^{-1}) a tin-oxygen bond ruptures ($k_{25} = 3.8$ sec^{-1}). Further, the free energy for the intramolecular pathway in this complex is of lower energy ($\Delta G^{\ddagger}_{25} = 13.95 \pm 0.09$ kcal/mole) than that of the intermolecular path ($\Delta G^{\ddagger}_{25} = 16.65 \pm 0.09$ kcal/mole (103)).

The case of the $(CH_3)ClGe(acac)_2$ complex presents a different problem. From the concentration dependence studies it was found that the rate is dependent on the concentration of methylchlorogermanium complex and consequently leads to the conclusion that the mechanism of rearrangement for this complex occurs via a bimolecular process. Dissociation of a methyl group is highly unlikely as has been explained earlier (see equation 9); also, dissociation of the chloride ion is also discounted for reasons already discussed (see equation 9). In addition, the rate of environmental averaging is second-order in the concentration of $(CH_3)ClGe(acac)_2$. A halide dissociation path would be expected to be first-order in the concentration of complex*.

---

* Consideration of several pathways involving a metal-chlorine bond breaking as a first step reveals no rate expression that contains second-order dependence on the concentration of the complex. In all the cases we have looked at the rate law was always first order with respect to [complex].

Also, the entropy of activation, -30 ± 1 eu, is inconsistent with a dissociative process. Brown (115) has pointed out that $\Delta S^{\ddagger}$ should be positive for a dissociative mechanism and negative for an associative one, in the absence of strong solvent effects. The latter effects probably amount to no more than about 10 eu for halogenated organic solvents (103).

A tentative pathway involves the intermolecular exchange of an acetylacetonate ligand. The process is viewed in the scheme below where the primed ligand, acac', represents a dangling ligand.

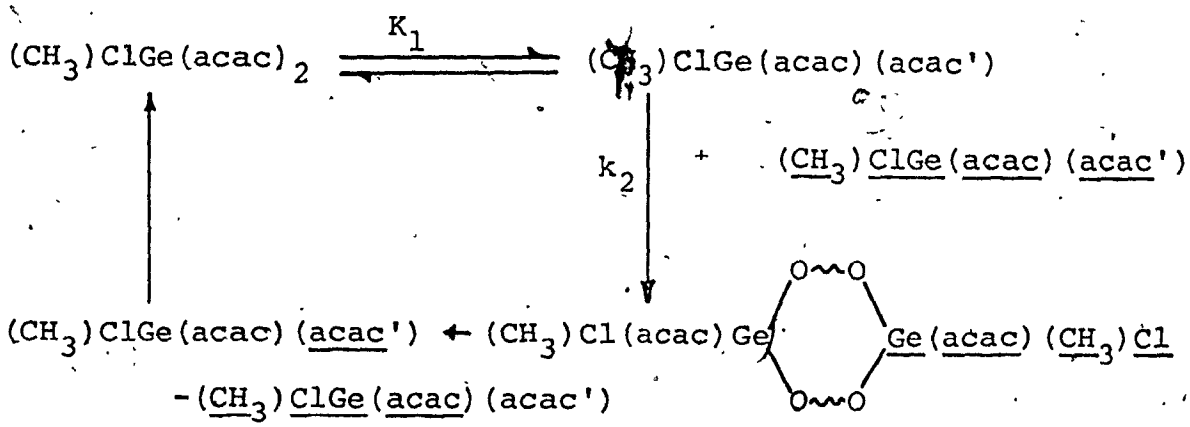

The equilibrium defined by K_1 must be shifted largely toward the six-coordinate species as we observed no nmr resonances attributable to the five-coordinate germanium species. The rate determining sequence, k_2, is thought to involve formation of the bis-acac bridged dimeric species, but prior to this, the five-coordinate

species would have to be in the correct orientation (the slow step) for attack by the dangling acetylacetonate ligand end onto the "vacant" coordination site (the "vacant" site may be occupied by a solvent molecule). The rate expression from the proposed mechanism is $R = k_2K_1 [(CH_3)-ClGe(acac)_2]^2$ consistent with observations reported earlier in this work.

IV. REFERENCES

1. N. Serpone and D.G. Bickley, Progr. Inorg. Chem., 17, 391 (1972).
2. J.J. Fortman and R.E. Seivers, Coord. Chem. Rev., 6, 331 (1971).
3. D.W. Thompson, Struct. Bond. (Berlin), 9, 27 (1971).
4. S.E. Livingstone, Coord. Chem. Rev., 7, 59 (1971).
5. M. Cox and J. Darben, Coord. Chem. Rev., 7, 29 (1971).
6. R.C. Fay, Ann. N.Y. Acad. Sci., 159, 152 (1969).
7. S.J. Lippard, Progr. Inorg. Chem., 8, 109 (1967).
8. J.P. Fackler Jr., Progr. Inorg. Chem., 7, 361 (1966).
9. R.M. Pike, Coord.Chem. Rev., 2, 163 (1967) and references therein.
10. L. Roncucci, G. Faraglia, and R. Barbieri, J. Organometal. Chem., 1, 427 (1964).
11. E.O. Schlemper, Inorg. Chem., 6, 2012 (1967).
12. M.M. McGrady and R.S. Tobias, J. Amer. Chem. Soc., 87, 1909 (1965).
13. W.H. Nelson and D.F. Martin, J. Inorg. Nucl. Chem., 27, 89 (1965).
14. M.M. McGrady and R.S. Tobias, Inorg. Chem., 3, 1157 (1964).
15. W. Kitching, J. Organometal. Chem., 6, 586 (1966).
16. T.N. Srivastava and K.L. Saxena, Ind. J. Chem., 9, 601 (1971).
17. R.Ueeda, Y. Kawasaki, T. Tanaka and R. Okawara, J. Organometal. Chem., 5, 194 (1966).
18. T. Tanaka, M. Komura, Y. Kawasaki, and R. Okawara, J. Organometal. Chem., 1, 484 (1964).
19. W.H. Nelson and M. Aroney, Inorg. Chem., 12, 132 (1973).
20. N. Serpone and R.C. Fay, Inorg. Chem., 8, 2379 (1969).

21. W.H. Nelson, Inorg. Chem., 6, 1509 (1967).

22. V. Doron and C. Fisher, Inorg. Chem., 6, 1917 (1967).

23. J.W. Faller and A. Davidson, Inorg. Chem., 6, 182 (1967).

24. J.A.S. Smith and E.J. Wilkins, J. Chem. Soc., A, 1749 (1966).

25. J.A.S. Smith and E.J. Wilkins, Chem. Commun., 381 (1965).

26. Y. Kawasaki, and T. Tanaka, Inorg. Nucl. Chem. Letters, 3, 13 (1967).

27. Y. Kawasaki, Mol. Phys., 12, 287 (1967).

28. Y. Kawasaki and T. Tanaka, J. Chem. Phys., 43, 3396 (1965).

29. Y. Kawasaki, R. Ueeda, T. Tanaka, International Symposium On Nuclear Magnetic Resonance, 2-M-16, Tokyo, Sept. 1965.

30. R.W. Jones Jr., Ph.D. Dissertation, Cornell University, Ithaca, N.Y. 14850 (1971).

31. M. Cox, R.J.H. Clark and J.H. Milledge, Nature, 212, 1357 (1966).

32. R.W. Jones Jr. and R.C. Fay, Inorg. Chem., 12, 2599 (1973); and references therein.

33. G.M. Bancroft and T.K. Sham, Can. J. Chem., 52, 1361 (1974).

34. N.N. Greenwood and J.N.R. Ruddick, J. Chem. Soc., A, 1679 (1967).

35. E.O. Schlemper, Private Communication to R.C. Fay. See ref. 32.

36. E.A. Miller and E.O. Schlemper, Inorg. Chem., 12, 677 (1973).

37. Y. Kawasaki, T. Tanaka, and R. Okawara, Bull. Chem. Soc. Japan., 37, 903 (1964).

38. V.B. Ramos and R.S. Tobias, Spect. Chim. Acta., 29A, 953 (1973).

39. B.W. Fitzsimmonds, N.J. Seeley and A.W. Smith, J. Chem. Soc., A, 143 (1969); Chem. Commun., 390 (1968).

40. R.H. Herber and H.A. Stockler, Tech. Rep. Ser. Int. Atom. Energy Agency, No. 50, 110 (1966).

41. C.Z. Moore and W.H. Nelson, Inorg. Chem., 8, 138 (1969).

42. J.W. Hayes, W.H. Nelson, and D.V. Radford, Austral. J. Chem., 26, 871 (1973).

43. N. Serpone and K.A. Hersh, Inorg. Nucl. Chem. Letters, 7, 115 (1971).

44. J.W. Hayes, R.J.W. LeFevre, and D.V. Radford, Inorg. Chem., 9, 400 (1970).

45. Y. Kawasaki, T. Tanaka and R. Okawara, Inorg. Nucl. Chem. Letters., 2, 9 (1966).

46. Y. Kawasaki, T. Tanaka, and R. Okawara, Spect. Chim. Acta., 22A, 1571 (1966).

47. D.W. Thompson, Private Communication (1971).

48. A.A. Lavigne, J.M. Tancrede, and R.M. Pike, Coord. Chem. Rev., 3, 497 (1968).

49. R.C. Mehrotra and S. Mathur, J. Organometal. Chem., 6, 11 (1966).

50. M. Cox, J. Lewis and R.S. Nyholm, J. Chem. Soc., A, 6113 (1964).

51. W.K. Ong and R.H. Prince, J. Inorg. Nucl. Chem., 27, 1057 (1965).

52. O.A. Osipov, V.L. Shelepina and O.E. Shelepin, J. Gen. Chem. USSR, 36, 274 (1966).

53. N. Serpone, Ph.D. Thesis, Cornell University, Ithaca, N.Y., 14850, (1968), (p. 144, Diss. Abstr. XXIX 1973-B)

54. T.J. Pinnavaia, L.J. Matienzo and Y.A. Peters, Inorg. Chem., 9, 993 (1970).

55. D.W. Thompson, Inorg. Chem., 8, 2019 (1969).

56. D.W. Thompson, J. Magn. Res., 1, 606 (1969).

57. N. Serpone and R.C. Fay, J. Amer. Chem. Soc., 90, 5701 (1968).

58. R.M. Pike and R.R. Luongo, J. Amer. Chem. Soc., 88, 2972 (1966); 87, 1403 (1965); 84, 3233 (1962).

59. C.E. Holloway, R.R. Luongo, and R.M. Pike, J. Amer. Chem. Soc., 88, 2060 (1966).

60. R. West, J. Amer. Chem. Soc., 80, 3246 (1958).

61. T.G. Selin (General Electric), U.S. Pat. Pend., Ger. Pat. 2000225. (Chem. Abstr. 73-78345t).

62. D.G. Holah, J. Chem. Educ., 42, 561 (1965).

63. T.J. Pinnavaia and R.C. Fay, Inorg. Syntheses, 12, 88 (1970).

64. See e.g., W.H. Nelson, W.J. Randall, and D.F. Martin, Inorg. Syntheses, 9, 52 (1967).

65. F. Rijkens and G.J.M. Van Der Kerk, Rec. Trav. Chim., 83, 723 (1964).

66. P.J. Paulsen and D.W. Cooke, Anal. Chem., 35, 1560 (1963).

67. J. Timmermans, "The Physico-Chemical Constants of Binary Systems in Concentrated Solutions", Vol. 1, Interscience Pub. Co. Inc., New York, N.Y., 1959.

68. A. Allerhand, H.S. Gutowsky, J. Jonas, and R.A. Meinzer, J. Amer. Chem. Soc., 88, 3185 (1966).

69. Varian Associates, Analytical Instrument Division, Pub. NBR. 87-202-006, HA-100 Manual. pp. 4-10, 4-13.

70. Varian Associates, Analytical Instrument Division, Pub. NBR. 87202-001, A-60A Manual. pp. 4-2, 4-4.

71. A.L. Van Geet, Abstract of Papers, 10th Experimental NMR. Conference, Mellon Institute, Pittsburgh, Pa., Feb. 1969, Session C-1.

72. A.L. Van Geet, Anal. Chem., 40, 2227 (1968); 42, 679 (1970).

73. R.C. Neuman and V. Jonas, J. Amer. Chem. Soc., 90, 1970 (1968).

74. O. Yamamoto and M. Yanogesama, Anal. Chem., 42, 1463 (1970).

75. D.A. Case and T.J. Pinnavaia, Inorg. Chem., 10, 482 (1971).

76. For a description of this program see, A. Granata, M.Sc. Thesis, Sir George Williams University, Montreal, H3G 1M8 (1972).

77. K.C. Williams and T.L. Brown, J. Amer. Chem. Soc., 88, 4134 (1966).

78. H.S. Gutowsky and C.H. Holm, J. Chem. Phys., 25, 1228 (1956).

79. J. Jonas, A. Allerhand and H.S. Gutowsky, J. Chem. Phys., 42, 3396 (1956).

80. L.W. Reeves and R.N. Shaw, Can. J. Chem., 48, 3641 (1970).

81. L.W. Reeves, Advan. Phys. Org. Chem., 3, 187 (1965).

82. C.S. Johnson Jr., Advan. Magn. Res., 1, 33 (1965).

83. M.T. Rogers and J.C. Woodbrey, J. Phys. Chem., 66, 540 (1962).

84. R.R. Shoup, E.D. Becker, and M.L. McNeil, J. Phys. Chem., 76, 71 (1972)

85. T.J. Pinnavaia, J.M. Seleson II and D.A. Case, Inorg. Chem., 8, 644 (1969).

86. J.A. Pople, W.G. Schneider and H.S. Bernstein, "High Resolution Nuclear Magnetic Resonance" McGraw-Hill Book Co. Inc., New York, N.Y., 1959. pp. 211,212, 458.

87. R.C. Fay and R.N. Lowry, Inorg. Chem., 6, 1512 (1967).

88. T.L. Brown and J.A. Ladd, Department of Chemistry, University of Illinois, Urbana, Ill. 61801.

89. We thank Professor R.C. Fay of Cornell University, Ithaca, New York. 14850 for providing us with the modified version of this program.

90. Y. Kawasaki, J. Inorg. Nucl. Chem., 29, 840 (1967).

91. We thank Professor L.D. Colebrook of Sir George Williams University, Montreal H3G 1M8, for supplying these programs.

92. For more details see the Operating and Service manual (1965) for the F-3B line follower, Hewlett-Packard, San Diego, California.

93. Ref. 86, Chap. 10.

94. Ref. 86, pp, 222-224.

95. J.R. Holmes and H.D. Kaesz, J. Amer. Chem. Soc., 83, 3903 (1961).

96. K. Nakamoto, "Infrared Spectra of Inorganic and Coordination Compounds", Wiley, New York, N.Y., 1963, p. 216 ff.

97. A. Allerhand and H.S. Gutowsky, J. Chem. Phys., 41, 2115 (1964).

98. T.J. Pinnavaia and R.C. Fay, Inorg. Chem., 7, 502 (1968).

99. R.C. Fay and T.J. Pinnavaia, Inorg. Chem., 7, 508. (1968).

100. R.N. Lowry, Ph.D. Thesis, Cornell University, Ithaca, N.Y. 14850 (1969),

101. G.M. Barrow, "Physical Chemistry", 2nd Ed., McGraw-Hill Book Company Inc., New York, N.Y., 1966.

102. G.E. Glass and R.S. Tobias, J. Organometal Chem., 15, 481 (1968).

103. N. Serpone and R. Ishayek, Inorg. Chem., 13, 52 (1974).

104. A. Mackor and H.A. Meinema, Rec. Trav. Chim., 91, 911 (1972).

105. H. Weingarten, M.G. Miles and N.K. Edelmann, Inorg. Chem., 7, 879 (1968).

106. We would like to thank Professor G. Binsch and the QCPE Section of Indiana University for supplying this program.

107. Commission on the Nomenclature of Inorganic Chemistry of IUPAC, Inorg. Chem., 9, 1 (1970).

108. Handbook of Chemistry and Physics, 51st Ed., The Chemical Rubber Co., Akron, Ohio., 1970-71.

109. J.M. Bull, M.J. Frazer, L.I.B. Haines, and J. Measures, Abstracts of Papers, A-14, Fall meeting of the Chemical Society (London), Southampton, 1969.

110. E.L. Muetteries, J. Amer. Chem. Soc., 90, 5097 (1968).

111. J.F. Harrod and K. Taylor, Chem. Commun., 696 (1971).

112. A. Werner, Ber., 45, 1228 (1912); 45, 3061 (1912).

113. N. Serpone and D.G. Bickley, Inorg. Chem., 13, 2908 (1974); references therein.

114. J.R. Hutchison, J.G. Gordon II, and R.H. Holm, Inorg. Chem., 10, 1004 (1971).

115. T.L. Brown, Accounts. Chem. Res., 1, 23 (1968).

116. T. Ignacz and N. Serpone, Unpublished Results.

117. C. Kutal and R.E. Sievers, Inorg. Chem., 13, 897 (1974).

V. APPENDIX

A. Attempted Syntheses

1. Dimethyl and Diphenylbis(2,4-pentanedionato) silicon(IV).-

Attempts to synthesize both these compounds produced the same results. If a stoichimetric ratio of 1:2 of diphenyl or dimethyldichlorosilane, $(C_6H_5)_2SiCl_2$ or $(CH_3)_2SiCl_2$, and thallium acetylacetonate, Tl(acac), are reacted in 50 ml of dichloromethane for 30 minutes as in the case of diphenyldichlorosilane or 10 minutes in the case of dimethyldichlorosilane, a red solution results. This solution was reduced with a water aspirator and the application of heat from a heat gun until the first signs of crystallization. The stoppered flask was then placed in a freezer (-4^oC) for one hour. The mixture was filtered through a fine modified frit funnel and washed with cold hexane (-4^oC). The residue was dried in vacuo overnight. In the cases of both dimethyl and diphenyl starting materials the same red compound was produced. The melting point ranged from 142^o to 154^o (with decomposition).

2. Dimethylbis(2,4-pentanedionato)germanium(IV).-

To 1.41 g of dimethylgermanium dichloride, $(CH_3)_2GeCl_2$, (0.00812 mol), in a solution of 50 ml of dichloromethane was added thallium acetylacetonate, Tl(acac), (4.75 g, 0.01565 mol). Molar ratios of starting materials in which there were excesses of either of the

two starting materials were also used (similar results were obtained). The mixture was stirred for 30 minutes and then filtered through a fine modified frit funnel. The yellow filtrate was reduced with a water aspirator and the application of heat from a heat gun until the first signs of turbidity. The stoppered flask was left in a freezer ($-4^{\circ}C$) for two hours. The resulting yellow-white compound was filtered and washed with cold hexane ($-4^{\circ}C$) to remove the yellow impurities and dried over a stream of dry nitrogen. Attempts to dry the compound *in vacuo* led to accelerated decomposition. Melting point on the freshly prepared white material was 104-107° (dec.). Attempts to recrystallize the compound also led to decomposition.

The infrared spectrum exhibited no uncomplexed CO bands below 1600 cm^{-1} and no OH bands. The nmr spectrum was difficult to obtain as the compound decomposed within minutes in solution. Chemical shifts (14.4 g/ml; $CDCl_3$/TMS; *ca.* 31°): $\delta\nu$ = 0.95 ppm ($Ge-CH_3$); 1.98 ppm, 2.04 ppm, 2.07 ppm (acac-CH_3 region) and 5.32 ppm, 5.53 ppm (-CH= region). The presence of three methyl signals and two ring proton signals might indicate the presence of a mixture of both *cis* and *trans* isomers. This compound was not worked up further in this study owing to its rapid decomposition.

B. Computer Programs

SLREG

This program performs a single linear regression analysis for up to 49 sets of an independent and a dependent variable (i.e. a X and Y value).

```
      FTN,B
      PROGRAM SLREG
      COMMON X(100),Y(100), Z(48)
      Z(1) = 12.706
      Z(2) = 4.3027
      Z(3) = 3.1825
      Z(4) = 2.7764
      Z(5) =2.5706
      Z(6) = 2.4469
      Z(7) = 2.3646
      Z(8) = 2.3060
      Z(9) = 2.2622
      Z(10) = 2.2281
      Z(11) = 2.201
      Z(12) = 2.1788
      Z(13) = 2.1604
      Z(14) = 2.1448
      Z(15) = 2.1315
      Z(16) = 2.1199
      Z(17) = 2.1098
      Z(18) = 2.1009
      Z(19) = 2.093
      Z(20) = 2.086
      Z(21) = 2.0796
      Z(22) = 2.0739
      Z(23) = 2.0687
      Z(24) = 2.0639
      Z(25) = 2.0595
      Z(26) = 2.0555
      Z(27) = 2.0518
      Z(28) = 2.0484
      Z(29) = 2.0452
      Z(30) = 2.0423
      DO 3 I = 31,35
      Z(I) = 2.04
    3 CONTINUE
      DO 5 I = 36,48
      Z(I) = 2.02
    5 CONTINUE
    2 DO 4 I = 1,100
      X(I) = 0.0
      Y(I) = 0.0
    4 CONTINUE
      CALL RESET
      N = 0
      NA = 0
      XSU = 0.0
      YSU = 0.0
      XY = 0.0
      XSQ = 0.0
      YSQ = 0.0
      WRITE(2,10)
   10 FORMAT(//'ENTER VALUES AS X AND Y'/)
```

```
C     VALUES ARE ENTERED AS "X , Y". THE INPUT IS TERMINATED BY
C     PLACING ",9" AT THE END OF LAST DATA EG. "X,Y,9".SHOULD THIS
C     BE OMITTED THEN THE VERY NEXT LINE SHOULD BE 0,0,9.IF IT IS
C     NECESSARY TO INPUT REPETITIVE X'S OR Y'S THEN THE VALUE IS
C     ENTERED ONCE AND THE NEXT LINE IS LEFT BLANK FOR THAT VARIABLE
C     EG. "2,4" IS FIRST LINE NEXT IS ",4" FOR A DUPLICATE X VALUE.
C     ALL VALUES MAY BE ENTERED IN ANY FORMAT EXCEPT THE ",9".
   11 READ(1,*)AAL,BAL,NA
      IF(AAL - 0.0)220,200,220
  200 IF(BAL- 0.0)220,210,220
  210 IF(NA-1)220,215
  220 N = N+1
      X(N) = AAL
      Y(N) = BAL
      XSU = XSU + X(N)
      YSU = YSU + Y(N)
      IF(NA-1) 11,15
   15 WRITE(2,12)
   12 FORMAT(//"IF RESTART DESIRED SET SSW 15")
      PAUSE
      IF(ISSW(15))2,13
   13 VDF2 = N-2
      NVE = N-2
      T = Z(NVE)
      XM = XSU/FLOAT(N)
      YM = YSU/FLOAT(N)
      DO 25 I = 1,N
      XY = XY + ((X(I) - XM)*(Y(I)-YM))
      XSQ = XSQ+ (X(I) -XM)**2
      YSQ = YSQ + (Y(I)- YM)**2
   25 CONTINUE
      B = XY/XSQ
      A = YM - (B*XM)
      VSQ1 = (B**2)*XSQ
      VSQ2 = YSQ - VSQ1
      V2 = VSQ2/VDF2
      TBET = T * (V2/XSQ)**0.5
      TAL = T * (V2**0.5)*((1.0/FLOAT(N)) + ((XM**2)/XSQ)**0.5)
      BY = T * ((V2/FLOAT(N))**0.5)
      WRITE(2,75) A, TAL
   75 FORMAT(//"INTERCEPT IS  ",E12.7," +- ",E12.7//)
      RB = BY + ABS(TBET * XM)
      RD = YM + (B*(-XM))
      WRITE(2,80)RD,RB,B,TBET
   80 FORMAT("Y= (",E12.7," +- ",E12.7,") + (",
     1 E12.7," +- ",E12.7,")X"//)
      WRITE(2,82)
   82 FORMAT("FOR CORRECTED VALUES SET SSW 14")
      PAUSE
      IF(ISSW(14))85,110
   85 WRITE(2,86)
   86 FORMAT(///"CORRECTED VALUES"//6X,"X",16X,"Y",10X,"DEVIATION(+-)")
```

```
      DO 90 I = 1,N
      RP = RD + (X(I) * B)
      RQ = Y819
      RQ = Y(I) - RP
      IF(X(I) - X(I+1)) 91,90,91
   91 WRITE(2,92)X(I),RP,RQ

   92 FORMAT(E12.7,4X,E12.7,6X,E13.7)
   90 CONTINUE
  110 WRITE(2,112)
  112 FORMAT(//"TO RERUN SET SSW 15")
      PAUSE
      IF(ISSW(15))2,150
  150 STOP
      END
      END$
```

TAB

This program calculates a number of parameters from a given set of τ values and an appropriate temperature. These include; the reciprocal of the temperature in the form of $1/T \times 10^3$, the average τ value, the mean, and standard deviations and their associated percentage deviations, TAUA ($= 2\tau$), the rate k, ln k, the mean and standard deviations of ln k, and log k and its standard deviation..

Each set of data is entered as follows:

Line 1: Temperature (^{o}C), and a single digit. If this digit is greater than 0 (zero), then a set of log k's will be produced in addition to ln k for the following set of τ values, if not, only a set of ln k's will be produced.

Line 2: The τ value in any format.

In order to terminate entering τ values the last τ value of the set is entered as follows;

Last Line: The last τ value, and a single digit. This single digit should be greater than 0 (zero).

```
      FTN,B
      PROGRAM TAB
      COMMON B(100),D(100),TEM(60),TAM(60),CAVG(60),AVKL(60),
     1 DEV(60),VKL(60),DAV(60)
    1 WRITE(2,80)
   80 FORMAT(////////////)
      K=0
    3 K=K+1
      KA = 0
      READ(1,*) TEM(K),KA
      TAM(K)  = 1000./(273.15+ TEM(K))
      I = 0
    5 I = I+1
      N=0
      READ(1,*)A,N
      B(I) = A
      IF(N-1)5,10
   10 IF(I-1)9,9,11
    9 I = 2
      B(2) = B(1)
   11 SUN = 0.0
      DO 15 LA = 1,I
      SUN = SUN+ B(LA)
   15 CONTINUE
      SAVG = (SUN/FLOAT(I))
      TOSM = 0.0
      DO 20 LA = 1,I
      TOSM = TOSM + (B(LA)-SAVG)**2
   20 CONTINUE
      FIN = (TOSM/FLOAT(I-1))**0.5
      DO 35 LA = 1,I
      D(LA) = ABS(B(LA) - SAVG)
   35 CONTINUE
      AMD = 0.0
      DO 49 LA = 1,I
      AMD = AMD + D(LA)
   49 CONTINUE
      DAVG = AMD/FLOAT(I)
      CAVG(K) = SAVG * 2.
      AVK = 1./CAVG(K)
      AVKL(K) = ALOG(AVK)
      STP = FIN/SAVG
      VKL(K) = AVKL(K) * 0.4342945
      DEP = DAVG/ SAVG
      DVK = DEP * AVK
      FINB =  STP * AVK
      CVKL = ALOG(AVK + DVK) - AVKL(K)
      DVKL = ALOG(AVK - DVK) -AVKL(K)
      FINC = ALOG(AVK + FINB) - AVKL(K)
      FIND = ALOG(AVK - FINB) - AVKL(K)
      DEV(K) = (ABS(FINC) + ABS(FIND))/2.0
      DAV(K) = DEV(K) * 0.4342945
```

```
      WRITE(2,50)TEM(K),TAM(K),SAVG,DAVG,DEP,FIN,STP,CAVG(K),AVK,
     1 AVKL(K),CVKL,DVKL,FINC,FIND
   50 FORMAT(/49X,"TEMP = ",F7.2," C *****"/38X,"RECIP = ",F6.4//
     1"TAU",E17.8,"  MEAN DEV",E17.8," FR DEV",E17.8/
     1 "STD DEV",E17.8," FRAC DEV",E17.8/"TAUA",E17.8,"   K",E17.8/
     2 "LN K",E17.8,"  DEVS",E17.8,E20.8/"STD DEVS",E17.8,E20.8///)
      IF(KA-1)52,54
   52 GO TO 3
   54 WRITE(2,57)
   57 FORMAT(//////////"NO.",5X,"TAUA",8X,"TEMP",5X,"RECIP",10X,
     1 "LN K",13X,"DEV(+-)")
      WRITE(2,62)(KB,CAVG(KB),TEM(KB),TAM(KB),AVKL(KB),DEV(KB),
     1 KB = 1,K)
   62 FORMAT(/I2,2X,E11.5,3X,F7.2,4X,F6.4,2E17.7)
      WRITE(2,70)
   70 FORMAT(//////////2X,"TEMP",5X,"RECIP",10X,"LOG K",
     1 12X,"DEV(+-)")
      WRITE(2,72)(TEM(KB),TAM(KB),VKL(KB),DAV(KB),KB = 1,K)
   72 FORMAT(/F7.2,4X,F6.4,2E17.7)
      GO TO 1
      STOP
      END
      ENDS
```

ACTP

This program calculates Arrhenius and Eyring activation parameters and 95% confidence intervals for inputted lifetimes and temperatures.

```
      PROGRAM ACTP  (INPUT,OUTPUT,TAPE5=INPUT,TAPE6=OUTPUT)
C
C     SIR GEORGE WILLIAMS UNIVERSITY.  NOVEMBER, 1971.
C     FORTRAN IV FOR CDC 6400.
C
C     CALCULATION OF ARRHENIUS AND EYRING ACTIVATION PARAMETERS USING
C     LINEAR REGRESSION ANALYSIS.
C
C     LINEAR REGRESSION ANALYSIS BASED ON
C     LARK, CRAVEN, AND BOSWORTH, 'THE HANDLING OF CHEMICAL DATA'.
C     CONFIDENCE LIMITS ARE BASED ON SLOPE AND INTERCEPT OF ARRHENIUS LINE
C     K = A*EXP(-EACT/RT)
C
      DIMENSION IDEN(7),TAU(50),TC(50),TK(50),TR(50),REXP(50),RFIT(50),
     1HEXP(50),SEXP(50),SFIT(50),GEXP(50),GFIT(50)
      DIMENSION ALKE(50),ALKR(50)
      GK=1.98640E-3
      BK=1.38049E-16
      PK=6.6254E-27
      RKH=BK/PK
      ALNR=ALOG(RKH)
    1 READ(5,100)NRUN,IDEN
  100 FORMAT(I3,7A10)
      IF (NRUN.EQ.0) STOP 1
      WRITE(6,101)
  101 FORMAT(15H1PROGRAM ACTPAR,///1X,15(1H*),* ARRHENIUS AND EYRING ACT
     1IVATION PARAMETERS AND 95 PERCENT CONFIDENCE INTERVALS *,15(1H*)//
     2/)
      I=1
    2 READ(5,103)TAU(I), TC(I)
  103 FORMAT(3X,2F10.0)
      IF (TAU(I).EQ.0.0.AND.TC(I).EQ.0.0) GO TO 3
      I=I+1
      GO TO 2
    3 NDATA=I-1
      READ(5,102)TEMP
  102 FORMAT(F10.0)
C
C     WRITE OUT EXPERIMENTAL DATA
      WRITE(6,105)NRUN,IDEN
  105 FORMAT(* CASE NUMBER *,I3,10X,7A10,///)
      WRITE(6,106)
  106 FORMAT(/1X,6(1H*),* EXPERIMENTAL LIFETIMES, RATE CONSTANTS, AND TE
     1MPERATURES *,6(1H*)//)
      WRITE(6,110)
  110 FORMAT(5X,*POINT*,5X,*LIFETIME*,5X,*RATE CONSTANT*,5X,*DEGREES C.*,
     1,5X,*DEGREES K.*/15X,*(SECONDS)*,5X,*(1/SECOND)*/)
      DO 4 I=1,NDATA
      TK(I)=TC(I)+273.16
      REXP(I)=1.0/TAU(I)
      TR(I)=1000.0/TK(I)
      WRITE(6,111)I,TAU(I),REXP(I),TC(I),TK(I)
  111 FORMAT(6X,I2,5X,E10.4,5X,F10.4,9X,F6.1,9X,F6.1)
    4 CONTINUE
C
```

```
C     LINEAR REGRESSION CALCULATIONS
      WRITE(6,120)
  120 FORMAT(////1X,21(1H*),* LINEAR REGRESSION TO ARRHENIUS EQUATION *,
     120(1H*)/)
      SUMX=SUMY=SUMXX=SUMYY=SUMXY=0.0
      DO 6 I=1,NDATA
      ALKE(I)=ALOG(REXP(I))
      SUMX=SUMX+1.0/TK(I)
      SUMY=SUMY+ALKE(I)
      SUMXX=SUMXX+(1.0/TK(I))**2
      SUMXY=SUMXY+(ALOG(REXP(I)))/TK(I)
      SUMYY=SUMYY+(ALOG(REXP(I)))**2
    6 CONTINUE
      NF=NDATA-2
      FN=NF
      PN=NDATA
      XAV=SUMX/PN
      YAV=SUMY/PN
      CSUMXX=SUMXX-PN*(XAV**2)
      CSUMYY=SUMYY-PN*(YAV**2)
      CSUMXY=SUMXY-PN*XAV*YAV
      SLOPE=CSUMXY/CSUMXX
      YINT=YAV-SLOPE*XAV
      EACT=-GK*SLOPE
      A = EXP(YINT)
C
C     ARRHENIUS PARAMETER CONFIDENCE INTERVAL CALCULATIONS
      DSUMYY=CSUMYY-SLOPE*CSUMXY
      STERR2=DSUMYY/FN
      STERR=SQRT(STERR2)
      ERSLOPE=STERR/SQRT(CSUMXX)
      W1=SUMXX/(PN*CSUMXX)
      ERINT=STERR*SQRT(W1)
      EACTER=GK*ERSLOPE
      WRITE(6,121)
  121 FORMAT(/* COMPARISON OF EXPERIMENTAL AND REGRESSION VALUES OF LN(R
     1ATE CONSTANT)*//5X,*POINT*,5X,*LN(KEXP)*,5X,*LN(KFIT)*,5X,*DIFFERE
     2NCE*,5X,*DIFF/STERROR*,5X,*DEGREES C.*/)
      DO 20 I=1,NDATA
      ALKR(I)=YINT+SLOPE/TK(I)
      DY=ALKE(I)-ALKR(I)
      RY=DY/STERR
      WRITE(6,122)I,ALKE(I),ALKR(I),DY,RY,TC(I)
  122 FORMAT(6X,I2,5X,F8.3,5X,F8.3,6X,F8.3,8X,F8.2,7X,F8.1)
   20 CONTINUE
      WRITE(6,123)
  123 FORMAT(////1X,4(1H*),* STANDARD LINEAR REGRESSION ERRORS *,5(1H*)/
     1/)
      WRITE(6,124)STERR
  124 FORMAT(5X,* STANDARD ERROR IN REGRESSION = *,F8.3/)
      WRITE(6,125)ERINT
  125 FORMAT(5X,*  STANDARD ERROR IN INTERCEPT = *,F8.3/)
      WRITE(6,126)ERSLOPE
  126 FORMAT(10X,* STANDARD ERROR IN SLOPE = *,F8.3/)
      ST=0.0
```

```
      CALL STUDENT(NF,ST)
C          95 PERCENT CONFIDENCE INTERVAL IN LN(K) AT A CHOSEN TEMPERATURE
      W2=1.0/PN+((1.0/TEMP-XAV)**2)/GSUMXX
      ERRY=STERR*SQRT(W2)
      CIY=ST*ERRY
C          95 PERCENT CONFIDENCE INTERVAL IN SLOPE
      CISLOPE=ST*ERSLOPE
C          95 PERCENT CONFIDENCE INTERVAL IN INTERCEPT
      CIYINT=ST*ERINT
      CLOGA=YINT/2.303
      CLOGIA=CIYINT/2.303
C          95 PERCENT CONFIDENCE INTERVAL IN ACTIVATION ENERGY
      CIE=GK*CISLOPE
      ELO=EACT-CIE
      EHI=EACT+CIE
      YINTHI=YINT+CIYINT
      YINTLO=YINT-CIYINT
      ALO=EXP(YINTLO)
      AHI=EXP(YINTHI)
      WRITE(6,130)
  130 FORMAT(///1X,38(1H*),* ARRHENIUS ACTIVATION PARAMETERS *,38(1H*)//
     1* ACTIVATION PARAMETERS AND STANDARD ERRORS*/)
      WRITE(6,134)EACT,EACTER
  134 FORMAT(/5X,*ACTIVATION ENERGY = *,F7.3,5X,*STANDARD ERROR = *,
     1F6.3)
      WRITE(6,135)YINT,ERINT
  135 FORMAT(/8X,*NATURAL LOG(A) = *,F7.3,5X,*STANDARD ERROR = *,F6.3/)
      WRITE(6,136)
  136 FORMAT(//* ACTIVATION PARAMETERS AND CONFIDENCE LIMITS*/)
      WRITE(6,131)EACT,CIE,ELO,EHI
  131 FORMAT(/5X,*ACTIVATION ENERGY = *,F8.4,3X,*(+OR-)*,F7.4,5X,
     1*LOWER LIMIT = *,F8.4,3X,*UPPER LIMIT = *,F8.4,2X,*KCAL/MOLE*)
      WRITE(6,132)A,ALO,AHI
  132 FORMAT(/6X,*FREQUENCY FACTOR = *,E10.4,5X,*LOWER LIMIT = *,E10.4,
     13X,* UPPER LIMIT = *,E10.4)
      WRITE(6,137)YINT,CIYINT
  137 FORMAT(/6X,*NATURAL LOG(A) = *,F8.4,3X,*(+OR-)*,F7.4)
      WRITE(6,133)CLOGA,CLOGIA
  133 FORMAT(/9X,*COMMON LOG(A) = *,F8.4,3X,*(+OR-)*,F7.4)
C
C     CALCULATE EYRING PARAMETERS
      WRITE(6,140)
  140 FORMAT(////,1X,31(1H*),* EYRING ACTIVATION PARAMETERS *,31(1H*)//)
      WRITE(6,142)
  142 FORMAT(5X,*POINT*,8X,*ENTHALPY*,10X,*-----ENTROPY (E.U.)-----*,
     110X,*FREE ENERGY (KCAL/MOLE)*/1X,*(KCAL/MOLE)*,9X,*EXP.*,6X,
     2*FIT*,5X,*DIFF.*,11X,*EXP.*,5X,*FIT*,5X,*DIFF.*/)
      DO 14 I=1,NDATA
      HEXP(I)=EACT-GK*TK(I)
      GEXP(I)=(GK*TK(I))*(ALNR+ALOG(TK(I))-ALOG(REXP(I)))
      SEXP(I)=1000.0*(HEXP(I)-GEXP(I))/TK(I)
      RFIT(I)=A*EXP(SLOPE/TK(I))
      GFIT(I)=(GK*TK(I))*(ALNR+ALOG(TK(I))-ALOG(RFIT(I)))
      SFIT(I)=1000.0*GK*(YINT-ALNR-ALOG(TK(I))-1.0)
      DIFFS=SEXP(I)-SFIT(I)
```

```
      DIFFG=GEXP(I)-GFIT(I)
      WRITE(6,141)I,HEXP(I),SEXP(I),SFIT(I),DIFFS,GEXP(I),GFIT(I),DIFFG
  141 FORMAT(6X,I2,10X,F7.3,10X,F7.2,5X,F7.2,F7.2,9X,F8.3,F9.3,F8.3)
   14 CONTINUE
C
C     CALCULATE EYRING PARAMETERS FOR A SPECIFIC TEMPERATURE
      YTEMP=YINT+SLOPE/TEMP
      YLO=YTEMP-CIY
      YHI=YTEMP+CIY
      EYTEM = EXP(YTEMP)
      TYTEM = 1./EYTEM
      ACL = EXP(YLO)
      ACH = EXP(YHI)
      ADL = 1./ACL
      ADH = 1./ACH
C          95 PERCENT CONFIDENCE INTERVAL IN FREE ENERGY
      RTEMP=A*EXP(SLOPE/TEMP)
      GT=(GK*TEMP)*(ALNR+ALOG(TEMP)-ALOG(RTEMP))
      GLO=(GK*TEMP)*(ALNR+ALOG(TEMP)-YHI)
      GHI=(GK*TEMP)*(ALNR+ALOG(TEMP)-YLO)
      GERR=GHI-GLO
      GERR2=GERR/2.0
C          95 PERCENT CONFIDENCE INTERVAL IN ENTHALPY
      HT=EACT-GK*TEMP
      HLO=ELO-GK*TEMP
      HHI=EHI-GK*TEMP
      HERR=HHI-HLO
      HERR2=HERR/2.0
C          95 PERCENT CONFIDENCE INTERVAL IN ENTROPY
      STD=1000.0*GK*(YINT-ALNR-ALOG(TEMP)-1.0)
      SLO=1000.0*GK*(YINTLO-ALNR-ALOG(TEMP)-1.0)
      SHI=1000.0*GK*(YINTHI-ALNR-ALOG(TEMP)-1.0)
      SERR=SHI-SLO
      SERR2=SERR/2.0
      WRITE(6,150)TEMP
  150 FORMAT(///* EYRING ACTIVATION PARAMETERS CALCULATED FOR *,F5.1,
     1* DEG. K.*//34X,*(+OR-)*,6X,*INTERVAL*,6X,*LOWER*,8X,*UPPER*/)
      WRITE(6,151)HT,HERR2,HERR,HLO,HHI
  151 FORMAT(7X,*ENTHALPY = *,F8.4,4(5X,F8.4),2X,*KCAL/MOLE*/)
      WRITE(6,152)STD,SERR2,SERR,SLO,SHI
  152 FORMAT(7X,*ENTROPY = *,F8.4,4(5X,F8.4),3X,*E.U.*/)
      WRITE(6,153)GT,GERR2,GERR,GLO,GHI
  153 FORMAT(4X,*FREE ENERGY = *,F8.4,4(5X,F8.4),2X,*KCAL/MOLE*/)
C
C     CALCULATE DATA FOR PLOTTING
      WRITE(6,160)
  160 FORMAT(///4(1H*),* DATA FOR PREPARATION OF ARRHENIUS PLOT *,4(1H*)
     1//5X,*POINT*,5X,*LN(KEXP)*,5X,*LN(KFIT)*,5X,*1000/T*/)
      DO 60 I=1,NDATA
      WRITE(6,161)I,ALKE(I),ALKR(I),TK(I)
  161 FORMAT(6X,I2,5X,F8.3,5X,F8.3,4X,F8.3)
   60 CONTINUE
      WRITE(6,1000)YTEMP,YHI,YLO,EYTEM,ACH,ACL,TYTEM,ADH,ADL
 1000 FORMAT(//30(1H*),10X,*RATE PARAMETERS*,10X,30(1H*)//* LN K = *,
     1    E20.8,
```

```
     120X,≠HI = ≠,E20.8,10X,≠LO = ≠,E20.8/≠ RATE = ≠,E20.8,20X,≠HI = ≠,
     2E20.8,10X,≠LO = ≠,E20.8/≠ TAU = ≠,E20.8,20X,≠HI = ≠,E20.8,10X,
     3 ≠LO = ≠,E20.8//)
      WRITE(6,199)
  199 FORMAT(////2(1X,110(1H*)/))
C
C     START NEXT CASE
      GO TO 1
      END
```

```
      SUBROUTINE STUDENT(NF,VAL)
      DIMENSION Z(48)
C     STUDENTS T VALUES FOR 95 PERCENT CONFIDENCE LIMITS
      Z( 1) =  12.706
      Z( 2) =  4.3027
      Z( 3) =  3.1825
      Z( 4) =  2.7764
      Z( 5) =  2.5706
      Z( 6) =  2.4469
      Z( 7) =  2.3646
      Z( 8) =  2.3060
      Z( 9) =  2.2622
      Z(10) =  2.2281
      Z(11) =  2.2010
      Z(12) =  2.1788
      Z(13) =  2.1604
      Z(14) =  2.1448
      Z(15) =  2.1315
      Z(16) =  2.1199
      Z(17) =  2.1098
      Z(18) =  2.1009
      Z(19) =  2.0930
      Z(20) =  2.0860
      Z(21) =  2.0796
      Z(22) =  2.0739
      Z(23) =  2.0687
      Z(24) =  2.0639
      Z(25) =  2.0595
      Z(26) =  2.0555
      Z(27) =  2.0518
      Z(28) =  2.0484
      Z(29) =  2.0452
      Z(30) =  2.0423
      DO 1 I=31,35
      Z(I) = 2.04
    1 CONTINUE
      DO 2 I=36,48
      Z(I) = 2.02
    2 CONTINUE
      VAL = Z(NF)
      RETURN
      END
```

NICKA

This program computes a normalized lineshape for an uncoupled two-site exchange system given the peak separation, the population of each site and the transverse relaxation times in the absence of exchange.

```
      PROGRAM NICKA(OUTPUT,INPUT,TAPE60=INPUT,TAPE61=OUTPUT)
C     COMMENT CARDS ON WHICH APE WRITTEN WRITE AND FORMAT STATEMENTS ARE TO BE
C     INCLUDED AS PART OF THE PROGRAM WHEN ONE WANTS TO PRINT OUT ALL OF THE
C     DATA. HOWEVER THEY MAY BE OMITTED WHEN ONE WANTS ONLY THE TABULATED RESULTS.
C     PROGRAM HAS BEEN REWRITTEN IN FORTRANIV AS OF MARCH 7,1968
      INTEGER  H
      DIMENSION V(3000), W(3000), T(1500),WID(3000), RH(1500),WSEP
     1(1500), VMX(1500), WSP(1500)
      TWOPI = 2.0*3.14159265
  200 READ (60,100) B,T2A,T2B,PA,PB,STEP1,STEP2,STEP3,STEP4,STEP5
  100 FORMAT (8F10.3/2F10.3)
      IF (B .EQ. 0.0) GO TO 47
    1 READ (60,50) STEPX, STEPY, STEP7,TEMP
   50 FORMAT (F10.2,F10.2,F10.3,44X,F6.1)
C     WRITE (61,99) PA,PB,B,T2A,T2B
C  99 FORMAT (1H1,4HPA =F10.3,6H, PB =F10.3,5H, B =F10.3,
C    1         7H, T2A =F10.3,7H, T2B =F10.3)
      K=0
      TAU = 0.00004
    2 TAU=TAU+STEP1*1.0E-6
    3 IF(TAU-1.0E-5)4,4,39
C   4 WRITE (61,5) TAU
C   5 FORMAT (1H1,5HTAU =E14.5)
    4 CONTINUE
      A=(PB/T2A+PA/T2B)*TAU+1.0
      U=1.0/T2B-1.0/T2A
      X=(1.0/(T2A*T2B)+B**2)*TAU+PA/T2A+PB/T2B
      Y=(PA-PB)*B
      Z=1.0+TAU/T2A+TAU/T2B
    6 I=1
    7 W7=-STEPX*TWOPI
    9 W(I)=W7
C SINCE PA WILL ALWAYS EQUAL PB FOR THE COMPOUNDS OF INTEREST TO US, THE NEXT
C     IF STATEMENT IS NOT NECESSARY
   10 IF (PA .EQ. PB) GO TO 67
   68 IF (W(I)-STEPX*TWOPI) 11,11,17
   67 IF (W(J)) 11,11,17
   11 P=X-(W(I)**2)*TAU
      Q=TAU*(W(I)-Y)
      R=W(I)*Z+Y
      V(I)=(P*A+(R+(TAU*U*B))*Q)/(P**2+R**2+(TAU*U*B)**2+2.0*R*(TAU*U*B
     1))
   15 I=I+1
    8 W7=W7+STEPY*TWOPI
      GO TO 9
   17 J=I
      W(J)=0.
      P=X-(W(I)**2)*TAU
      Q=TAU*(W(I)-Y)
      R=W(I)*Z+Y
      V(I)=(P*A+(R+(TAU*U*B))*Q)/(P**2+R**2+(TAU*U*B)**2+2.0*R*(TAU*U*B
     1))
      DO 66 I=1,J
   66 W(I)=W(I)/TWOPI
C  37 WRITE (61,98) (W(I),V(I), I=1,J)
```

```
C  AFTER THE ABOVE WRITE STATEMENT WILL COME THE PLOT     STATEMENTS WHICH HAVE
C    BEEN DELETED BECAUSE THE PLOT     IS NOT AS ACCURATE AS THE NUMERICAL
C      DATA    WHICH CAN BE EXTRAPOLTED
C  98 FORMAT (3(14X,1HW,19X,1HV)/3(10X,F10.4,10X,F10.5))
   37 CONTINUE
C AFTER FORMAT STATEMENT 98, INSERT THE SUBPROGRAM TO SORT OUT VALLES OF LINE-
C  WIDTHS AND OTHER PARAMETERS FOR MATCHING EXPERIMENTAL TO THEORETICAL SPECTRA
      K=K+1
      M=K
      L=3*K-2
      T(K)=TAU
      IF(V(J) .GT. V(J-1)) GO TO 20
C     POST-COALESCENCE CALCULATION
      GO TO 21
   20 VMAX=V(J)
      RH(K)=0.
      WSEP(K)=0.
      VQRT=VMAX/4.
      VQ=VQRT
   26 DO 22 I=1,J
      IF(VQRT .LT. V(I)) GO TO 23
   22 CONTINUE
   23 WID(L) =(-2.0/TWOPI)*(W(I)*TWOPI+(STEPY*TWOPI*((V(I)-VQRT)/(V(I)-
     1V(I-1)))))
      VQRT=VQRT+VQ
      IF(VQRT .GT. (.8L*VMAX) GO TO 24
   25 L=L+1
      GO TO 26
C  24 WRITE (61,27) TAU, WID(3*K-2),WID(3*K-1),WID(3*K)
C  27 FORMAT (1HC,11X,83HTAU      LINEWIDTH AT    ONE FOURTH      ONE HALF
C     1    THREE-FOURTHS    MAXIMUM AMPLITUDE/
C     11H0,F14.5,F30.5,F13.5,F17.5)
   24 CONTINUE
      GO TO 2
C     PRE-COALESCENCE CALCULATION
   21 DO 28 I=1,J
      IF(V(I) .GT. V(I+1)) GO TO 29
   28 CONTINUE
   29 H=1
      N=I
      WSP(H)=W(I-1)*TWOPI
      VMX(H)=V(I-1)
   71 H=H+1
      WSP(H)=WSP(H-1)+TWOPI*STEPZ
      P=X-(WSP(H)**2)*TAU
      Q=TAU*(WSP(H)-Y)
      R=WSP(H)*Z+Y
      VMX(H)=(P*A+(R+(TAU*U*B))*Q)/(P**2+R**2+(TAU*U*B)**2+
     12.0*R*(TAU*U*B))
      IF(VMX(H) .LT. VMX(H-1)) GO TO 70
      GO TO 71
   70 VMAX=VMX(H-1)
      VQRT=VMAX/4.0
      VQ=VQRT
      WMAX=(-2.0/TWOPI)*WSP(H-1)
```

```
      WSEP(K)=WMAX
      RHX=VMAX/V(J)
      RH(K)=RHX
   52 DO 30 I=1,J
      IF(VQRT .LT. V(I)) GO TO 31
   30 CONTINUE
   31 WID1= (W(I)*TWOPI-(STEPY*TWOPI*((V(I)-VQRT)/(V(I)-V(I-1)))))
      DO 32 I=N,J
      IF(VQRT .GT. V(I)) GO TO 34
   32 CONTINUE
      WID(L)= (-2.0*WID1)/TWOPI
   51 VQRT=VQRT+VQ
      L=L+1
      IF(VQRT .GT. 0.80*VMAX)  GO TO 36
      GO TO 52
   34 WID2= (W(I)*TWOPI-((V(I)-VQRT)/(V(I)-V(I-1)))*STEPY*TWOPI)
      WID(L)=(WID2-WID1)/TWOPI
      GO TO 51
C  36 WRITE (61,54) TAU, WID(3*K-2), WID(3*K-1), WID(3*K), RHX, WMAX
C  54 FORMAT (1H0,11X,83HTAU      LINEWIDTH AT   ONE FOURTH      ONE HALF
C     1   THREE-FOURTHS   MAXIMUM AMPLITUDE/
C     11H0,E14.5,F30.5,F13.5,F17.5///
C     11H0,12X,22HRATIO (MAX. TO MIN.) =F10.4,10X,17HFULL-SEPARATION =
C     1F10.4)
   36 CONTINUE
      GO TO 2
   39 TAU=TAU+STEP2*1.0E-5
   40 IF(TAU-1.0E-4)4,4,41
   41 TAU=TAU+STEP3*1.0E-4
   42 IF(TAU-1.0E-3)4,4,43
   43 TAU=TAU+STEP4*1.0E-3
   44 IF(TAU-1.0E-2)4,4,45
   45 TAU=TAU+STEP5*1.0E-2
   46 IF(TAU-0.300)4,4,300
C     VALUE IN STATEMENT 46 IS LAST TAU CALC. - CAN BE CHANGED
  300 WRITE (61,207)
  207 FORMAT(1HR)
      WRITE (61,97) B,T2A,T2B,PA,PB,TEMP
   97 FORMAT(1H1,* B =*,F10.3,* T2A =*,F10.3,* T2B =*,F10.3* PA =*,
     1  F10.3,* PB =*, F10.3,20X,*TEMP = *,F6.1,* C*///)
      WRITE (61,55)
   55 FORMAT(  7X,   *TAU*,12X,*RATIO     FULL SEPARATION      WIDTH AT
     1ONE-FOURTH     ONE-HALF       THREE-FOURTHS    MAXIMUM*/)
      DO 301 K=1,M
      WRITE (61,56) T(K),RH(K),WSEP(K),WID(3*K-2),WID(3*K-1),WID(3*K)
   56 FORMAT (1H ,E13.4,F13.3,F15.3,F28.3,F13.3,F17.3)
  301 CONTINUE
      GO TO 200
   47 STOP
      END
```

DNMR3

This program calculates the lineshape for a multisite exchange system given the number of sites, the initial chemical configuration, the final chemical configuration, the chemical shifts, the populations of each site, the transverse relaxation time in the absence of exchange, the number of magnetically equivalent sites and the coupling constants.

```
      PROGRAM DNMR3(INPUT,OUTPUT,PUNCH,TAPE1,TAPE5 = INPUT,TAPE6 =
     1 OUTPUT)
C
C     GENERAL NMR LINE-SHAPE PROGRAM
C     WITH SYMMETRY AND MAGNETIC EQUVALENCE FACTORING
C     BY G. BINSCH AND D.A. KLEIER
C     ADAPTED FOR S.G.W.U. CDC 6400 BY K. HERSH
C     VERSION D    JUNE 1/72.
      INTEGER P
      LOGICAL TWICE
      REAL TIME
      DIMENSION WS(5),AJS(4,5)
      COMPLEX A(48,48),CR(48,48),CL(48,48),EIG(48), Q(136),D(136),TEMP
      COMMON /PAR/W(3,5),AJ(3,4,5)
      COMMON /SUB/NO(7),LL(7),FZ(32,5),NS,ISY(7),P(32)
      COMMON /HAM/H(3252),HT(32,32)
      COMMON /INDEX/IROW(210),JCOL(210),IT(32,32)
      COMMON /VEC/V(210),POV(210)
      COMMON /DYNPAR/RC(3,3),T2
      COMMON /VECT/C,D
      COMMON /EIVEC/CR,CL,EIG
      COMMON /PLTPAR/SCALE,HEIGHT,FR1,FR2
      COMMON /PERMT/IE(3,5),PT(2,32,32),MU
      COMMON /MAG/IME(6,5),WF(6)
      COMMON /NAME/NTEXT(7)
      COMMON N,NP,MAX,MAXM,NE,NM,NEM,NEN,NMES,NMESM,NNMES(5),NSYM,MRC
      EQUIVALENCE (CR(1,1),A(1,1))
      DIMENSION POP(3)
      PRINT 100
  100 FORMAT (* EXECUTION BEGINS *)
      DO 6001 I = 1,32
      DO 6001 J = 1,5
      FZ(I,J) = 0.0
 6001 CONTINUE
      DO 6002 I = 1,3
      DO 6002 J = 1,5
      IE(I,J) = 0
 6002 CONTINUE
      DO 6003 I = 1,7
      LL(I) = 0
 6003 CONTINUE
      IREP = 0
    1 CALL STADAT
      KEN = 0
      DO 5001 I = 1,32
      P(I) = 0
 5001 CONTINUE
      NSAVE = N
      NSYMS = NSYM
      MRC = 0
      RMIN = W(1,1)
      RMAX = W(1,1)
      RMAX1 = 0.0
      DO 221          I = 1, NEN
      DO 222 J = 1,NMES
```

```
      RMIN = AMIN1(W(I,J),RMIN)
      RMAX = AMAX1(W(I,J),RMAX)
      JP = J + 1
      IF(JP .GT. NMES) GO TO 222
      DO 21 K = JP, NMES
      AB = ABS(AJ(I,J,K))
      RMAX1 = AMAX1(RMAX1,AB)
   21 CONTINUE
  222 CONTINUE
  221 CONTINUE
      RMAX = RMAX - RMIN
      RMAX = AMAX1(RMAX,RMAX1)
      IF(N.NE.NMES) GO TO 12
      WF(1) = 1.0
      DO 67 I = 1 , NMES
   67 IME(1,I) = 0.5
      GO TO 20
   12 CALL MAGEQ(NIC)
   20 NP = N + 1
      MAX = 2**N
      MAXM = MAX - 1
      NEM = NE - 1
      READ(5,1001) NRS,LPUNCH,LPLOT,NPSR,FR1,FR2,SCALE,HEIGHT
 1001 FORMAT(I2,2I1,I2,4X4F10.0)
      WRITE(6,1002) FR1,FR2,SCALE,HEIGHT
 1002 FORMAT(1X/////≠ PLOTTING PARAMETERS≠//10X≠LEFT PLOT FREQENCY≠,
     111X≠=≠,F8.3,≠ CPS≠/10X≠RIGHT PLOT FREQUENCY≠,10X≠=≠,F8.3,≠ CPS≠/9)
     2≠SCALE≠,25X,≠=≠,F8.3,≠ MM/CPS≠/10X≠HEIGHT≠,24X,≠=≠,F8.3,≠ MM≠////)
      IF(MU .EQ. 1) GO TO 8
      WRITE(6,1010)
 1010 FORMAT(≠POPULATIONS≠)
      READ(5,1003) (POP(I),I=1,NE)
 1003 FORMAT(3F10.3)
      WRITE(6,1004) (I,POP(I),I= 1,NE)
 1004 FORMAT(10X≠POP(≠,I1,≠) = ≠,F6.3)
    8 IF(EOF(5)) 2030,2008
 2030 WRITE(6,2050) N,NE,MU,NMES,NSYM
 2050 FORMAT(5I5)
      STOP
 2008 READ(5,1101) T2
 1101 FORMAT(F10.0)
      WRITE(6,1102) T2
 1102 FORMAT(1X///≠ RELAXATION TIME =≠,F8.3,≠ SEC≠//)
      IF(NE.EQ.1) NRS = 1
      DO 5000 NIR = 1,NRS
      K = 0
      IF(NE.EQ.1) GO TO 27
      WRITE(6,1005)
 1005 FORMAT(1X///≠ RATE CONSTANTS IN (1/SEC)≠//)
      IF(MU .EQ. 0) GO TO 10
      READ(5,1006) RC(1,2)
      RMIN = RC(1,2)
      WRITE(6,1009) RC(1,2)
 1009 FORMAT(≠ K = ≠,F15.6///)
      IF(N.EQ.NMES) GO TO 16
```

```
      DO 19 I = 1,NE
      DO 19 J = 1, NE
   19 RC(I,J) = RC(1,2)
      GO TO 16
   10 DO 2 I = 1, NEM
      IP = I + 1
      DO 2 J = IP,NE
      READ(5,1006) RC(I,J)
 1006 FORMAT(F10.0)
      RC(J,I) = RC(I,J)*POP(I)/POP(J)
      IF(I.EQ.1 .AND. J..EQ. 2) RMIN = RC(1,2)
      RMIN = AMIN1(RMIN,RC(J,I),RC(I,J))
    2 WRITE(6,1007) I,J,RC(I,J)
 1007 FORMAT(10X≠K(≠,I1,≠,≠,I1,≠) = ≠,F15.6)
   13 WRITE(6,1008)
 1008 FORMAT(1X///)
   16 IF((RMIN/RMAX) - 1.0E+03) 27,27,28
   28 MRC = 1
      NENS = NEN
      NEN = 1
      IF(MU .EQ. 0) GO TO 36
      DO 37 I = 2,NE
      DO 38 J = 1, NMES
      L = IE(I,J)
   38 W(I,L) = W(1,J)
      DO 37 J = 1, NMESM
      JP = J +1
      L = IE(I,J)
      K1 = K
      DO 37 K = JP, NMES
      M = IE(I,K)
      IF(L .LT. M) GO TO 39
      AJ(I,M,L) = AJ(1,J,K)
      GO TO 37
   39 AJ(I,L,M) = AJ(1,J,K)
   37 CONTINUE
      K = K1
   36 DO 29 I = 1 , NMES
      WS(I) = W(1,I)
      IF(MU .EQ. 0) W(1,I) = POP(1)*W(1,I)
      IF(MU .EQ. 1) W(1,I) = (1./FLOAT(NE)*W(1,I))
      DO 30 J = 2,NE
      IF(MU .EQ. 0) GO TO 34
      W(1,I) = (1./FLOAT(NE)) * W(J,I) + W(1,I)
      GO TO 30
   34 W(1,I) = POP(J) *W(J,I) + W(1,I)
   30 CONTINUE
      IP = I + 1
      IF(IP .GT. NMES) GO TO 27
      DO 29 KK = IP, NMES
      AJS(I,KK) = AJ(1,I,KK)
      IF(MU .EQ.0) AJ(1,I,KK) = POP(1)*AJ(1,I,KK)
      IF(MU .EQ. 1) AJ(1,I,KK) = (1./FLOAT(NE))* AJ(1,I,KK)
      DO 29 J = 2, NE
      IF(MU .EQ. 0) GO TO 35
```

```
      AJ(1,I,KK) = (1./FLOAT(NE)) * AJ(J,I,KK) + AJ(1,I,KK)
      GO TO 29
   35 AJ(1,I,KK) = POP(J)*AJ(J,I,KK) + AJ(1,I,KK)
   29 CONTINUE
   27 IF(N.EQ.NMES) NIC = 1
      DO 4099 ITE = 1,NIC
      IF(MRC .NE. 1) GO TO 4097
      GO TO 15
 4097 IF(N.EQ.NMES.AND.NIR.GT.1.AND.MRCS.EQ.0) GO TO 4
      IF(N.EQ.NMES.OR.MU.EQ.0) GO TO 15
      DO 11 I = 2,NE
      DO 11J = 1,NMES
      KO = IE(I,J)
      IF(IME(ITE,J) .NE. IME(ITE,KO)) GO TO 14
   11 CONTINUE
      NEN = 1
      GO TO 15
   14 NEN=NE
   15 IF (IREP.EQ.N) GO TO 3
      CALL BASIS(IREP,ITE)
    3 CALL HAMILT(ITE)
      CALL PROJCT(POP,ITE)
   17 IF (MU.EQ.0.OR.NEN.NE.1.OR.MRC.EQ.1) GO TO 4
   18 CALL PERMUT(KEN)
      IF(KEN .EQ. 1) GO TO 1
    4 KC = 1
      K = K + 1
      NB=0
      TWICE=.FALSE.
      ND = N
      IF (N.NE.NMES) ND = NS-1
      NOSS = 0
      NOS = 0
      DO 51 II=1,ND
      NOS = NOS + (NO(II))**2
      IF (NSYM.NE.0) GO TO 63
      NTR=NO(II)*NC(II+1)
      GO TO 64
   63 IF (TWICE) GO TO 65
      NTR=((NO(II)+ISY(II))/2)*((NO(II+1)+ISY(II+1))/2)
      TWICE=.TRUE.
      GO TO 64
   65 NTR=((NO(II)-ISY(II))/2)*((NO(II+1)-ISY(II+1))/2)
      TWICE=.FALSE.
      IF (NTR.EQ.0) GO TO 66
   64 IF (NEN.EQ.1) GO TO 5
      NT=NTR*NE
      GO TO 6
    5 NT=NTR
    6 CALL TRAMAT(A,NTR,NT,NB,ITE,NOSS,NOS,II)
      CALL ALLMAT(A,NT,CL,EIG,KEN)
      IF(KEN .NE. 0) GO TO 1
      CALL CONVEC(K,KC,NT,ITE)
      NB = NB + NTR
      IF (TWICE) GO TO 63
```

```
      66 NOSS = NOS
      51 CONTINUE
         K=K-1
         IF (ITE.NE.NIC) GO TO 4099
    4096 WRITE (6,1021)
    1021 FORMAT (1X///17X16HCONTRACTED SHAPE10X19HCONTRACTED SPECTRAL/24X6H
        1VECTOR21X6HVECTOR///)
         KM = K -1
         DO 24 I = 1,KM
         IP1 = I+1
         DO 24 J = IP1,K
         IF (AIMAG(Q(I)).LE.AIMAG(Q(J))) GO TO 24
         TEMP = Q(I)
         Q(I) = Q(J)
         Q(J) = TEMP
         TEMP = D(I)
         D(I) = D(J)
         D(J) = TEMP
      24 CONTINUE
         J = 1
         DO 62 I = 1,K
         IF (ABS(REAL(Q(I))).LE.1.E-03) GO TO 62
         Q(J) = Q(I)
         D(J) = D(I)
         WRITE (6,1022) J,Q(J),D(J)
    1022 FORMAT(I5,5X4E14.6)
         J= J + 1
      62 CONTINUE
         J = J-1
         IF(LPUNCH .EQ. 0) GO TO 4089
         PUNCH 1382,NTEXT,RC(1,2)
    1382 FORMAT(4X,7A10,F6.2)
         IF( NPSR .LT. 1) NPSR = 1
         DO 4088 JAB = 1, NPSR
         PUNCH 1024, J, NTEXT , RC(1,2)
         PUNCH 1023,(Q(JAB),D(JAB), JAB = 1,J)
    1023 FORMAT(4E20.13)
    1024 FORMAT(I3,1H1,7A10, F6.2)
    4088 CONTINUE
    4089 IF (LPLOT.EQ.0) GO TO 4099
         CALL SPECT(J)
    4099 IF (NIC.NE.1) IREP=0
         MRCS = MRC
         IF (MRC.NE.1) GO TO 5000
         MRC = 0
         NEN = NENS
         DO 32 I = 1,NMFS
         W(1,I) = WS(I)
         IP = I +1
         IF (IP.GT.NMES) GO TO 5000
         DO 32 J = IP,NMES
      32 AJ(1,I,J) = AJS(I,J)
    5000 CONTINUE
         WRITE(6,7070)
    7070 FORMAT(*THIS IS A ERROR*)
```

```
PROGRAM     DNMR3
            GO TO 1
            END
```

```
      SUBROUTINE STADAT
C
C     THIS SUBROUTINE READS AND PRINTS THE STATIC PARAMETERS
C
      COMMON N,NP,MAX,MAXM,NE,NM,NEM,NEN,NMES,NMESM,NNMES(5),NSYM,MRC
      COMMON /PAR/W(3,5),AJ(3,4,5)
      COMMON /PERMT/IE(3,5),PT(2,32,32),MU
      COMMON /NAME/NTEXT(7)
      READ 1001,NRUN,N,NE,MU,NMES,NSYM
 1001 FORMAT(I3,5I1)
      IF (NRUN.EQ.0) STOP
      IF (N.EQ.NMES) GO TO 15
      READ 1007,(NNMES(J),J=1,NMES)
 1007 FORMAT (5I1)
   15 READ 1011, NTEXT
 1011 FORMAT(7A10)
      WRITE (6,1021) NRUN,NTEXT,N,NE,NSYM
 1021 FORMAT (1H1,10HRUN NUMBERI4,5X7A10//20XI1,12H NUCLEI      I1,24H ELECTRO
     1NICAL CONFIGURATIONS,6X,I2,* SYMMETRY PAIRS*////)
      NEN=NE
      IF (MU.EQ.1) NEN=1
      DO 1 I=1,NEN
      READ 1002,(W(I,J),J=1,NMES)
 1002 FORMAT(5F10.0)
      NMESM=NMES-1
      IF (NMES.EQ.1) GO TO 1
      DO 18 J=1,NMESM
      JP=J+1
      READ 1003,(AJ(I,J,K),K=JP,NMES)
 1003 FORMAT(4F10.0)
   18 CONTINUE
    1 CONTINUE
      IF (MU.EQ.0) GO TO 21
      DO 2 I=2,NE
      READ 1004,(IE(I,K),K=1,NMES)
 1004 FORMAT(5I1)
      WRITE(6,6) I
    6 FORMAT (9H THE NO. I1,16H EXCHANGE VECTOR)
      DO 7 K=1,NMES
    7 WRITE (6,5) K, IE(I,K)
    5 FORMAT (4H IE(I1,4H) = I1)
    2 CONTINUE
      IF (N.EQ.NMES) GO TO 13
      DO 22 I = 2,NE
      DO 23 J =1,NMES
      JT = IE(I,J)
      W(I,JT) = W(1,J)
      JP = J + 1
      IF (JP.GT.NMES) GO TO 23
      DO 24 K = JP,NMES
      KT = IE(I,K)
      AJ(I,JT,KT) = AJ(1,J,K)
   24 AJ(I,KT,JT) = AJ(I,JT,KT)
   23 CONTINUE
   22 CONTINUE
```

```
   21 IF (N.EQ.NMES) GO TO 13
      WRITE(6,1005)
 1005 FORMAT(29H MAGNETICALLY EQUIVALENT SETS//5H SET 5X14H NO. OF NUCLE
     1I)
      DO 14 J=1,NMES
      IF (NNMES(J).EQ.3) NNMES(J)=1
   14 WRITE(6,1006) J,NNMES(J)
 1006 FORMAT(2XI1,14XI1)
   13 DO 11 I=1,NEN
      WRITE (6,1022) I
 1022 FORMAT (1X/////27H CHEMICAL CONFIGURATION NO.I2///10X15HCHEMICAL S
     1HIFTS//)
      DO 11 J=1,NMES
   11 WRITE (6,1023) J,W(I,J)
 1023 FORMAT (13X2HW(I1,4H) = F8.3)
      WRITE (6,1024)
 1024 FORMAT (1X//10X18HCOUPLING CONSTANTS//)
      IF (NMES.EQ.1) GO TO 44
      DO 12 J=1,NMESM
      JP=J+1
      DO 12 K=JP,NMES
   12 WRITE (6,1025) J,K,AJ(I,J,K)
 1025 FORMAT (13X2HJ(I1,1H,I1,4H) = F10.7)
   44 CONTINUE
   10 CONTINUE
      RETURN
      END
```

```
      SUBROUTINE MAGEQ(NIC)
C
C     THIS SUBROUTINE GENERATES THE TOTAL SPIN QUANTUM NUMBERS AND
C     WEIGHTING FACTORS FOR THE VARIOUS COMBINATIONS OF COMPOSITE NUCLE.
      DIMENSION BI(2)
      REAL IME
      COMMON /PERMT/IE(7,5),PT(2,32,32),MU
      COMMON N,NP,MAX,MAXM,NF,NM,NSM,NEN,NMES,NMESM,NNMES(5),NSYM,MRC
      COMMON/MAG/IME(6,5),WF(6)
      DO 1 I=1,NMES
    1 IME(1,I)=(.5)*(FLOAT(NNMES(I)))
      I = 1
    2 J=0
   10 J=J+1
      IF (J.GT.NMES) GO TO 11
      IP=I+1
      IME(IP,J)=IME(I,J)-1.
      IF (IME(IP,J).GE.0) GO TO 9
      IME(IP,J)=IME(1,J)
      GO TO 10
    9 JP=J+1
      IF(JP.GT.NMES) GO TO 4
      DO 8 K=JP,NMES
    8 IME(IP,K)=IME(I,K)
    4 I = I + 1
      GO TO 2
   11 NIC=I
      IF (MU.EQ.0) GO TO 17
      WF(1) = 1.0
      WF(2) = 1.0
      IF (NIC.LT.3) GO TO 17
      K = 2
      DO 18 I = 3,NIC
      DO 19 IS =2,K
      DO 19 J = 2,NE
      DO 20 L = 1,NMES
      LT = IE(J,L)
      IF (IME(I,L) - IME(IS,LT)) 19,20,19
   20 CONTINUE
      WF(IS) = WF(IS) + 1.0
      GO TO 18
   19 CONTINUE
      K = K + 1
      WF(K) = 1.0
      DO 21 M = 1,NMES
   21 IME(K,M) = IME(I,M)
   18 CONTINUE
      NIC = K
   17 DO 7 I = 1,NMES
      IF (IME(NIC,I)) 7,7,12
    7 CONTINUE
      NIC = NIC - 1
   12 DO 3 J = 1,NIC
      IF (MU.EQ.1) GO TO 29
      WF(J)=1.
```

```
   29 DO 3 I = 1,NMES
      N = 2.*IME(1,I)
      DO 5 K=1,2
      M=IME(1,I)-IME(J,I)-FLOAT(K) + 1.
      IF (K.EQ.1.AND.M.EQ.0) GO TO 3
      NBIN=1
      NBID=1
      IF(M.EQ.0) GO TO 5
      DO 6 L=1,M
      LL=L-1
      NBIN=NBIN*(N-LL)
    6 NBID = NBID*L
    5 BI(K)=NBIN/NBID
      WF(J)=WF(J)*(BI(1)-BI(2))
    3 CONTINUE
      RETURN
      END
```

```
      SUBROUTINE BASIS (IREP,ITE)
C
C     SPIN BASIS FUNCTIONS ARE GENERATED, ORDERED, AND THEIR
C     IZ COMPONENTS ACCUMULATED. DIMENSIONS AND INDEX VECTORS
C     FOR HAMILTONIAN SUBMATRICES ARE COMPUTED.
C
      COMMON/MAG/IME(6,5),WF(6)
      INTEGER P
      COMMON /SUB/NO(7),LL(7),FZ(32,5),NS,ISY(7),P(32)
      COMMON N,NP,MAX,MAXM,NE,NM,NEM,NEN,NMES,NMESM,NNMES(5),NSYM,MRC
      REAL IME
C
      IREP=N
      NO(1)=1
      LL(1)=1
      LL(2)=2
      IF (N.EQ.NMES) GO TO 8
      RMAX=1
      DO 18 I=1,NMES
   18 RMAX=RMAX*(2.*IME(ITE,I)+1.0)
      MAX=RMAX+.1
      MAXM = MAX - 1
    8 DO 1 I = 1,NMES
    1 FZ(1,I)=IME(ITE,I)
      NS=2
      I=2
      KT=1
      KTSP=2
      KK=1
      K=0
    2 DO 3 J=1,NMES
    3 FZ(I,J)=FZ(KK,J)
      K=K+1
      FZ(I,K)=FZ(I,K)-1.0
      IF (FZ(I,K)+IME(ITE,K)) 4,6,6
    6 IM=I-1
      IF (IM.LT.KTSP) GO TO 17
      DO 19 J = KTSP,IM
      DO 16 JJ=1,NMES
      IF (FZ(J,JJ).EQ.FZ(I,JJ)) GO TO 16
      GO TO 19
   16 CONTINUE
      I=I-1
      GO TO 17
   19 CONTINUE
   17 IF (I.EQ.MAX) GO TO 10
      IF (K.EQ.NMES) GO TO 5
    4 I=I+1
      GO TO 2
    5 K=0
      IF (KK.EQ.KT) GO TO 7
      KK=KK+1
      I=I+1
      GO TO 2
    7 NO(NS) = I - KT
```

```
      LL(NS+1)=LL(NS)+NO(NS)
      KT=I
      KTSP=KT+1
      NS=NS+1
      GO TO 5
    4 IF (K.NE.NMES) GO TO 2
      I=I-1
      GO TO 5
   10 NO(NS)=1
      IF (NSYM.EQ.0) GO TO 20
      ISY(1)=1
      ISY(NP)=1
      P(1)=1
      P(MAX) = MAX
      DO 21 I=2,N
   21 ISY(I)=0.
      NC=2*NSYM-1
      DO 22 I=2,N
      NA=LL(I)
      JI=LL(I)
      JF=LL(I)+NO(I)-1
      DO 23 J=JI,JF
      DO 24 K=1,NC,2
      IF (FZ(J,K)-FZ(J,K+1)) 23,24,23
   24 CONTINUE
      DO 26 K=1,N
      FZT=FZ(NA,K)
      FZ(NA,K)=FZ(J,K)
   26 FZ(J,K)=FZT
      ISY(I)=ISY(I)+1
      P(NA) = NA
      NA=NA+1
   23 CONTINUE
      KI=LL(I)+ISY(I)
      KF=LL(I)+(NO(I)+ISY(I))/2-1
      IF (KF.NE.KI) GO TO 27
      P(KI)=KF+1
      P(KF+1)=KI
      GO TO 22
   27 KFM=KF-1
      NA=KF+1
      DO 28 K=KI,KFM
      KPI=K+1
      DO 30 KP=KPI,MAX
      DO 29 L=1,NC,2
      IF (FZ(K,L)-FZ(KP,L+1)) 30,31,30
   31 IF (FZ(K,L+1)-FZ(KP,L)) 30,29,30
   29 CONTINUE
      DO 32 L=1,N
      FZT=FZ(NA,L)
      FZ(NA,L)=FZ(KP,L)
   32 FZ(KP,L)=FZT
      GO TO 33
   30 CONTINUE
   33 P(K)=NA
```

```
      P(NA)=K
      NA=NA+1
      KK = K
   28 CONTINUE
      K = KK
      P(K+1) = NA
      P(NA) = K+1
   22 CONTINUE
   20 CONTINUE
      RETURN
      END
```

```
      SUBROUTINE HAMILT(ITE)
C
C     THIS SUBROUTINE ASSEMBLES THE HAMILTONIAN MATRICES
C
      COMMON /HAM/H(3,252),HT(32,32)
      INTEGER P
      COMMON /SUB/NO(7),LL(7),FZ(32,5),NS,ISY(7),P(32)
      COMMON /PAR/W(3,5),AJ(3,4,5)
      COMMON/MAG/IME(6,5),WF(6)
      REAL IME
      COMMON N,NP,MAX,MAXM,NE,NM,NEM,NEN,NMES,NMESM,NNMES(5),NSYM,MRC
C
      MAXT = 0
      IF (N.NE.NMES) NP = NS
      DO 43 I = 1,NP
   43 MAXT = MAXT + (NO(I))**2
      DO 20 I = 1,NEN
      DO 20 J = 1,MAXT
   20 H(I,J) = 0.0
      DO 42 I = 1,NEN
      LC = 0
      NOS = 0
      DO 41 K = 1,MAX
      DO 41 J = 1,MAX
   41 HT(K,J) = 0.0
      DO 42 IA=1,NP
      MM=NO(IA)
      DO 22 J=1,MM
      DO 22 K=J,MM
      JJ=LL(IA)+J-1
      KK=LL(IA)+K-1
      IF (J.EQ.K) GO TO 23
      KINV=0
    1 DO 2 M=1,NMES
      IF (FZ(JJ,M)-FZ(KK,M))- 3,2,3
    3 KINV=KINV+1
      IF (KINV-1) 2,4,5
    4 MA=M
      GO TO 2
    5 IF (KINV-2) 2,6,22
    6 MB=M
    2 CONTINUE
      IF ((FZ(JJ,MA)-FZ(KK,MA))*(FZ(JJ,MB)-FZ(KK,MB))+1.) 22,7,22
    7 HT(JJ,KK) =.5*AJ(I,MA,MB)*SQRT(IME(ITE,MA)*(IME(ITE,MA)+1.)-FZ(JJ,
     1MA)*FZ(KK,MA))*SQRT(IME(ITE,MB)*(IME(ITE,MB)+1.)-FZ(JJ,MB)*FZ(KK,M
     2B))
      HT(KK,JJ)=HT(JJ,KK)
      GO TO 22
   23 DO 30 M = 1,NMES
   30 HT(JJ,JJ)=HT(JJ,JJ)-FZ(JJ,M)*W(I,M)
      IF(NMES.EQ.1) GO TO 22
      DO 31 M=1,NMESM
      MP=M+1
      DO 31 NN=MP,NMES
   31 HT(JJ,JJ)=HT(JJ,JJ)+FZ(JJ,M)*FZ(JJ,NN)*AJ(I,M,NN)
```

```
   22 CONTINUE
      IF (NSYM.EQ.0) GO TO 21
      NCUT = LL(IA) + (NO(IA) + ISY(IA))/2
      ITI = LL(IA)
      ITF = LL(IA) + NC(IA) - 1
      DO 35 IT = ITI,ITF
      DO 35 JT = IT,ITF
      LC = NOS + (IT - LL(IA))*NO(IA) + JT - LL(IA) + 1
      IF (JT.LT.NCUT) GO TO 34
      IF (IT.LT.NCUT) GO TO 33
      IP=P(IT)
      JP=P(JT)
      H(I,LC) = .5*(HT(IT,JT)+HT(IP,JP)-HT(IT,JP)-HT(JT,IP))
      GO TO 37
   34 IF (IT.GE.NCUT) GO TO 33
      IF (P(JT).EQ.JT) GO TO 37
      IF (P(IT).EQ.IT) GO TO 38
      IP=P(IT)
      JP=P(JT)
      H(I,LC) = .5*(HT(IT,JT)+HT(IT,JP)+HT(JT,IP)+HT(IP,JP))
      GO TO 33
   38 JP=P(JT)
      H(I,LC) = (1./SQRT(2.))*(HT(IT,JT) + HT(IT,JP))
      GO TO 33
   37 H(I,LC) = HT(IT,JT)
   33 LCT = NOS + (JT-LL(IA))*NO(IA) + IT - LL(IA) + 1
   35 H(I,LCT) = H(I,LC)
      NOS = NOS + (NO(IA))**2
      GO TO 42
   21 DO 29 J = 1,MM
      DO 29 K = 1,MM
      LC = LC+1
      JJ = LL(IA) + J - 1
      KK = LL(IA) + K - 1
   29 H(I,LC) = HT(JJ,KK)
   42 CONTINUE
      RETURN
      END
```

```
      SUBROUTINE PERMUT(KEN)
C
C     PERMUT GENERATES NECESSARY PERMUTATION MATRICES IN CASES
C     OF MUTUAL EXCHANGE
C
      COMMON N,NP,MAX,MAXM,NE,NM,NEM,NEN,NMES,NMESM,NNMES(5),NSYM,MRC
      COMMON /HAM/H(3,252),PTEMP(32,32)
      COMMON /PERMT/IE(3,5),P(2,32,32),MU
      COMMON /SUB/NO(7),LL(7),FZ(32,5),NS,ISY(7),PX(32)
      INTEGER PX
C
      DO 1 NPR = 2,NE
      NPRM = NPR - 1
      DO 2 I=1,MAX
      DO 2 J=1,MAX
      PTEMP(I,J) = 0.0
    2 P(NPRM,I,J) = 0.0
      M = 1
      DO 12 I = 1,MAX
      IF (I.LE.(NO(M) + LL(M) -1)) GO TO 3
      M = M+1
    3 DO 4 J = 1,NMES
      JT = IE(NPR,J)
      IF (FZ(I,J) - FZ(I,JT)) 6,4,6
    4 CONTINUE
      PTEMP(I,I) = 1.0
      GO TO 12
    6 K = LL(M)
   11 DO 7 L = 1,NMES
      LT = IE(NPR,L)
      IF (FZ(I,L)-FZ(K,LT)) 9,7,9
    9 K = K+1
      IF(K .LE. 32) GO TO 30
      WRITE(6,204)
  204 FORMAT(///*ABORT DUE TO INFINITE K IN PERMUT*)
      KEN = 1
      RETURN
   30 GO TO 11
    7 CONTINUE
      PTEMP(K,I) = 1.0
   12 CONTINUE
      IF (NSYM.NE.0) GO TO 13
      DO 14 I=1,MAX
      DO 14 J=1,MAX
   14 P(NPRM,I,J)=PTEMP(I,J)
      GO TO 1
   13 P(NPRM,1,1) = 1.0
      P(NPRM,MAX,MAX) = 1.0
      DO 15 I = 2,MAXM
      IF (PX(I).EQ.I) GO TO 16
      DO 19 J = 2,MAXM
      IF (PTEMP(J,I)) 20,19,20
   19 CONTINUE
   20 IF (PX(I).LT.I) GO TO 18
      IF (PX(J).GT.J) P(NPRM,J,I) = 1.0
```

```
      JS = PX(J)
      IF (PX(J).LT.J) P(NPRM,JS,I) = 1.0
      GO TO 15
   18 IF (PX(J).LT.J) P(NPRM,J,I) = 1.0
      JS = PX(J)
      IF (PX(J).GT.J) P(NPRM,JS,I) = -1.0
      GO TO 15
   16 DO 17 J = 1,MAX
   17 P(NPRM,J,I) = PTEMP(J,I)
   15 CONTINUE
    1 CONTINUE
      RETURN
      END
```

```
      SUBROUTINE PRJECT(POP,ITE)
C
C     THIS SUBROUTINE GENERATES VARIOUS AUXILIARY INDEX ARRAYS,
C     NEEDED FOR THE PROJECTION OF THE DENSITY VECTOR INTO THE
C     PROPER LIOUVILLE SUBSPACE, AND COMPUTES THE POPULATION
C     VECTOR
C
      COMMON /INDEX/IROW(210),JCOL(210),IT(32,32)
      COMMON /VEC/V(210),POV(210)
      INTEGER PI,PJ,P
      COMMON /SUB/NO(7),LL(7),FZ(32,5),NS,ISY(7),P(32)
      COMMON /PERMT/IE(3,5),PT(2,32,32),MU
      COMMON/MAG/IME(6,5),WF(6)
      REAL IPL
      COMMON /HAM/H(3,252),IPL(32,32)
      REAL IME
      COMMON N,NP,MAX,MAXM,NE,NM,NEM,NEN,NMES,NMESM,NNMES(5),NSYM,PRO
      DIMENSION POP(3)
      LOGICAL TWICE
C
      POP(1) = 1.0
      IF (NEN - 1) 2,2,3
    2 PS = POP(1)
      GO TO 5
    3 IF (N.EQ.NMES.OR.MU.EQ.0) GO TO 5
      DO 18 I = 1,NE
   18 POP(I) = 1./FLOAT(NE)
    5 DO 80 I = 1,MAX
      DO 80 J=1,MAX
   80 IT(I,J)=0
      L=0
      ND=N
      IF (N.NE.NMES) ND=NS-1
      DO 51 I=1,ND
      TWICE = .FALSE.
   52 K=0
      IF (NSYM.EQ.3) GO TO 6
      IF (TWICE) GO TO 7
      IA = LL(I)
      JA = LL(I+1)
      IEE = IA + (NO(I) + ISY(I))/2 - 1
      JE = JA + (NO(I+1) + ISY(I+1))/2 - 1
      GO TO 8
    7 IA = IEE+ 1
      JA = JE + 1
      IEE= LL(I) + NO(I) - 1
      JE = LL(I+1) + NO(I+1) - 1
      IF (IA.GT.IEE.OR.JA.GT.JE) GO TO 51
      GO TO 8
    6 IA=LL(I)
      JA=LL(I+1)
      IEE = IA + NO(I) - 1
      JE=JA+NO(I+1)-1
    8 DO 50 I1=IA,IEE
      DO 50 J=JA,JE
```

```
      L=L+1
      IROW(L)=I1
      JCOL(L)=J
      K=K+1
   50 IT(I1,J)=K
      IF (NSYM.EQ.0) GO TO 51
      IF (TWICE) GO TO 51
      TWICE = .TRUE.
      GO TO 52
   51 CONTINUE
      L=0
      DO 9 I=1,MAX
      DO 9 J=1,MAX
    9 IPL(I,J)=0.0
      DO 62 II=1,NO
      IB=LL(II)
      IF=LL(II)+NO(II)-1
      JB=LL(II+1)
      JF=LL(II+1)+NO(II+1)-1
      DO 62 I=IB,IF
      DO 62 J=JB,JF
      KINV = 0
      DO 63 M=1,NMES
      IF (FZ(J,M)-FZ(I,M)+1.) 68,67,68
   68 IF (FZ(J,M)-FZ(I,M)) 65,63,65
   67 MS=M
      KINV=KINV+1
      IF(KINV.GT.1) GO TO 65
   63 CONTINUE
      IPL(I,J)=1.0
      IF(N.NE.NMES) IPL(I,J)=SQRT((IME(ITE,MS)-FZ(J,MS))*(IME(ITE,MS)+FZ
     1(J,MS)+1.))
      GO TO 62
   65 IPL(I,J)=0.0
   62 CONTINUE
      TWICE=.FALSE.
      DO 69 II=1,NO
      IF(NSYM.NE.0) GO TO 10
      MM=NO(II)*NO(II+1)
      MA=LL(II)
      ME=MA+NO(II)-1
      MX=LL(II+1)
      MY=MX+NO(II+1)-1
      DO 70 I=MA,ME
      DO 70 J=MX,MY
      L=L+1
      V(L)=IPL(I,J)
   70 POV(L)=.5*V(L)*POP(1)
      GO TO 71
   10 IF(TWICE) GO TO 17
      GO TO 11
   17 TWICE=.FALSE.
      MM=((NO(II)-ISY(II))/2)*((NO(II+1)-ISY(II+1))/2)
      IF(MM.EQ.0) GO TO 69
      MA=LL(II)+(ISY(II)+NO(II))/2
```

```
      ME=LL(II)+NO(II)-1
      MX=LL(II+1)+(ISY(II+1)+NO(II+1))/2
      MY=LL(II+1)+NC(II+1)-1
      DO 12 I=MA,ME
      DO 12 J=MX,MY
      L=L+1
      PI=P(I)
      PJ=P(J)
      V(L)=.5*(IPL(I,J)+IPL(PI,PJ)-IPL(PI,J)-IPL(I,PJ))
   12 POV(L)=(.5)*POP(1)*V(L)
      GO TO 71
   11 TWICE=.TRUE.
      MM=((ISY(II)+NO(II))/2)*((ISY(II+1)+NO(II+1))/2)
      MA=LL(II)
      ME=LL(II)+((ISY(II)+NO(II))/2)-1
      MX=LL(II+1)
      MY=LL(II+1)+((ISY(II+1)+NO(II+1))/2)-1
      DO 13 I=MA,ME
      DO 13 J=MX,MY
      L=L+1
      IF (I.LT.(LL(II)+ISY(II))) GO TO 14
      IF (J.LT.(LL(II+1)+ISY(II+1))) GO TO 15
      PI=P(I)
      PJ=P(J)
      V(L)=(.5)*(IPL(I,J)+IPL(I,PJ)+IPL(PI,J)+IPL(PI,PJ))
      GO TO 13
   15 PI=P(I)
      V(L) = (1./SQRT(2.))*(IPL(I,J)+IPL(PI,PJ))
      GO TO 13
   14 IF (J.LT.(LL(II+1)+ISY(II+1))) GO TO 16
      PJ=P(J)
      V(L) = (1./SQRT(2.))*(IPL(I,J)+IPL(I,PJ))
      GO TO 13
   16 V(L)=IPL(I,J)
   13 POV(L)=(.5)*POP(1)*V(L)
   71 IF (NEN.EQ.1) GO TO 72
      DO 73 JJ=1,NEM
      JM=JJ-1
      LA=L+1+MM*JM
      LE=L+MM*JJ
      DO 73 LX=LA,LE
      LY=LX-MM
      IF (POV(LY)) 92,91,92
   92 POV(LX)=V(LY)*(.5)*(POP(JJ+1))
      GO TO 93
   91 POV(LX)=0.
   93 V(LX)=V(LY)
   73 CONTINUE
      L=LE
   72 IF (TWICE) GO TO 10
   69 CONTINUE
      IF (NEN.NE.1) GO TO 4
      POP(1) = PS
    4 CONTINUE
      RETURN
```

```
SUBROUTINE PRJECT
      END
```

```
      SUBROUTINE TRAMAT(A,NTR,NT,NB,ITE,NOSS,NOS,ID)
C
C     THIS SUBROUTINE CONSTRUCTS THE SUBMATRICES OF THE LIOUVILLE
C     MATRIX.  THE TRANSITION SUBMATRICES INCLUDING EXCHANGE AND
C     RELAXATION TERMS ARE ALSO GENERATED.
C
      COMPLEX A(48,48)
      INTEGER O
      COMPLEX IM
      COMMON /SUB/NC(7),LL(7),FZ(32,5),NS,ISY(7),O(32)
      COMMON /INDEX/IROW(210),JCOL(210),IT(32,32)
      COMMON N,NP,MAX,MAXM,NE,NM,NEM,NEN,NMES,NMESM,NNMES(5),NSYM,MRC
      COMMON /HAM/H(3,252),HT(32,32)
      COMMON /DYNPAR/RC(3,3),T2
      COMMON /PERMT/IE(3,5), P(2,32,32),MU
      INTEGER U,V
C
      IM=CMPLX(0.,1.)
      PI=3.14159
      DO 52 I=1,NT
      DO 52 J=1,NT
   52 A(I,J)=CMPLX(0.,0.)
      INC=0
      DO 53 KK=1,NE
      DO 4 I=1,NTR
      II=I+NB
      IC=I+INC
      IF (NEN.EQ.1) GO TO 13
      DO 55 IR=1,NE
      IF (IR.EQ.KK) GO TO 55
      A(IC,IC)=-RC(KK,IR)+A(IC,IC)
   55 CONTINUE
   13 DO 4 J=I,NTR
      JJ=J+NB
      JC=J+INC
      IF (JCOL(II).EQ.JCOL(JJ)) GO TO 59
   62 IF (IROW(II).EQ.IROW(JJ)) GO TO 60
      GO TO 4
   59 U=IROW(II)
      V=IROW(JJ)
      LC = NOSS+NO(ID)*(U-LL(ID))+V-LL(ID) + 1
      A(IC,JC) = -2.*IM*PI*H(KK,LC)+ A(IC,JC)
      GO TO 62
   60 U=JCOL(II)
      V=JCOL(JJ)
      LC=NOS+NO(ID+1)*(U-LL(ID+1))+V-LL(ID+1)+1
      A(IC,JC) = 2.*IM*PI*H(KK,LC)+ A(IC,JC)
    4 A(JC,IC) = A(IC,JC)
      IF(MRC.EQ.1) GO TO 5
      IF (MU.EQ.1.AND.NEN.EQ.1) GO TO 15
      INC=INC+NTR
   53 CONTINUE
      GO TO 5
   15 DO 6 NPR=1,NEM
      DO 7 I=1,NT
```

```
      II=NB+1
      U=IROW(II)
      V=JCOL(II)
      DO 7 J=1,NT
      JJ = NB + J
      K=IROW(JJ)
      L=JCOL(JJ)
    7 A(I,J) = A(I,J) + RC(1,2)*P(NPR,U,K)*P(NPR,V,L)
    6 CONTINUE
      DO 14 I = 1,NT
      DO 14 J = 2,NE
   14 A(I,I) = A(I,I) - RC(1,2)
    5 DO 54 I = 1,NT
   54 A(I,I) = A(I,I) -1./T2
      IF (NEN.EQ.1) GO TO 61
      NA=1
      IF (NE.EQ.1) GO TO 61
      DO 56 IR=1,NEM
      NTRR=NTR*IR
      DO 57 I2=NA,NTRR
      I2P=I2+NTR
      I3=IR
      DO 58 I4=I2P,NT,NTR
      I3=I3+1
      A(I2,I4)=RC(I3,IR)
      A(I4,I2)=RC(IR,I3)
   58 CONTINUE
   57 CONTINUE
      NA=NA+NTR
   56 CONTINUE
   61 CONTINUE
      RETURN
      END
```

```
      SUBROUTINE CONVEC(K,KC,NT,ITE)
C
C     THIS SUBROUTINE GENERATES THE SHAPE VECTOR
C     AND RADIOFREQUENCY INDEPENDENT PART OF THE
C     SPECTRAL VECTOR
C
      COMPLEX CR(48,48),CL(48,48),EIG(48),Q(135),D(136)
      COMPLEX CRS,CLS
      COMMON /EIVEC/CR,CL,EIG
      COMMON /VECT/C,D
      COMMON /VEC/V(210),POV(210)
      COMMON/MAG/IME(6,5),WF(6)
      REAL IME
C
      K1=1
      KK = KC - 1
   82 Q(K)=CMPLX(0.,0.)
      CRS=CMPLX(0.,0.)
      DO 91 LA=1,NT
      LAK=LA+KK
   91 CRS = CRS + 2.*V(LAK)*CR(LA,K1)
      CLS=CMPLX(0.,0.)
      DO 92 NU=1,NT
      NUK=NU+KK
   92 CLS=CLS+POV(NUK)*CL(K1,NU)
      Q(K) = WF(ITE)*CRS*CLS
      D(K)=EIG(K1)
      KC = KC +1
      K=K+1
      K1=K1+1
      IF (K1.LE.NT) GO TO 82
      RETURN
      END
```

```
      SUBROUTINE SPECT(NTOT)
C     THIS SUBROUTINE PLOTS THE SPECTRUM
C     S.G.W.U. VERSION.
      COMPLEX Q(136),D(136),V,G,IM
      DIMENSION KRAY(6)
      COMMON /PLTPAR/ SCALE,HEIGHT,FR1,FR2
      COMMON /VECT/ Q,D
      COMMON /ETVEC/ Y(9312)
      COMMON /DYNPAR/ RC(3,3),T2
      COMMON /NAME/IDEN(7)
      IF (HEIGHT.GT.250.0) HEIGHT=250.0
      PI=3.14159
      IM=CMPLX(0.,1.)
      DENS=100.0
      XMAX=SCALE*(FR2-FR1)/25.4
      NPOINT=DENS*XMAX
      STEP=(FR2-FR1)/NPOINT
      FR=FR1-STEP
      DO 16 L=1,NPOINT
      FR=FR+STEP
      G=CMPLX(0.,0.)
      V=2.*PI*IM*FR
      DO 15 K=1,NTOT
   15 G=G+Q(K)/(D(K)-V)
   16 Y(L)=-REAL(G)
      YMAX=Y(1)
      YMIN=Y(1)
      DO 21 I=2,NPOINT
      IF (YMAX.GT.Y(I)) GO TO 22
      YMAX=Y(I)
   22 IF (YMIN.LT.Y(I)) GO TO 21
      YMIN=Y(I)
   21 CONTINUE
      FACTOR=HEIGHT/(25.4*(YMAX-YMIN))
      DO 23 I=1,NPOINT
   23 Y(I)=(Y(I)-YMIN)*FACTOR
      LY=XMAX+1.0
      YL=(FR2-FR1)*FLOAT(LY)/XMAX
      CALL SAXESX (     1,10,LY,1.0,10.0,YL,0.0,0.0,0.0,0.0)
      CALL PLOTXYX(0.0,0.0,1,0)
      CALL PLOTXYX(0.0,YL,1,0)
      CALL PLOTXYX(10.0,YL,1,0)
      YT = YL
   30 YT=YT-5.0
      IF( YT .LT. 0.0)GO TO 36
      CALL PLOTXYX(10.0,YT,1,0)
      CALL PLOTXYX(9.95,YT,1,0)
      CALL PLOTXYX(10.0,YT,1,0)
      YT=YT-5.0
      IF( YT .LT. 0.0)GO TO 36
      CALL PLOTXYX(10.0,YT,1,0)
      CALL PLOTXYX(9.90,YT,1,0)
      CALL PLOTXYX(10.0,YT,1,0)
      GO TO 30
   36 CALL PLOTXYX(0.0,0.0,1,0)
```

```
      ENCODE(40,110,KRAY(1)) RC(1,2),T2
  110 FORMAT(16HRATE CONSTANT = ,F8.2,*    T2 =*,F8.4)
      Y1=YL*(FLOAT(LY)-0.2)/FLOAT(LY)
      IFR1=FR1
      IFR2=FR2
      IRF=0
      ILF=0
      ENCODE(4,111,IRF)IFR1
      ENCODE(4,111,ILF)IFR2
  111 FORMAT(I4)
      CALL PLOTXYX(0.15,0.0,0,0)
      CALL LABELX(4,3,3,ILF)
      CALL PLOTXYX(1.0,2.0,0,0)
      CALL LABELX(70,3,4,IDEN(1))
      X=0.
      YYY=9.85-Y(NPOINT)
      CALL PLOTXYX(YYY,X,0,0)
      DO 24 I=2,NPOINT
      J=NPOINT-I+1
      X=X+STEP
      YYY=9.85-Y(J)
   24 CALL PLOTXYX(YYY,X,1,0)
      Y2=YL*(FLOAT(LY)-0.6)/FLOAT(LY)
      CALL PLOTXYX(9.0,Y1,0,0)
      CALL LABELX(40,3,2,KRAY(1))
      CALL PLOTXYX(0.15,Y2,0,0)
      CALL LABELX(4,3,3,IRF)
      CALL ENDPLTX
      WRITE(6 ,100)
  100 FORMAT(///29H SUMMARY OF PLOT CALCULATIONS/)
      WRITE(6 ,102)NPOINT
  102 FORMAT(25H NO. OF POINTS PLOTTED = ,I4)
      WRITE(6 ,105)LY
  105 FORMAT(37H LENGTH OF FREQUENCY AXIS (INCHES) = ,I3)
      WRITE(6 ,106)YL
  106 FORMAT(34H LENGTH OF FREQUENCY AXIS IN HZ = ,F7.2)
      XG=FR1+X
      WRITE(6 ,107)FR1,XG
  107 FORMAT(27H FREQUENCY RANGE PLOTTED = ,F7.2,4H TO ,F7.2,3H HZ)
      RETURN
      END
```

```
      SUBROUTINE ALLMAT (A,M,CL,LAMBDA,KEN)
C ALLMAT DIAGONALIZES THE NT BY NT DIMENSIONAL A MATRIX.  THE
C EIGENVECTORS ARE OVERWRITTEN ON THE ORIGINAL A MATRIX. THE INVERSE OF
C THE EIGENVECTOR MATRIX IS CALCULATED AS THE CL MATRIX. THE EIGEN-
C VALUES ARE CONTAINED IN THE ONE DIMENSIONAL LAMBDA ARRAY.
C PROG. AUTHORS JOHN RINZEL,P.E.FUNDERLIC,UNION CARBIDE CORP.
C NUCLEAR DIVISION,CENTRAL DATA PROCESSING FACILITY,
C OAK RIDGE TENNESSEE
C
      DIMENSION INT(48)
      COMPLEX A(48,48),H(48,48),HL(48,48),LAMBDA(48),
     1VECT(48),MULT(48),SHIFT(3),TEMP,SIN,COS,TEMP1,TEMP2,
     1CR(48,48),CL(48,48),EIG(48),TRACE,SUMEIG
      INTEGER R,RP1,RP2
      LOGICAL INTH(55),TWICE
      COMMON /EIVEC/ CR,H,EIG
      COMMON/TEM/ HL
      KEN = 0
      N=M
      TRACE = 0.0
      DO 61 I = 1,N
   61 TRACE = TRACE + A(I,I)
      NCAL=N
      IF(N.NE.1)GO TO 1
      LAMBDA(1)=A(1,1)
      A(1,1)=1.
      CL(1,1) = 1.0
      GO TO 57
    1 ICOUNT=0
      SHIFT(1) = (0.,0.)
      SHIFT(2) = (0.,0.)
      SHIFT(3) = (0.,0.)
      IF(N.NE.2)GO TO 4
    2 TEMP=(A(1,1)+A(2,2)+CSQRT((A(1,1)+A(2,2))**2-
     14.*(A(2,2)*A(1,1)-A(2,1)*A(1,2))))/2.
      IF(REAL(TEMP).NE.0..OR.AIMAG(TEMP).NE.0.)GO TO 3
      LAMBDA(M)=SHIFT(1)
      LAMBDA(M-1)=A(1,1)+A(2,2)+SHIFT(1)
      GO TO 37
    3 LAMBDA(M)=TEMP+SHIFT(1)
      LAMBDA(M-1)=(A(2,2)*A(1,1)-A(2,1)*A(1,2))/(LAMBDA(M)-SHIFT(1)
     1 ) + SHIFT(1)
      GO TO 37
C
C     REDUCE MATRIX A TO HESSENBERG FORM
    4 NM2=N-2
      DO 15 R=1,NM2
      RP1=R+1
      RP2=R+2
      ABIG=0.
      INT(R)=RP1
      DO 5 I=RP1,N
      ABSSQ=REAL(A(I,R))**2+AIMAG(A(I,R))**2
      IF(ABSSQ.LE.ABIG)GO TO 5
      INT(R)=I
```

```
      ABIG=ABSSQ
    5 CONTINUE
      INTER=INT(R)
      IF(ABIG.EQ.0.)GO TO 15
      IF(INTER.EQ.RP1)GO TO 8
      DO 6 I=R,N
      TEMP=A(RP1,I)
      A(RP1,I)=A(INTER,I)
    6 A(INTER,I)=TEMP
      DO 7 I=1,N
      TEMP=A(I,RP1)
      A(I,RP1)=A(I,INTER)
    7 A(I,INTER)=TEMP
    8 DO 9 I=RP2,N
      MULT(I)=A(I,R)/A(RP1,R)
    9 A(I,R)=MULT(I)
      DO 11 I=1,RP1
      TEMP=0.
      DO 10 J=RP2,N
   10 TEMP=TEMP+A(I,J)*MULT(J)
   11 A(I,RP1)=A(I,RP1)+TEMP
      DO 13 I=RP2,N
      TEMP=0.
      DO 12 J=RP2,N
   12 TEMP=TEMP+A(I,J)*MULT(J)
   13 A(I,RP1)=A(I,RP1)+TEMP-MULT(I)*A(RP1,RP1)
      DO 14 I=RP2,N
      DO 14 J=RP2,N
   14 A(I,J)=A(I,J)-MULT(I)*A(RP1,J)
   15 CONTINUE
C
C     CALCULATE EPSILON
C
      EPS=0.
      DO 16 I=1,N
   16 EPS=EPS+CABS(A(1,I))
      DO 18 I=2,N
      SUM=0.
      IM1=I-1
      DO 17 J=IM1,N
   17 SUM=SUM+CABS(A(I,J))
   18 IF(SUM.GT.EPS)EPS=SUM
      EPS=SQRT(FLOAT(N))*EPS*1.E-12
      IF(EPS.EQ.0.)EPS=1.E-12
      DO 19 I=1,N
      DO 19 J=1,N
   19 H(I,J)=A(I,J)
   20 IF(N.NE.1)GO TO 21
      LAMBDA(M)=A(1,1)+SHIFT(1)
      GO TO 37
   21 IF(N.EQ.2)GO TO 2
   22 MN1=M-N+1
      IF(REAL(A(N,N)).NE.0..OR.AIMAG(A(N,N)).NE.0.) GO TO 99
      GO TO 23
   99 IF(ABS(REAL(A(N,N-1)/A(N,N)))+ABS(AIMAG(A(N,N-1)/A(N,N)))-1.E-9)
```

```
      1 24,24,23
   23 IF(ABS(REAL(A(N,N-1)))+ABS(AIMAG(A(N,N-1))).GE.EPS)GO TO 25
   24 LAMBDA(MN1)=A(N,N)+SHIFT(1)
      ICOUNT=0
      N=N-1
      GO TO 21
C
C     DETERMINE SHIFT
C
   25 SHIFT(2)=(A(N-1,N-1)+A(N,N)+CSQRT((A(N-1,N-1)+A(N,N))**2
     1-4.*(A(N,N)*A(N-1,N-1)-A(N,N-1)*A(N-1,N))))/2.
      IF(REAL(SHIFT(2)).NE.0..OR.AIMAG(SHIFT(2)).NE.0.)GO TO 26
      SHIFT(3)=A(N-1,N-1)+A(N,N)
      GO TO 27
   26 SHIFT(3)=(A(N,N)*A(N-1,N-1)-A(N,N-1)*A(N-1,N))/SHIFT(2)
   27 IF(CABS(SHIFT(2)-A(N,N)).LT.CABS(SHIFT(3)-A(N,N)))GO TO 28
      INDEX=3
      GO TO 29
   28 INDEX=2
   29 IF (CABS(A(N-1,N-2)).GE.EPS) GO TO 30
      LAMBDA(MN1)=SHIFT(2)+SHIFT(1)
      LAMBDA(MN1+1)=SHIFT(3)+SHIFT(1)
      ICOUNT=0
      N=N-2
      GO TO 20
   30 SHIFT(1) = SHIFT(1) + SHIFT(INDEX)
      DO 31 I=1,N
   31 A(I,I)=A(I,I)-SHIFT(INDEX)
C
C     PERFORM GIVENS ROTATIONS, OR ITERATES
C
      IF (ICOUNT.LE.10) GO TO 32
      NCAL=M-N
      GO TO 37
   32 NM1=N-1
      TEMP1=A(1,1)
      TEMP2=A(2,1)
      DO 36 R=1,NM1
      RP1=R+1
      RHO=SQRT(REAL(TEMP1)**2+AIMAG(TEMP1)**2+
     1REAL(TEMP2)**2+AIMAG(TEMP2)**2)
      IF (RHO.EQ.0) GO TO 201
      COS=TEMP1/RHO
      SIN=TEMP2/RHO
      INDEX=MAXU(R-1,1)
      DO 33 I=INDEX,N
      TEMP=CONJG(COS)*A(R,I)+CONJG(SIN)*A(RP1,I)
      A(RP1,I)=-SIN*A(R,I)+COS*A(RP1,I)
   33 A(R,I)=TEMP
  201 TEMP1 = A(RP1,RP1)
      IF(R+2 .GT. N) GO TO 203
      TEMP2=A(R+2,R+1)
      IF (RHO.EQ.0) GO TO 36
  203 DO 34 I=1,R
      TEMP=COS*A(I,R)+SIN*A(I,RP1)
```

```
      A(I,RP1)=-CONJG(SIN)*A(I,R)+CONJG(COS)*A(I,RP1)
   34 A(I,R)=TEMP
      INDEX=MIN0(R+2,N)
      DO 35 I=RP1,INDEX
      A(I,R)=SIN*A(I,RP1)
   35 A(I,RP1)=CONJG(COS)*A(I,RP1)
   36 CONTINUE
      ICOUNT=ICOUNT+1
      GO TO 22
C
C     CALCULATE VECTORS
C
   37 IF(NCAL.EQ.0)GO TO 57
      NCALM = NCAL - 1
      DO 68 I = 1,NCALM
      IP1 = I + 1
      K = NCAL
      DO 68 J = IP1,K
      IF (CABS(LAMBDA(I)) - CABS(LAMBDA(J))) 68,68,69
   69 TEMP = LAMBDA(I)
      LAMBDA(I) = LAMBDA(J)
      LAMBDA(J) = TEMP
   68 CONTINUE
      DO 70 I = 1,NCALM
      IP1= I+1
      DO 71 J = IP1,NCAL
      IF (CABS(LAMBDA(I) - LAMBDA(J)) - (3.0E-07)*(CABS(LAMBDA(I)))) 72,
     172,71
   72 LAMBDA(1) = LAMBDA(I) - (3.0E-07)*LAMBDA(I)
      IM = I-1
      DO 73 K = 1,IM
      IF (CABS(LAMBDA(I) - LAMBDA(I-K)) -(3.0E-07)*(CABS(LAMBDA(I)))) 74
     1,74,71
   74 LAMBDA(I-K) = LAMBDA(I-K) - (3.0E-07)*LAMBDA(I)
   73 CONTINUE
   71 CONTINUE
   70 CONTINUE
      N=M
      NM1=N-1
      IF(N.NE.2)GO TO 38
      EPS=AMAX1(CABS(LAMBDA(1)),CABS(LAMBDA(2)))*1.E-8
      IF(EPS.EQ.0.)EPS=1.E-12
      H(1,1)=A(1,1)
      H(1,2)=A(1,2)
      H(2,1)=A(2,1)
      H(2,2)=A(2,2)
   38 DO 56 L=1,NCAL
      DO 40 I=1,N
      DO 39 J=1,N
   39 HL(I,J)=H(I,J)
   40 HL(I,I)=HL(I,I)-LAMBDA(L)
      DO 44 I=1,NM1
      MULT(I)=0.
      INTH(I)=.FALSE.
      IP1=I+1
```

```
      IF(CABS(HL(I+1,I)).LE.CABS(HL(I,I)))GO TO 42
      INTH(I)=.TRUE.
      DO 41 J=I,N
      TEMP=HL(I+1,J)
      HL(I+1,J)=HL(I,J)
   41 HL(I,J)=TEMP
   42 IF(REAL(HL(I,I)).EQ.0..AND.AIMAG(HL(I,I)).EQ.0.)GO TO 44
      MULT(I)=-HL(I+1,I)/HL(I,I)
      DO 43 J=IP1,N
   43 HL(I+1,J)=HL(I+1,J)+MULT(I)*HL(I,J)
   44 CONTINUE
      DO 45 I=1,N
   45 VECT(I)=1.
      TWICE=.FALSE.
   46 IF(REAL(HL(N,N)).EQ.0..AND.AIMAG(HL(N,N)).EQ.0.)HL(N,N)=EPS
      VECT(N)=VECT(N)/HL(N,N)
      DO 48 I=1,NM1
      K=N-I
      DO 47 J=K,NM1
   47 VECT(K)=VECT(K)-HL(K,J+1)*VECT(J+1)
      IF(REAL(HL(K,K)).EQ.0..AND.AIMAG(HL(K,K)).EQ.0.)HL(K,K)=EPS
   48 VECT(K)=VECT(K)/HL(K,K)
      SSS = 0.
      DO 1001 I = 1,N
 1001 SSS = SSS + (REAL(VECT(I)))**2 + (AIMAG(VECT(I)))**2
      SSS = SQRT(SSS)
      DO 50 I = 1,N
   50 VECT(I) = VECT(I)/SSS
      IF(TWICE)GO TO 52
      DO 51 I=1,NM1
      IF(.NOT.INTH(I))GO TO 51
      TEMP=VECT(I)
      VECT(I)=VECT(I+1)
      VECT(I+1)=TEMP
   51 VECT(I+1)=VECT(I+1)+MULT(I)*VECT(I)
      TWICE=.TRUE.
      GO TO 46
   52 IF(N.EQ.2)GO TO 55
      NM2=N-2
      DO 54 I=1,NM2
      N1I=N-1-I
      NI1=N-I+1
      DO 53 J=NI1,N
   53 VECT(J)=H(J,N1I)*VECT(N1I+1)+VECT(J)
      INDEX=INT(N1I)
      TEMP=VECT(N1I+1)
      VECT(N1I+1)=VECT(INDEX)
   54 VECT(INDEX)=TEMP
   55 DO 56 I = 1,N
   56  A(I,L) =VECT(I)
      IF (NCAL.NE.N) GO TO 64
      CALL NVRT(A,CL,N)
      SUMEIG = 0.0
      DO 59 I=1,NCAL
   59 SUMEIG = SUMEIG + LAMBDA(I)
```

```
      WRITE (6,60) TRACE, SUMEIG
   60 FORMAT (9H TRACE = E14.7,3H + E14.7,1HI10H SUMEIG = E14.7,3H + E14
     1.7,1HI)
      GO TO 57
   64 NCALP = NCAL + 1
      WRITE (6,65) NCALP
   65 FORMAT (43H CONVERGENCE FAILURE IN CALCULATION OF NO. I2,28H EIGEN
     1VALUE -- RUN TERMINATED)
      KEN = 1
   57 RETURN
      END
```

```
      SUBROUTINE NVRT(Q,QNV,N)
C
C     NVRT-INVERTS THE EIGENVECTOR MATRIX GENERATED BY ALLMAT
C
      COMPLEX Q(48,48),QQNV(48,48),TEMP(48,48),QNV(48,48),P(48)
      COMPLEX TFR
      COMMON/TEM/ TEMP
C
      IF (N.NE.1) GO TO 1
      QNV(1,1) = 1./Q(1,1)
      GO TO 120
    1 DO 410 I = 1,N
      DO 410 J=1,N
      TEMP(I,J)=Q(I,J)
  410 QQNV(I,J)=CMPLX(0.,0.)
      DO 11 I=1,N
   11 QQNV(I,I)=CMPLX(1.,0.)
      K=1
   92 I=K
      L=K
    9 S=CABS(TEMP(I,K))
      T=CABS(TEMP(L,K))
      IF (S-T) 10,10,20
   20 L=I
   10 IF (I-N) 30,40,30
   30 I=I+1
      GO TO 9
   40 IF (K-K) 50,60,50
   50 J=K
    6 TFR=TEMP(K,J)
      TEMP(K,J)=TEMP(L,J)
      TEMP(L,J)=TFR
      IF (J-N) 8,7,8
    8 J=J+1
      GO TO 6
    7 DO 69 IN=1,N
      TFR=QQNV(K,IN)
      QQNV(K,IN)=QQNV(L,IN)
   69 QQNV(L,IN)=TFR
   60 I=K+1
   71 TFR=TEMP(I,K)/TEMP(K,K)
      TEMP(I,K)=CMPLX(0.,0.)
      J=K+1
    3 TEMP(I,J)=TEMP(I,J)-TFR*TEMP(K,J)
      IF (J-N) 5,4,5
    5 J=J+1
      GO TO 3
    4 DO 39 IN=1,N
   39 QQNV(I,IN)=QQNV(I,IN)-TFR*QQNV(K,IN)
      IF (I-N) 70,80,70
   70 I=I+1
      GO TO 71
   80 IF (K-N+1) 90,91,90
   90 K=K+1
      GO TO 92
```

```
 91 DO 750 IN=1,N
750 QNV(N,IN)=QQNV(N,IN)/TEMP(N,N)
    I=N-1
 99 J=I+1
    DO 751 IN=1,N
751 P(IN)=CMPLX(0.,0.)
102 DO 752 IN=1,N
752 P(IN)=P(IN)+TEMP(I,J)*QNV(J,IN)
    IF (J-N) 100,101,100
100 J=J+1
    GO TO 102
101 DO 753 IN=1,N
753 QNV(I,IN)=(QQNV(I,IN)-P(IN))/TEMP(I,I)
    IF (I-1) 110,120,110
110 I=I-1
    GO TO 99
120 RETURN
    END
```